ANALYSIS OF SET-UP ERRORS IN BREAST CANCER PATIENTS UNDERGOING EXTERNAL BEAM RADIOTHERAPYAT NATIONAL HOSPITAL ABUJA

BY

ONUH, ECHECHE

BSc PHYSICS (UNIJOS, 2010)

MSc PHYSICS (A.B.U, 2014)

P16PSPY9012

A THESIS SUBMITTED TO THE SCHOOL OF POSTGRADUATE STUDIES, AHMADU BELLO UNIVERSITY, ZARIA, IN PARTIAL FULFILMENT OF THE REQUIREMENTS FOR THE AWARD OF DOCTORATE DEGREE OF SCIENCE IN RADIATION BIOPHYSICS, DEPARTMENT OF PHYSICS, FACULTY OF PHYSICAL SCIENCES, AHMADU BELLO UNIVERSITY, ZARIA NIGERIA.

APRIL, 2023

DECLARATION

I hereby declare that the work in this thesis titled "**Analysis of Set-up Errors in Breast Cancer Patients Undergoing External Beam Radiotherapy"** was carried out by me in the Department of Physics, Faculty of Physical Sciences, Ahmadu Bello University, Zaria, under the supervision of **Professor RabiuNasiru, Dr. NuraddeenNasiruGarba and Dr. Adamu Abdullahi.** The work of other researchers has been duly acknowledged and referenced. No part of this thesis has been presented for another degree or diploma at this or any other institution.

_____ _____ _____

ONUH ECHECHE **Signature** **Date**

CERTIFICATION

This thesis titled "**ANALYSIS OF SET-UP ERRORS IN BREAST CANCER PATIENTS UNDERGOING EXTERNAL BEAM RADIOTHERAPY"** meets the regulations governing the award of the degree of doctorate of Radiation Biophysics in the Department of Physics, Faculty of Physical Sciences, Ahmadu Bello University and is approved for its contribution to knowledge and literary presentation.

Prof. RabiuNasiru	_____	_____
Chairman Supervisory Committee	(Signature)	(Date)
Dr. N. N. Garba	_____	_____
Member Supervisory Committee,	(Signature)	(Date)
Dr. A. Abdullahi	_____	_____
Member, Supervisory Committee,	(Signature)	(Date)
.		
Prof. RabiuNasiru	_____	_____
Head of Department	(Signature)	(Date)
Prof. Sani A. Abdullahi	_____	_____
Dean, School of Postgraduate Studies,	(Signature)	(Date)

DEDICATION

This research work is dedicated to my late dad, my beloved mum, my darling husband, my family and friends. Thank you for a life full of adventure.

ACKNOWLEDGEMENT

My sincere appreciation goes to my supervisors, Professor RabiuNasiru, Dr N.N. Garba and Dr. A. Abdullahi as well as my mentors Professor Sunday Jonah, Mr. A.S. Ajuji and Professor U. Sadiq for theirstewardship and guidance in this work. I am indebted to these persons for their scientific expertise, dedication, guidance and friendship throughout the last five years. It was very satisfying (on many levels) to work with them and an honour to be one of the students they have mentored. I believe I have learned much from them, they showed me how to approach difficult problems in a coherent and reasonable manner. I am immensely proud to say I have been their student.

Many thanks goes to all those who have taught me from my primary school up to this stage. I cannot thank you enough. In the same vein, I thank my colleagues at National Hospital Abuja particularly, Dr. T. Ige, Obinna Asogwa, Mrs Khadija and Maruf Adewole for assisting with the data collection. I would also like to thank all staff of the department of Physics for their support and encouragement.

Finally, I thank my spouse and all my family members and friends for their unconditional support throughout this journey.

ABSTRACT

Radiotherapy plays an important role in breast cancer treatment. The main goal of radiationtherapy is to ensure tumor control while avoiding complications to the organs at risks. Uncertainty in the dose deposited in the tumor exists due to a variety of factors which include patient positioning errors. This study assessed and quantified breast cancer patients' set-up errors using an electronic portal imaging device and evaluated the dosimetric and biological impact in terms of generalized equivalent uniform dose (gEUD) using predictive models, such as Tumour Control Probability (TCP) and Normal Tissue Complication Probability (NTCP). About 200 breast cancer patients were considered at the Radiotherapy-Oncology department of National Hospital Abuja (NHA). Systematic and random errors were quantified, in addition,three-dimensional treatment planning was performed using CT scan images of the patients. The total prescribed dose was 5000 cGy per 25 fractions for most of the patients. The dosimetric and biological impact of these set-up errors on the target volume and the organ at risk (OARs) coverage were assessed by evaluating the Dose– Volume Histogram (DVH), gEUD, TCP and NTCP. The standard deviations (SDs) of the systematic set-up and random set-up errors were calculated for the Lateral, Anterior-Posterior and Superior-Inferior fields and were found to be 6.6055(4.477), 4.608(3.591), 11.432(8.1748) respectively. Thus, a planning target volume (PTV) margin of 5 mm was defined around the OARs, and around the clinical target volume (CTV). The toxicity of OARs was quantified using gEUD, TCP and NTCP. The data represented that NTCP values for conformal technique was one (1) for the combined lungs at D50, D75, D90 and D98 of the planning target volume ($p = 0.05$). In addition, NTCP values of the heart were equal to 0.99 at D_{50}, D_{75}, D_{90} and D_{98}. The TCP outcome shows a negative and not so good correlation with calculated dose to 50%, 75%, 90% and 95% of the target volume (D95%). In conclusion, this research confirmed that more relevant and robust radiobiological parameters should be integrated with more recent dose calculation methods to obtain reliable prediction of organ at risks toxicity and avoid over/under estimating of TCP and NTCP. This is critical if medical decisions have to be based on NTCP estimations in routine practice.

TABLE OF CONTENTS

LIST OF TABLES

LIST OF FIGURES

LIST OF ABBREVIATIONS AND ACRONYMS

A	Adenine
ACS	American Cancer Society
AC	Alternating Current
AIWH	Australian Institute for Health and Welfare
A-P	Anterior-Posterior
BB	Breast Board
BED	Biological Effective Dose
C	Cytosine
CB	Contralateral Breast
CI	Conformity Index
CL	Contralateral Lung
CLD	Central Lung Distance
CTV	Critical Target Volume
CT	Computed Tomography
CTCAE	Common Terminology Criteria for Adverse Effects Schema
D	Dose
DC	Direct Current
Deff	Effective Dose
Dmax	Maximum Dose
Dmean	Mean Dose
Dmin	Minimum Dose
DNA	Deoxyribose-Nucleic Acid
DRR	Digital Reconstructed Radiography
DVHs	Dose Volume Histograms
EBRT	External Beam Radiotherapy

EPID	Electronic Portal Imaging Device
EUD	Equivalent Uniform Dose
FSUs	Function Sub Units
G	Guanine
gEUD	generalise Equivalent Uniform Dose
GTV	Gross Tumour Volume
Gy	Gray
IB	Ipsilateral Breast
ICRU	International Commission on Radiological Units and Measurements
IGRT	Image Guided Radiotherapy
IL	Ipsilateral Lung
IMRT	Intensity Modulated Radiation Therapy
L	Lateral
LEM	Local Effect Model
LET	Linear Energy Transfer
LINAC	Linear Accelerator
LKB	Lyman Kutcher and Burman
LQ	Linear Quadratic
MeV	Mega electron Volts
MLCs	Multileaf Collimators
MRI	Magnetic Resonance Image
MUs	Monitor Units
MV	MegaVoltage
NHA	National Hospital Abuja
NIH	National Institute of Health
NTCP	Normal Tissue Complication Probability
OARs	Organ at Risks

PD/fr	Prescribed Dose per fraction
PET	Positron Emission Tomography
PIs	Portal Images
PTV	Planning Target Volume
QA	Quality Assurance
QUANTEC	Qualitative Analysis of Normal Tissue Effects in Clinic
RE	Relative Effectiveness
RT	Radiotherapy
RTOG	Radiotherapy Oncology Group
SDs	Standard Deviatons
S-I	Superior-Inferior
SPECT	Single-Photon Emission Computerized Tomography
SPSS	Statistical Package for Social Sciences
SSD	Source to Surface Distance
T	Thymine
TCD	Tumour Control Dose
TCP	Tumour Control Probability
TD	Tolerance Dose
TPS	Treatment Planning System
US	United States
VC	Vacuum Cushion
VMAT	Volumetric Modulated Arc Therapy
Vref	Reference Volume
WHO	World Health Organisation
3D-CRT	Three Dimensional-Conformal Radiotherapy

CHAPTER ONE

INTRODUCTION

1.1 Background of study

Cancer is a malignant disease condition arising from uncontrolled division of cells in the body to form mass of tissues. These cells have the capacity to infiltrate adjacent or surrounding structures or spread to distant site in the body where they can go on proliferating uncontrollably thus, causing significant morbidity and mortality (ACS, 2019). There are various types of human cancers such as anal cancer, bladder cancer, bone cancer, breast cancer, cervical cancer, colon cancer, endometrial cancer, kidney cancer, leukemia, liver cancer lymphoma, ovarian cancer, pancreatic cancer amongst others. Breast cancer is a disease in which malignant cells form in breast tissue. Breast tissue consists mainly of fatty tissue, glandular tissue arranged in lobes (which produce milk), and ducts (the tubes that carry milk to the nipple), as well as connective tissue (Figure 1.1). Breast cancers can invade and damage the tissue around the tumour and can spread to other parts of the body through the lymphatic or vascular system.

The menace of cancer in the society today cannot be over-emphasized because it has become such a chronic disease and it claims millions of lives every year (WHO, 2020). Cancer incidence keeps on rising from year to year with death rate following the same pattern. The World Health Organization, (WHO), in December, 2020, reported cancer as one of the leading causes of morbidity and mortality worldwide, with nearly 14 million new cases in 2012 alone, which is expected to rise by about 70% in the next two decades. In 2015 about 8.8 million cancer deaths were recorded (Christina, 2018).

WHO rated cancer as the second leading cause of death globally with 70% of these deaths from low and middle-income countries (Stewart *et al*., 2016). The United States (US) reported in 2018 that 266,120 new cases of invasive breast cancer were diagnosed in women, 2,550 cases diagnosed in men and an additional 63,960 cases of in situ breast lesions diagnosed in women (ACS, 2019). From 2005 to 2014, invasive breast cancer incidence rates were stable in white women and increased slightly (by 0.3% per year) in black women with an estimated 41,400 breast cancer deaths occurrence (40,920 women, 480 men) in 2018 (United States Report, 2018). The female breast cancer death rate peaked at 33.2% (per 100,000) in 1989, and then declined by 39% to 20.3 in 2015. This progress, which is attributed to improvements in early detection (through screening, as well as increased awareness) and treatment, translates to an estimated 322,600 fewer breast cancer deaths than would have been expected if the death rate had remained unchanged. Decline in annual percentage from 2006 to 2015 was slightly higher for white women (1.8%) than for black women (1.5%) (ACS, 2019).

Cancer was ranked as the 7th leading cause of death in Africa in 2004, with an expected annual incidence of 1.28 million cases and 970,000 deaths by 2030 (Ferlay*et al*., 2012). Cancer is becoming a public health problem in Africa because of the following factors: aging, growth of the population and increased incidence of economic transition-associated cancer risk factors such as smoking,obesity, physical inactivity, poor diet, and reproductive factors (Jemal et al., 2012). Despite the increasing rate of cancers in Africa, there is no enough public policy about the disease. Hence, additional research policy needs to be carried out in order to decrease the rate of cancers in the continent (Akinde*et al*., 2015). According to WHO, over 71,000 people died from cancer related causes in Nigeria, with about 102,000 new cases reported in 2012 (Ferlay*et al*., 2012).

It was reported that in developed countries like the United States of America and other western countries, incidence and mortality rates of most cancers are decreasing, but in developing countries like Nigeria the situation is on the contrary (Jemal *et al*., 2012). For instance, in Kano State of Nigeria, the pattern of cancer recorded in its cancer registry for a period of ten years(1995-2004) showed a progressive increase in number of cancer cases which was in agreement with the predicted increase in cancer cases by the World Health Organization (WHO, 2005)**.** In 2008, there were 12.7 million new cases and 7.6 million cancer-related deaths worldwide (Ferlay*et al*., 2010). Fifty six percent of these newly reported cancer cases occurred in developing countries and it is projected that by 2030, 70% of all new cases of cancer will be found in developing countries (Boyle *et al*., 2008).

Nigeria, between 2006 and 2012, recorded 102,079 cases of cancer, out of which 27,255 (26.7%) cases were for breast, 14,087 (13.8%) for cervix uteri, 12,045 (11.8%) for liver and 11,944 (11.7%) for prostate (Globocan, 2012). The age standardized incidence rates (ASR) for these common cancers; breast, cervix uteri, liver and prostate were 50.4, 29.0, 11.5, and 30.7 per 100,000 respectively with a 5-year prevalence study in Nigeria also showing almost the same trend. The mortality showed that breast cancer caused 13,960 (19.5%) deaths, cervix uteri 8,240 (11.5%) deaths, liver 11,663 (16.3%) deaths and prostate 9628 (13.5%) deaths in Nigeria (Globocan, 2012).

Breast cancer (BC) is a global disease of significant burden and its incidence continues to rise especially in the sub-Saharan Africa (Akpo*et al*., 2010).Therefore, the cause of this significant rise particularly in its mortality rate needs to be investigated.Breast cancer was described as the most common cancer in women worldwide and accounted for 24.45% of all the cancer types. Huge differences have been observed in the behavior of the tumor, clinical manifestation, treatment response and prognosis across the various regions of the world especially between the developed and the developing world (ACS, 2009). Incidence data

from two population based cancer registries in Nigeria suggested substantial increase in mortality rates of breast cancer patients in recent times. Hence, the need to investigate the cause of high mortality rate of breat cancer which could be as a result of errors in clinical procedures. Recent observations also showed that the frequency of breast cancer had risen over that of cervical cancer in Nigeria. In 2012, WHO also estimated 27,304 cases with age standardized incidence rates of 50.4 per 100,000 and 13,960 deaths with ASR of 25.9 per 100,000. In 2008 there was a suggestion on public enlightenment, where screening of all women at risk, early detection of the lesion, and proper management in our health institution as the ways to slow down the progressive increase in breast cancer cases and deaths in our environment, Nigeria (Ngadda*et al*., 2008).

In this study, set up errors for breast cancer patients was quantified and analyzed in order to contribute to decreasing the mortality rate for breast cancer patients in Nigeria.

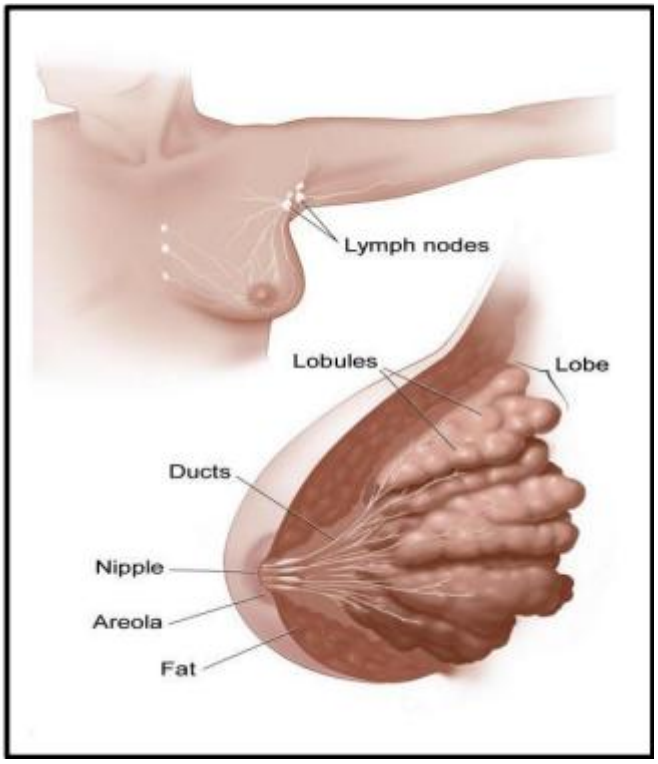

Figure 1.1 Anatomy of the female breast Source: National Cancer Institute, 2009. (AIHW, 2009).

1.2 Statement of Research Problem

Set-up errors are an inherent part of the radiation treatment process. They are defined as the difference between the actual and intended position with respect to radiation delivery. Coverage of target volume is a direct function of set-up margins, which should be optimized to prevent inadvertent irradiation of adjacent normal tissues. Planning target volume (PTV) that encompasses the clinical target volume (CTV) with some margins to account for such uncertainties in patient positioning, organ motion, and beam geometry is universally accepted today as the benchmark for radiotherapy (RT) dose prescription (ICRU 1994,2000). The use of portal imaging to measure set-up errors is an acceptable standard practice (Herman, 2005). The widespread availability of electronic portal imaging devices (EPID), coupled with a demand to reduce PTV margins, particularly for high-precision radiotherapy has provided impetus for such assessments across the radiation oncology community (Herman, 2005). The experience, training, commitment and time available with radiation therapy staff can have a major impact on daily positioning accuracy.

Set-up uncertainties in patient positioning can produce under treatment of some part of the tumor, increasing the possibility of local tumor recurrence, while some non-target tissues may be over-irradiated. Geometric uncertainties are important in three dimensional conformal radiotherapy (3D-CRT) planning as well as with conventional treatments and it is worthwhile to quantify, and if possible to reduce, patient set-up errors during treatment. Different immobilization and reliable alignment systems have been used to reduce the patient setup error (Williner and Gilbeau, 2015). However, patient positioning is based on the outer surface of the body and therefore effects of patient dependent factors, such as weight loss and cooperation in most cases, are not taken into account.

Additionally, it is generally recommended worldwide that every radiotherapy institution generate data on its set-up accuracy without blindly adopting published margin recipes due to

the fact that the efficacy of the radiotherapy treatment depends on patient's set-up at each fraction, especially when the breast region is treated, and where safety margins are narrow due to the close proximity of organs at risk, such as the lungs and heart. However, in developing countries, Nigeria in particular, there is a paucity of data on the analysis of set up errors for cancer patients (breast cancer). This is pertinent on the background that globally, set up errors in the treatment of breast cancer now constitute a distinct field of study and practice. Radiotherapy treatment facilities are just beginning here in Nigeria so there is the need for comparison with the results of standard settings. It is in this context that this study is planned at a newly commissioned radiotherapy unit of National Hospital Abuja (NHA) in order to necessitate more contributions through clinical research in Cancer Oncology.

1.3 Aim and Objectives

The aim of this study is to quantify and analyze set-up errors in breast cancer patients undergoing external beam radiotherapy **(**E.B.R.T**)** at National Hospital radiotherapy centre.

The objectives of this study are to;

1. determine set-up errors for breast cancer patients using electronic portal imaging device (EPID).
2. evaluate the magnitude of these set up errors with respect to standard margins with a view to minimizingthem.
3. determine the impact of unwanted radiation dose to organs at risk, target coverage and treatment compliance in breast cancer patients treated with 3-D Conformal Radiotherapy Technique (3D-CRT).
4. calculate the biological and dosimetric impact of patients set up errors in terms of generalized Equivalent Uniform Dose (gEUD), Tumor Control Probability (TCP) and Normal Tissue Complication Probability (NTCP).

5. evaluate the differences between NTCP and TCP models for treatment prediction of breast cancer using radiobiological models.
6. determine tumor control and normal tissue toxicity using NTCP and TCP radiobiological models.

1.4 Justification of the study

With the recent advancements in technology, there is a great optimism and expectation of the precise diagnostic approach and the efficient treatment mechanism amongst breast cancer patients. The advanced diagnostic and treatment imaging modalities such as computed tomography (CT) scan, positron emission tomography (PET) scan, magnetic resonance imaging (MRI), mammography, ultrasound and linear accelerators are the primary basis of the efficient diagnosis and treatment of the various types of cancers. However, various types of mechanical factors such as set up errors, delineation errors, positioning errors amongst others have limited its implications in the accurate diagnosis of the disease. Such drawbacks in the diagnostic imaging and treatment need to be addressed properly to achieve the good prognosis in the advanced treatment procedures of various types of cancers especially breast cancers. As a result of these errors, cancer therapies have experienced tremendous setbacks in the past 30 years due to the associated toxic response, resulting in a significant number of treatment-induced deaths rather than disease-induced fatalities (Mohammed*et al*., 2018).In this pretext, the majority of this work will be formed around the understanding of the volume delineation of the tumor targets, the radiotherapy treatment planning and assessments, predicting the outcomes of treatment using radiobiological models such as NTCP and TCP models, prevention or reduction of set up errors in breast cancer treatments as well as achieving great tumor control.

1.5 Scope of the Study

This study focuses on the assessment of the treatment plans established in the case of breast cancer when set-up errors occur and then assess and quantify the impact of these set up errors on the calculation of generalized Equivalent Uniform Dose (gEUD), Tumor control Probability (TCP) and Normal Tissue Complication Probability (NTCP). Firstly, this study made use of the concept of Equivalent Uniform Dose (EUD) and the predictive models TCP and NTCP. The assessment took into account the cases when patient setup errors occur. The choice of the EUD approach provides better protection for Organs at Risk (OARs) and better dose distributions in the PTV. The TCP and NTCP demonstrates the unavoidable biological impact of patient set-up errors on tumors and OARs when they were not corrected, especially in the case of the lungs and heart. Data was obtained from the electronic portal imaging device, treatment planning system and the CT simulator and inputed in the systematic error, random error, NTCP and TCP equations to obtain the respective values.

1.6 Limitations of Study

As with most research work, there are limitations involved. Interpretation of the results should be done bearing in mind that amajor drawback of this study was the lack of automatic anatomy matching and image fusion facilities in iView GT elekta portal imaging device which could have resulted in reduction in the accuracy of measurements. Secondly, the introduction of a predictive model into clinical practice has to be prudent as it is necessary to assess if it is based on calculations and treatments similar to those for which the NTCP has to be calculated. There are large uncertainties in the biological models and its associated parameters. As more clinical data are collected, it may help in the formulation of models to predict radiobiological response and result in more accurate prediction of TCP and NTCP. This research is therefore, restricted by the few number of breast cancer patients participating in this study and lack of follow-up effort.

Similarly, the models used in this study do not account for variations in dose rate;3D-CRT treatment can be significantly shorter than techniques used in other studies and this may affect the tumor dose-response. Also due to the method of delivery, the dose rate can vary spatially across the tumor volume. Furthermore, the radiobiological parameters used in the models to characterize the dose response curves, the D_{50}, γ and α/β are subject to significant uncertainty. This limits the use of the simple models in calculating an absolute measure of tumor control probability and normal tissue complication probability; however, we suggest that they can be used as a valuable tool in comparing and evaluating different treatment techniques and protocols.

Finally, we did not control the breathing in this study, which is important because the main cause of radiation under-dosing in breast- cancer patients is the respiratory motion of the target.

CHAPTER TWO

LITERATURE REVIEW

2.1 Radiotherapy

Radiation therapy is a type of cancer treatment that uses beams of intense energy to kill cancer cells. Radiation therapy most often uses X-rays and photons, but protons or other types of energy also can be used. The term "radiation therapy" most often refers to external beam radiation therapy and includes unsealed source therapy (radioisotope or ‘molecular’ radiotherapy), sealed-source radiation therapy (brachytherapy), and external-beam radiotherapy (EBRT). Early EBRT, also known as Röntgen therapy, involved directing kilovoltage X-rays towards a tumor to damage malignant tissue with poor or no control over the size and field of exposure. Despite this lack of geometrical precision (relative to current practice), there was sufficient reason to advocate the use of radiation to treat different types of cancer depending on the size and the extent of disease (Hirsch andHolzknecht, 1926; Pfahlery*et al*., 1931).A successful cancer treatment means successful killing of the cancer target whilst avoiding serious damage to normal tissue cells. However, considerable harm can be done to surrounding normal (non-cancerous) organs.

2.1.1 Developments in External Beam Radiotherapy (EBRT)

Early radiotherapy was performed by directing X-rays onto a rectangular area marked on the patient. The implications of this were quite severe as a high dose of radiation was imparted to the healthy parts of the patient's body and also to the radiographers, which was gradually realised as the late effects of radiation exposure came to light (Lambert, 2001; Stirling and Gee, 2002). The idea of dividing the total dose into smaller amounts (fractionation) was introduced in order to reduce normal-tissue complications for a given effect on the tumor (Chapman and Nahum, 2015; Lambert, 2001). 3-D treatment planning was later introduced with the development of three-dimensional conformal radiotherapy (3D-CRT). This not only involved deposition of radiation dose in the tumor by beams from various directions but also planning of the distribution of the dose to organs at risk (OARs) according to a 3-D representation of the patient anatomy generated using computed tomography (CT). However, imparting a radical dose to the tumor can result in high dose deposition in the surrounding normal tissues with the risk of severe side effects (complications). With the evolution of treatment delivery technologies, the therapeutic ratio has improved, i.e. lower toxicity levels for the same or improved tumor control.The concept of 3D-CRT entails conforming (or 'shaping') the radiation dose to the 3D tumor volume, thereby reducing the dose outside the tumor as much as possible. This is done using computer-controlled geometric field shaping. Despite the sophisticated manual and electronic equipment developed in this field, various errors still occur. In general, the error can be subdivided into systematic and random error. Further developments in radiotherapy delivery have involved the introduction of intensity-modulated radiotherapy (IMRT) from the early 90s and, in the last decade, Image-guided radiotherapy (IGRT) was introduced.

2.1.2 Conformal Radiotherapy

The concept of 3D-CRT has to do with shaping the radiation beam to the tumor volume in three dimension thereby maximizing the dose to the target and minimizing dose to surrounding tissue as much as possible. This is done using computer-controlled geometric field shaping as opposed to the rectangular-field radiotherapy employed earlier. The concept of 3D-CRT is easy to understand. The problem is that depth dose of a homogeneous photon field is described by an exponentially decreasing function of depth. Dose deposition is normally higher close to the surface than at the depth of the tumor. To improve this situation normally more than one beam is used. Within the overlapping region of the beams a higher dose is deposited. If the apertures of the beams are tailored (three dimensionally) to the shape of the planning target volume (PTV) masking the organs at risk (OAR), then the overlapping region should fit the PTV (Schlegel, 2006). In the case of an OAR close to the PTV, this is not true for such a simple beam configuration. In such cases one needs a more complex beam configuration to achieve an acceptable dose distribution; however, the general thesis is that, using enough beams, it should be possible to a certain extent to fit a homogeneous dose distribution to the PTV while sparing the OARs. The conformity of dose distributions can be increased using individually tailored beams compared with, for example, a beam arrangement using simple rectangular-shaped beams, and for the majority of cases this is true. Nevertheless, there are cases, especially with concave-shaped target volumes and moving targets, where conventional conformal treatment planning and delivery techniques fail. It is hoped that these problems will be solved using intensity-modulated and adaptive respectively (Schlegel, 2006).

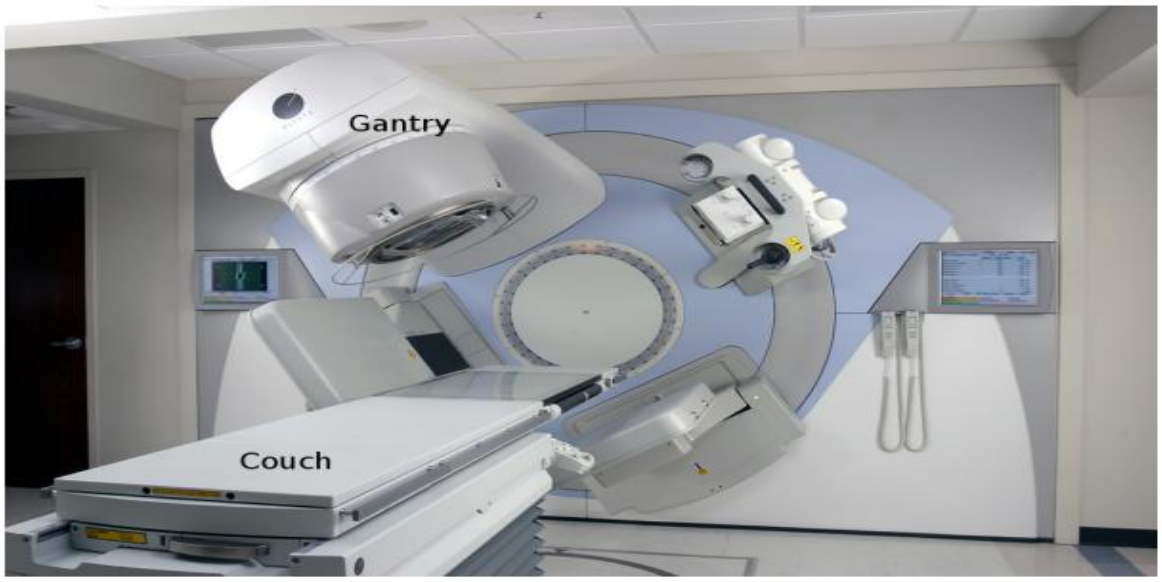

Figure 2.1: The front of a medical linear accelerator (LINAC) including the couch on which the patient is positioned. Image courtesy of Elekta (www.elekta.com, Stock-holm, Sweden).

3D-CRT is a treatment method that gives the planner control over many parameters that define the treatment from beam placement, Multileaf collimator (MLC) position, beam weighting, accessory use, etc. As such, it is a widely used method of treatment for many patients. It provides good coverage of the target site while sparing the normal tissue using the MLCs to shape the beam as needed. A sample 3D plan is shown in figure 2.

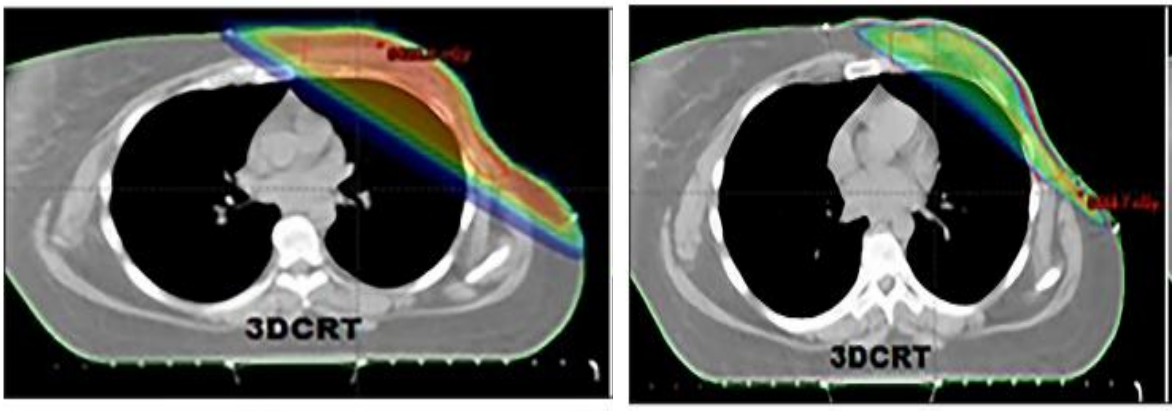

Figure 2.2: Sample 3D-CRT dose distribution patterns obtained for taken from patient selection(Aras *et al*., 2019. Dosimetric Comparison for Radiotherapy Techniques).

2.1.3 VMAT, IMRT and IGRT

Intensity Modulated Radiation Therapy (IMRT) uses modulation of beam intensity and beam shape (using multileaf collimator). This is undertaken either continuously (dynamic / sliding

window IMRT technique) or in step and shoot (static IMRT) mode delivered from different angles relative to the delivery target with the beam turned off between each delivery angle. The beam shape is constricted such that the OARs in the path of the beam (directed towards the target) are avoided as much as possible from a given delivery angle. IMRT enables development of concave and inhomogeneous dose distributions that selectively spare Organs-at-Risk (OARs) whilst depositing the required radiation dose in the tumor. Current IMRT planning systems use the beam's eye view technique to design irregularly shaped radiation-dose fields that conform to the target volume in 3D. These fields are then delivered by means of the multileaf-collimator (MLC) controlled beam shapes (Gerstner *et al*., 1999). IMRT represents an improvement in conforming high dose to the tumor volume by modulating the intensity of each beam in a plane perpendicular to the beam direction (Bhide and Nutting, 2010). There is credible evidence that IMRT is better at sparing organs at risk compared to the MLC-shaped beams of 3D conformal therapy. For head and neck tumors, IMRT has been beneficial in the sparing of optical nerves, digestive-tract mucosa, salivary glands, cochlea, brain and spinal cord (Chao *et al*., 2001; Feng *et al*., 2007; Nutting *et al*., 2011). Reduction of doses to the above organs has resulted in significant improvements in patients' quality of life post-radiotherapy. This improved normal organ sparing also presents clinicians with the opportunity to increase tumor dose, thereby increasing the chances of achieving local control. Improved local control and reduction in OAR toxicities have been reported for prostate cancer treatments via the use of IMRT and other advanced radiotherapy techniques. Prostate tumour treatment dose is limited due to genito-urinary and gastrointestinal toxicities. There is considerable evidence that the use of IMRT has resulted in acceptable bladder and rectal toxicities even for hypofractionated escalated doses (Kupelian*et al*., 2005; Kupelian*et al*., 2002; Zelefsky*et al*., 2001, Dearnaley*et al*., 2016; Livsey*et al*., 2003; Wolff *et al*., 2015). A disadvantage of IMRT is increased delivery time which can result in patient discomfort,

lower overall patient throughput and most importantly an increase in the possibility of patient movement. Further, compared to conventional conformal radiotherapy, IMRT plans require more monitor units (MUs) which results in increased radiation dose to the whole patient body. The solution to the above disadvantages is the arc-based (rotational) therapies that deliver radiation through continuous rotation of the gantry allowing treatment over the full 360° arc around the patient (Teoh *et al*., 2011). The two primary forms of arc therapies are volumetric arc therapy and Tomotherapy. Tomotherapy is a hybrid of a linear accelerator (LINAC) and a CT scanner, delivering radiation from a continuously moving narrow slit while the patient is translated along an axis perpendicular to the slit direction. Tomotherapy can be delivered axially, serial (slice by slice) or helically (as a continuous spiral). VMAT, on the other hand, is delivered by varying three parameters related to the delivery system which are beam dose rate, gantry rotation speed and beam shape (via movement of MLC leaves). Conventional linear accelerators can be configured to have VMAT capabilities which is a distinct advantage compared to Tomotherapy as investment in a new piece of equipment is not required. Compared to standard fixed-field IMRT, arc therapies are delivered faster which is very useful clinically. The most recognized arc therapy systems are Elekta VMAT (Elekta), RapicArc (Varian) and SmartArc (Philips) as shown in figure 2.1.

Image Guided Radiotherapy (IGRT) is characterisedas “Increasing the accuracy by repeated imaging of target and/or healthy tissues before the therapeutic action and matching the image with the therapy” (Van Herk, 2007). The purpose of IGRT is to use advanced imaging methods to aid better delineation of tumor’s and OARs resulting in a potential reduction in margins and uncertainties in treatment planning. This results in more precise target dose deposition and improved sparing of OARs. During a course of radiotherapy, 3D imaging in the form of cone-beam CT is repeated multiple times to assess changes in tumors location, size and shape. Pre-treatment-fraction observation of these changes allows the treatment

delivery to be modified to improve delivery of dose to the target and reduce the dose to the OARs. One other important use of IGRT is to accommodate organ motion (through pre-treatment 4D CT) especially in the case of lung, liver and prostate glands. IGRT also uses PET, SPECT and MRI marker based imaging techniques to guide precise target delineation (Arabloo*et al*., 2016). Today, it is well established that technological improvements in radiotherapy beam delivery, tumor and OAR delineation have delivered significant reductions in organ dose. However, the potential to individualize increase in tumor dose remains largely unexploited. Limiting the side effects of radiotherapy is essential but maximizing tumor control probability is of paramount importance as that is the primary objective of radiotherapy treatment.

2.2 Photon Production with Medical Linear Accelerators

A medical LINAC produces X-ray photons by accelerating electrons which then strike a target. The electrons are accelerated in a high frequency electromagnetic field. A typical medical LINAC uses a magnetron or klystron to generate microwaves in a waveguide accelerator. An electron gun then inserts low energy electrons into the waveguide which are accelerated to very high velocities near the speed of light. When the high energy electrons leave the waveguide, they are usually bent into the final direction of the beam by a bending magnet and eventually hit a small target thereby producing bremsstrahlung X-rays. The X-rays then travel through the treatment head and eventually strike the patient (Figure 2.3a).

2.2.1 Electron Source

The electron gun is the LINAC's source of low speed electrons. It consists of a tungsten cathode and an anode in a vacuum tube. The cathode is heated to high temperatures (T > 1000◦C) in order to produce free electrons via thermionic emission. These free electrons are then accelerated by the electric field between the cathode and the anode. Typical electron

guns operate at 30-100 kV. At the anode, the electrons are inserted into the acceleration waveguide of the LINAC.

2.2.2 Microwave Production

The microwaves in linear accelerators are produced by either a klystron or a magnetron. Klystrons do not generate microwaves but rather amplify an existing microwave. They consist of an electron gun that generates an electron beam which then passes through a buncher and a catcher cavity that both resonate at the frequency of the low power microwave to be amplified. The low power microwave is fed into the buncher cavity, where it generates an oscillating electric field in the path of the electron beam. Electrons that pass through the cavity become velocity modulated. That is, electrons that pass the cavity while the electric field points in the same direction as the electron flow will be decelerated, whereas electrons passing through the cavity when the electric field points in the opposite direction will be accelerated. The electrons then enter a drifting space in between the buncher cavity and the catcher cavity, where they form bunches due to the acceleration and deceleration they experienced in the buncher cavity. The distance between the cavities is designed such that the electrons pass through the second cavity when they are maximally bunched. At the catcher cavity, they induce a retarding electric field that decelerates the electron bunches, thereby producing high power microwave oscillations in the cavity. These microwaves are of the same frequency as the initial low power microwaves. In contrast to klystrons, magnetrons produce microwaves rather than amplifying existing microwaves. A magnetron consists of a cylindrical copper anode with several holes (cavities) and a heated cathode at the center of the cylinder. The cathode emits electrons via thermionic emission and a direct current (DC) electric field between the cathode and the anode combined with an external static magnetic field perpendicular to the magnetron cross section causes them to travel towards the anode in

a circular path. The magnetron is tuned such that the electrons do not initially reach the anode but pass it closely in a circular motion and then move back towards the cathode. The holes in the anode are connected to the evacuated space in between the anode and the cathode via small slits that act as capacitors, while the cavities themselves form one loop induction coils. Thus the sections of the anode can act as parallel resonant circuits which resonate at microwave frequencies. When the spiralling electrons pass the cavity slits in the anode, they induce an alternating current (AC) electric field across the anode slits by transferring some of the energy of the DC field. This AC field in turn velocity modulates the electrons and bunches them based on the same principles as the klystron leading to a stronger AC field which generates microwaves in the anode cavities. In medical LINACs, magnetrons create pulsed microwaves of about 3000 MHz.

2.2.3 Acceleration and Bending Magnet

The microwaves produced by the klystron or magnetron are eventually fed into the accelerating waveguide of the medical LINAC where they are used to accelerate the electrons inserted by the electron guns. The waveguide consists of several copper cavities in which the electrons are bunched and reach near speed of light velocity. Some current LINACs have travelling waveguides, where the microwaves enter on one side and leave on the other. A more efficient approach is standing waveguides where the microwaves are reflected at the end and create a standing wave. More details on the principles of waveguides in LINACs can be found for example in (Khan, 2010; Krieger, 2012). After the electron beam leaves the waveguide it needs to be bent towards the patient (Figure 2.3a). This is accomplished by using a bending magnet. However, electrons of different energies follow different paths through the field of a bending magnet and thus the electron beam will diverge after deflection by a single 90° bending magnet. Therefore, either three 90° bending magnets bending the

beam by 270°, or two 44° magnets in combination with one 112° magnet that bend the beam along a snake like curve are typically used in LINACs to allow refocusing the electron beam.

2.2.4 Treatment Head

The treatment head consists of several components that shape and monitor the beam, such as the X-ray target, a flattening filter, ion chambers and collimators (Figure 2.3b). The target is made of tungsten and emits bremsstrahlung and characteristic X-rays when the high energy electrons collide with it. Bremsstrahlung is generated when the incoming electrons are deflected by fields of the target nuclei and experience deceleration. The consequent loss of kinetic energy is compensated by the production of photons. The angular distribution of photons depends on the energy of the electrons striking the target. At higher photon energies of at least a few hundred kV, the majority of photons are emitted in the forward direction while at lower energies (e.g. 100 kV) photons are emitted more laterally. Bremsstrahlung has a continuous spectrum with energies up to the initial kinetic electron energy since the electrons may lose all or part of their energy in the process. Just below the target is a fixed primary collimator that prevents leakage followed by a flattening filter. The flattening filter is used to obtain a uniform beam profile. However, the filter, usually composed of steel, copper or tungsten, leads to significant attenuation. Since in recent radiotherapy the beam fluence is often modulated, flattening filters may be omitted in favor of a higher dose rate. The flattening filter also leads to changes in the (angular) energy spectrum of the beam, because the mass attenuation coefficient depends on the energy of the photons. Lower energy photons are attenuated more easily than higher energy photons, which leads to an increase in the average energy of the photon beam. This effect is called ’beam hardening’. Beam hardening also occurs when the photon beam interacts with the patient’s tissues. Below the flattening filter are ion chambers that monitor dose rate, beam symmetry and beam homogeneity.

Below are four or two movable lead or tungsten jaws that can create a rectangular opening. In addition to the jaws, modern LINACs have multi leaf collimators (MLCs) in order to create irregular field shapes. The treatment head can be rotated along the central beam axis. Finally, the treatment head is surrounded by thick shielding that prevents X-rays from leaking.

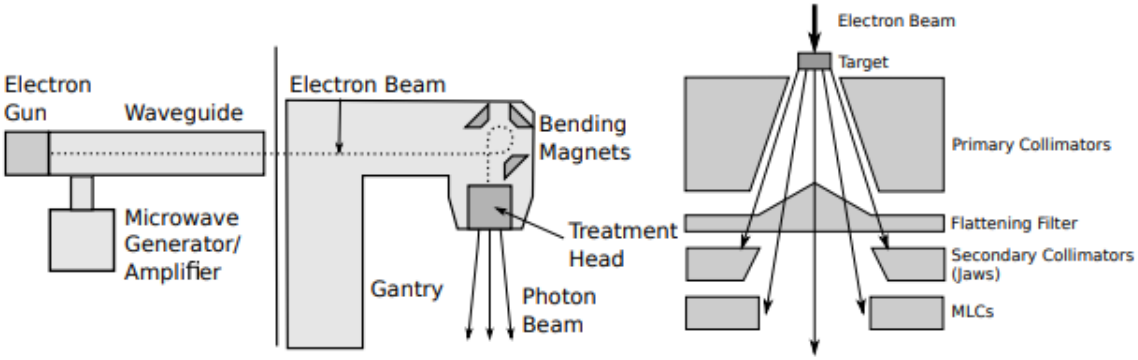

(a) LINAC body.

(b) Treatment head of a medical LINAC.

Figure 2.3: Simplified schematic view of a medical linear accelerator (LINAC).

2.3 Important Radiotherapy Concepts

Some important concepts of radiation therapy explicitly used throughout this thesis are now introduced.

2.3.1 Patient positioning (set-up) errors

In external beam radiotherapy, patients are positioned for about 30 fractions of treatment based on initial measurements done at treatment planning. Set-up errors which are a combination of systematic and random errors occurs during simulation and treatment and may be calculated individually for each patient and each direction (x, y and z) and according to the number of portal images (PIs). A patient set-up error is defined as the difference between the real and the intended positions. These set up errors are usually measured using landmarks clearly visible on the Electronic Portal Imaging Device (EPID).

2.3.2 Radiotherapy treatment planning

This thesis involves analyzing radiotherapy treatment data for cohorts of patients treated using the 3D-confortmal radiotherapy (3D-CRT). To ensure radiation treatment planning is consistent across centers, the International Commission on Radiological Units and Measurements (ICRU), established in 1925, coined the terms planning target volume (PTV), gross tumorvolume (GTV) and clinical target volume in report 50 (ICRU, 1993a), report 62 (ICRU 1999) and report 83 (ICRU, 2010). The upper and lower dose limits to the above volumes relative to the prescribed dose are also defined. GTV refers to the tumor that can be seen, palpated or imaged. GTV delineation aims to identify the demonstrable extent of the tumor and its location (Figure 2.4). The GTV should also include any involved lymph nodes or noticeable spread into adjacent tissues. Surrounding the GTV is the CTV which is GTV plus a margin that will cover the microscopic spread of disease. The addition of a margin to the GTV to create the CTV is a matter of clinical assessment through biopsy or judgement based on experience which should take into account microscopic infiltrations of disease outside the GTV (Burnet, 2004). The local infiltration of a given tumor delineated by CTV is very variable. Some of the anatomical structures like bone cortex, muscular fascia and ligaments act as barriers and limit microscopic tumor infiltration. CTV delineation ideally accounts for such clinical information. However, the CTV covers the volume suspected of harboringclonogenictumor cells and thus should be treated with the prescribed dose as survival of even a single clonogenic cell can result in tumor relapse (i.e. treatment failure). and external variations such as beam and patient positioning errors. The PTV encompasses the CTV in order that the prescribed dose is delivered to the whole of the CTV ensuring there is no under dosage to any part of the CTV.

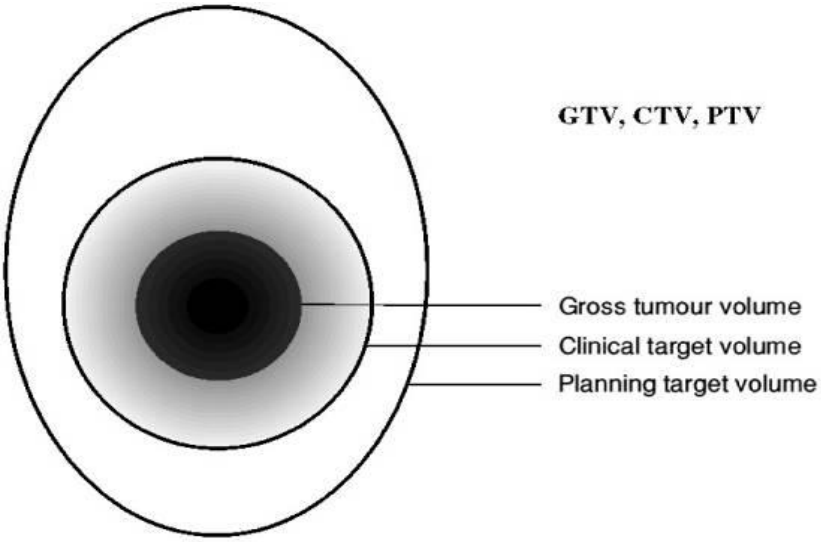

Fig 2.4; Diagram to illustrate the main radiotherapy planninning volumes, taken from ICRU Report 50.

2.3.3 Organs at Risks

The organs that surround a tumors or are in close proximity to the tumors, thereby receiving a high dose of radiation are known as Organs at Risk (OAR) (ICRU, 1999). This current investigation analyzes breast radiotherapy treatment data. As far as clinical complications are concerned, this tumor site have OARs whose physiological function can be compromised as part of radiotherapy related side effects. In the case of breast tumors, the OARs are healthy lung (ipsilateral and contralateral), heart, oesophagus,thyroid, brachial plexus and spinal cord(Ateane*t al*., 2012). The radiotherapy related side effects to different OARs are usually reported using the radiation oncology group foundation's reporting schema (RTOG, 2015) or the Common Terminology Criteria for Adverse Events schema [CTCAE v5.0] (National Institute of Health, 2010). These scoring systems allow quantification of the severity of an adverse event by means of a grade. The grade of an adverse event refers to a defined level of severity of the adverse event in relation to a patient's health. RTOG has defined toxicity grades from 1 to 5 for 15 tissues. Such scoring methods benefit clinicians as it allows

justification for allocation and prioritization of resources required to manage a given patient's condition based on the severity of the event.

2.3.4 Dose Fractionation

Radiation therapy is usually divided or "fractionated" over a treatment course lasting multiple weeks. Fractionation in the context of radiotherapy is the process of dividing a dose of radiation into multiple "fractions". This practice seeks to maximize the destruction of malignant cells while minimizing damage to healthy tissues. Several of the mechanisms which represent the rationale behind fractionation include redistribution, re-oxygenation and repair. In the 1920s, as of today, fractionation can be divided into the following categories: Hypofractionation, Conventional fractionation, Hyper-fractionation, Accelerated fractionation and Protracted fractionation. The definitions of these fractionation types are taken from Dale and Jones (2007). Conventional fractionation refers to 1.8 - 2 Gy per day each weekday. Hypofractionation schedules are of fraction size greater than 2 Gy/fraction, and hyperfractionation refers to fractions less than 2 Gy (1-1.2 Gy per fraction - The Royal College of Radiologists, 2016). Accelerated fractionation means imparting more than 10 Gy per week total dose, and protracted fractionation refers to total doses of less than 10 Gy per week as per Dale and Jones (2007). The point being made here is that fractionation regimens are a compromise between many fractions or too few fractions to balance the sparing of normal tissues versus minimizing tumor repopulation. One may justifiably ask why one should prefer empirically derived fractionation schedules when radiobiological modelling based analysis can yield a more rationalized patient-specific fractionation schedule. Also, it is important to remember that fraction size is not the only parameter to optimize; dose-rate within a fraction, total dose, tumor volume and overall treatment time have a complex inter-relationship that govern the success of treatment for a given patient.

2.3.5 Depth Dose Distribution

The important quantity absorbed dose is defined as the expectation value of the energy imparted by ionizing radiation to matter per unit mass at a point of interest (ICRU, 1980). It is expressed in units of Gray (Gy) where 1 Gy = 1 J/kg. High energetic photons used in radiation therapy such as X-rays dose energy to the traversed material mainly by three processes: 1) photoelectric effect, in which the photon interacts with a bound inner shell electron in an atom of the traversed material and transfers its total energy to the electron which is emitted; 2) Compton scattering,inwhichthephotoninteractswithanouterorbitalelectronandtransfers part of its energy to the emitting electron, after which the photon is scattered with reduced energy; and 3) pair production, in which the photon energy is converted to the mass and kinetic energy of an electron-positron pair. The likelihood of each of these processes depends on the energy of the photon and the atomic number of the target atom. The emitted electrons in the different processes lose energy in turn by further ionization and excitation events. A typical photon depth dose curve, the dose distribution on the central axis, in a patient shows a low surface dose giving a so-called skin sparing effect. The dose is" built-up" by secondary electrons and increases with depth to a maximum, at a depth (a few millimeters to a few centimeters) depending mainly on the beam energy, and then decreases almost exponentially until the beam exit point (Figure 2.5). Except for very superficial tumors, it is not opportune to treat with a single photon beam. The proximal dose in the normal tissue would be higher than the dosedeliveredtothe tumor, and thedosebeyondthetumorwouldalsobetoohigh. Instead multiple beams from several directions are combined. High-energetic ions, on the other hand, interact with tissue mainly through Coulomb interactions with the atomic electrons of the material. The energy loss per unit path length of a particle, referred to as the stopping power, depends on the electron density of the traversed medium, the atomic number of the ion, the velocity of

the ion, and the effective charge of the ion. Since the rate of energy transferisinverselyproportionaltothesquareof thevelocityoftheion, theenergy deposition is small at high velocities. As a consequence, the deposited dose is low at small depths where the ions have their highest energy (Wedenber*et al*., 2013). As the ions slow down, the dose increases with depth and forms a sharp maximum at the end of the range, the Bragg peak. For protons, the fall-off in energy depositions beyond the Bragg peak is sharp. With increasing atomic number of the ion, nuclear fragmentation increases causing energy depositions beyond the Bragg peak forming a so called fragmentation tail. Thus, for carbon ions some dose is deposited beyond the peak. The height of the Bragg peak depends on the mass of the ions, and the range of an ion, and thus the location of the Bragg peak, is determined by the initial energy. At the depth of the Bragg peak there is a spread of energies due to fluctuations between ions in the number of collisions and transferred energies. This is known as range straggling or energy-loss straggling. In summary, a low dose is obtained at the entrance, the dose peaks at the end of the track, and very little dose is deposited behind the peak. This feature of ions is utilized in radiation therapy to obtain a more focused dose to deep-seated tumors than would be possible with photons, while lowering the dose to the normal tissue. The width of a Bragg peak is too small to cover an entire tumor. By super positioningseveralBraggpeaksofdifferentenergiessocalledspread-outBraggpeak is obtained, shown in Figure 2.5

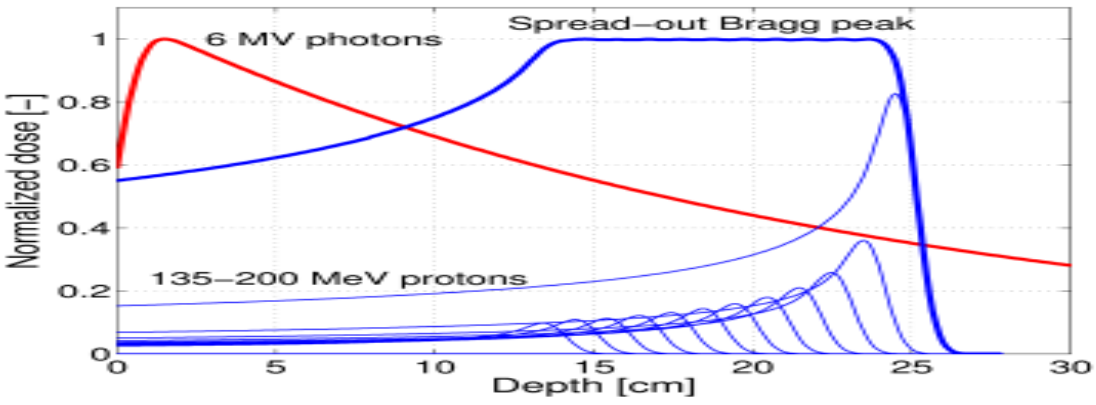

Figure 2.5: Depth dose profiles for broad beams of 6MV photons and 135-200 MeV protons. By super positioning several Bragg peaks of different energies, a spread out Bragg peak is produced. (Courtesy of Albin Fredriksson.)

2.3.6 Dose-Volume Histograms

A dose-volume histogram (DVH) is a histogram that relates radiation dose to the irradiated tissue volume in a given radiotherapy treatment plan. A DVH can be differential or cumulative in type. A histogram of the absolute (or percentage) dose received by a given structure versus the absolute (or percentage) volume of the structure receiving dose in a dose bin is called a differential DVH. The histogram can also be cumulative which for a given dose (interval) can show the total volume receiving that given dose or greater. A set of DVHs can be used for preliminary plan analysis and/or to rank different plans. The DVHsare also used as inputs to radiobiological models to calculate tumor control probability (TCP) and normal tissue complication probability (NTCP). TCP and NTCP models together with DVHs are a means to assess treatment plans quantitatively. The standard DVH is still commonly employed for plan scoring and dose reporting possibly due to its simplicity. The definition of various dose-volume metrics for tumor and normal tissue that can be derived using a DVH are given below. Dmean, Dmax, Dmin, Dref, and Vrefare some of the metrics often reported.

Minimum Dose (Dmin): The minimum dose received by a specific percentage (mostly it would be 95% or 99%) volume of a given structure. This is a useful metric in terms of target dose as minimum dose could be used to set a definite curative dose for a given tumor PTV.

Maximum Dose (Dmax): The maximum dose received by a specific percentage volume (mostly it would be 1% organ/tissue volume) of a given structure. This metric is used to limit dose to critical organs that have a serial architecture

Dref: It is the volume of the structure receiving greater than or equal to the ‘reference’ dose.

Vref: This is defined as the minimum dose received by a ‘reference’ percentage volume of a given structure (Kharia, 2018).

Dmean: This is defined as the mean dose received by the Planning Target Volume (Tome, 2002).

2.3.7 DNA Damage

The DNA (Deoxyribo-Nucleic Acid) in the cell nucleus is considered to be the most important target for radiobiological effects. DNA has a double helix structure with two polynucleotide strands held together by hydrogen bonds between the bases of the nucleotides. The double-ringed nucleobases adenine (A) and guanine (G) pair with the single-ringed thymine (T) and cytosine (C) respectively. The double helix interacts with small protein complexes called histones and arranged in a compact structure called chromatin. The structure of chromatin depends on the stage of the cell cycle: during replication and transcription the chromatin is loosely structured whereas during cell division it is tightly packed (Jackson, 2002).

Radiation may cause damage to the DNA, e.g. in the form of breaks on the strands, either directly by ionizing the DNA or indirectly by forming free radicals that damage the DNA. However, DNA damage is not always lethal to the cell. Single strand breaks rarely cause cell death in normal cells since they are easily repaired by the repair system of the cell using the opposite strand as a template. Double strand breaks, breaks close to each other on both of the strands, are more difficult to repair. Cells have two main processes to repair these latter lesions: homologous recombination and non-homologous end joining (Jackson, 2002). In homologous recombination, the sister chromatid or the homologous chromosome is used as a template and the information is copied. In non-homologous end joining the broken strands are simply rejoined and this process is therefore more error-prone. An even more severe damage

is multiple strand breaks close to each other, sometimes called clustered DNA damage. In the repair process, DNA breaks may fail to rejoin correctly and form chromosome aberrations.Seriouschromosomechangeshindercorrectcelldivisionand lead to mitotic death.

High-LET radiation is believed to cause damage that is more difficult to repair compared to low-LET radiation due to the dense ionization pattern which causes multiplestrandbreakscloseinspacetoahigherdegree(Goodhead,1994; Karlsson and Stenerlöw, 2004). Consequently, the ability of high-LET radiation to cause non-repairable DNA damage is less dependent on alterations such as mutations affecting the cell's repair capacity, cell cycle phase, and environmental conditions such as oxygen pressure.

2.3.8 Organ and Tumor Response to Radiation

Clinical radiation biology often focuses on the relationship between the absorbed dose and resulting response, and on factors influencing this relation. The response is often described as a probability of a specific outcome for the normal tissue or the tumor, typically showing a sigmoid dose-response curve. Tissues can be classified as serial or parallel, or somewhere in between, based on how their functional subunits are organized. Serial tissues, such as the spinal cord and brain stem, may lose their function even if only a small proportion is severely damaged. Parallel tissues, such as lung and liver, can function even when substantial parts are damaged. Tumors are always assumed to have a parallel function since all clonogenic cells need to be eradicated in order to achieve tumor control. Theresponseofnormaltissuescanalsobedividedintoearlyandlateoccurring damage, reflecting the time of occurrence of side effects. Rapidly dividing tissues such as skin, bone-marrow, and intestinal epithelium respond early to radiation (Wedenber*et al.*, 2013).

There are many publications that analyze various radiobiological effects of normal tissues and determines guidelines and dose limitations for organs depending on treatment modalities.

One example of this type of publication is Quantitative Analysis of Normal Tissue Effects in the Clinic (QUANTEC) published in 2010. According to QUANTEC for the lung, 20% of the volume should be <=30% of the total dose with <20% toxicity presented as symptomatic pneumonitis. The mean dose cannot exceed 27 Gy as toxicity becomes 40% for symptomatic pneumonitis. According to QUANTEC for the heart, 25% of the volume can receive <10% of the total dose for <1% toxicity rate presented as long-term cardiac mortality. The pericardium has a mean dose limit of <26Gy for <15% toxicity as pericarditis and 30% of the volume can receive <46% of the total dose for the same toxicity (Mark *et al*., 2010). The dose constraints for the chest wall and ribs are equivalent, the Dmax cannot exceed 125% of the prescribed dose. For the skin, Dmax cannot exceed 145% of the prescribed dose.

2.4 Radiobiological Models

Mathematical radiobiological models are used for a variety of purposes: to describe the relation between physical quantities of radiation and biological response, to interpolate between known outcomes and to extrapolate beyond what has been studied, to suggest hypotheses to be tested experimentally, to estimate the possible gain of a new treatment strategy, to compare treatment plans, to assist in combining treatment modalities, to re-plan after a non-scheduled treatment interruption, to compensate for earlier delivered over- or under dosage, generally to assist in decision-making, and more. It is not possible to experimentally test all combinations of irradiation conditions of interest. With mathematical models, what-if analyses are easily made to explore the impact of changes in the input assumptions. Radiobiological models are also used to convert the absorbed dose to clinically more relevant quantities such as biologically equivalent dose, tumor control probability and normal tissue complication probability. In ion radiation therapy, radiobiological models are used to estimate the relative biological effectiveness (Wedenber*et al*., 2013).

2.4.1 Equivalent Uniform Dose

EUD was proposed by Niemierko in 1997 and is defined as the uniform dose that, if delivered over the same number of fractions as the non-uniform dose distribution of interest, yields the same radiobiological effect (Niermierko., 1997). In 1999 Niemierko extended the notion of EUD to normal tissues with the generalized EUD (Niermierko., 1999).

$$gEUD = \left(\sum_i V_i D_i^{\alpha} \right)^{\frac{1}{\alpha}} \quad 2.3$$

Where V_i is the fractional organ volume receiving the dose D_i and a is a parameter describing the volume effect which is tissue specific.

2.4.2 Biological Effective Dose

The linear quadratic (LQ) model was first proposed by Chadwick et al. (1973), but it was the article by Fowler (1989) incorporating the overall treatment time factor in the LQ-equation and introducing the concept of BED (biologically effective dose), that was responsible for the renaissance in the use of mathematical models in the radiobiology of radiotherapy. Fowler (1989) coined $\frac{E}{\alpha}$ as the biologically effective dose (BED), which is radiation damage expressed as a function of total dose imparted. Thus, the total damage inflicted by a given prescription dose D in *n* fractions of size d is given by

$$\text{Relative Effectiveness (RE)} = \left\{ 1 + \frac{\beta}{\alpha} d \right\} \quad 2.4$$

where $BED = D \times RE$

α *and* β ratio determines the fractional sensitivity to irradiation of a particular cell type.

Assuming now that there is a new fractionation regimen which yields the same biological damage, this new regimen will have the same BED as the reference regimen.

2.4.3 Linear Quadratic Cell Survival Model

The fraction of surviving cells as a function of dose is usually not an entirely exponential process as assumed by the linear cell survival model, but exhibits a curvature. The linear-quadratic (LQ) model (Lea and Catcheside, 1942; Sinclair, 1966; Kellerer and Rossi, 1978; Chadwick and Leenhouts, 1973; Barendsen, 1982) can handle this type of response. This is a well-established and widely used model. For a single dose (one dose fraction) the model is expressed as:

$$S_{LQ}(d) = e^{-\alpha d - \beta d^2} \qquad 2.5$$

where α and β are the parameters of the model. α is associated with the initial slope and β with the curvature. The α/β ratio describes the fractionation sensitivity of a tissue and the inherent sensitivity of a cell type. As a general rule of thumb, late-responding tissuese.g spinal cord, lung and kidney have low α/β values (around3Gy) while early-responding normal tissue and most tumors have a larger α/β value (around 10 Gy). There are exceptions such as prostate tumors with biological properties more like those of slowly proliferating late-responding tissues (Brenner and Hall,1999) and exhibit a low α/β ratio around 1.5 Gy (Dasu and Toma-Dasu, 2012; Fowler *et al*., 2013). A small α/β value indicates that large fractional doses are not well tolerated. The total survival fraction after n dose fractions is obtained as;

$$S_{LQ} = \prod_{k=1}^{n} S_{LQ}(d_k) = \prod_{k-1}^{n} e^{\alpha d_k - \beta {d_k}^2} = \exp\left(\sum_{k-1}^{n}\left(-\alpha d_k - \beta {d_k}^2\right)\right)$$

$$= \exp\left(\sum_{k-1}^{n} -\alpha d_k \left(1 + \frac{d_k}{\alpha/\beta}\right)\right) \qquad 2.6$$

d_k is the dose of the kth fraction. When the fractional doses are equal this expression simplifies to

$$S_{LQ}(D) = \left(S_{LQ}(d)\right)^n = e^{-\alpha nd - \beta nd^2} = e^{-\alpha d\left(1+\frac{d}{\alpha/\beta}\right)} \quad 2.7$$

where D denotes the total dose.

In its simplest form, it is assumed that full repair of sub-lethal damage occurs between each dose fraction and that no repopulation occurs. The LQ model can be reformulated to account for incomplete repair due to dose fractions close in time, and to account for the effect that cells may start to divide at a higher rate after some time following irradiation (Dale and Jones, 2007). Furthermore, the inducible repair model (Joiner and Johns, 1988) is a modified LQ model to handle low-dose hypersensitivity, the phenomenon observed experimentally of high radiation sensitivity to doses below around 0.5 Gy (Joiner *et al*., 2001). A drawback with this model is the constant curvature which is not consistent with experimental observations which indicate that the survival curve becomes more or less linear (in a log-linear scale) at high doses. The model is therefore modified in the local effect model (LEM), where the LQ model is a part, used clinically in the carbon ion treatment in Heidelberg (Scholz *et al*., 1997; Elsässer and Scholz, 2007; Elsässer*et al*., 2008, 2010). In LEM, the curve is simply extrapolated by a straight line at doses higher than at threshold dose d_t:

$$S_{LQ'} = \begin{cases} e^{-\alpha d - \beta d^2} & \text{If } d \le d_t \\ e^{-\alpha d - \beta d^2 - (\alpha + 2\beta\beta\beta(d - d_t))} & \text{If } d > d_t \end{cases} \quad 2.8$$

The LQ model may also be inappropriate for treatments with high doses per fractions used in stereotactic radiation therapy and in hypofractionation (Kirkpatrick et al., 2009), and for ions showing a cell survival curve with a small shoulder that transform into an exponential curve already at low doses.

2.4.4 Main Radiobiological Models

2.4.4.1 Normal Tissue Complication Probability

Similar to mathematical descriptions which calculate tumor control, it is also possible to calculate damage to normal tissue. NTCP can be determined through equation 2.10, also known as the Lyman-Kutcher-Burman (LKB) NTCP model. In order to bridge the gap between uniform irradiation and partial irradiation, the equivalent uniform dose (EUD) was devised (Kutcher *et al*., 1991). The EUD describes the dose that yields an equivalent survival fraction as a heterogeneous dose distribution, if delivered uniformly to the entire volume of a structure. The phenomenological, generalized EUD (gEUD) formalism, for OARs is postulated as follows (Niemierko, 1997).

$$gEUD = \left(\frac{1}{N} \left(\sum_{i=1}^{n} \left(D_i \right)^{\alpha} \right) \right)^{\frac{1}{\alpha}} \qquad 2.9$$

Where N is the number of voxels in the structure of interest, Di the total dose in the ith voxel, and α is the phenomenological model parameter that describes the magnitude of the volume effect (Chvetsov *et al*., 2007). Based upon the gEUD metric, the response of OARs for a given RT regime can be described by the following model (Lyman 1985).

$$NTCP = \frac{1}{\sqrt{2\pi}} \int_{0}^{t} e^{-\frac{x^2}{2}} dx \qquad 2.10$$

where

$$t = \frac{gEUD - TD_{50}}{mTD_{50}} \qquad 2.11$$

Here TD_{50} is the uniform dose given to the entire OAR which results in a 50% risk of complication, m is a measure of the slope of the sigmoid curve represented by the integral of the normal distribution (Stewart and Li, 2007). The volume effect represents the architecture of OARs, which are assumed to consist of independent functional sub units (FSUs) (Withers et al. 1988), arranged in series, parallel, or some combination of the two. The volume effect plays an important role in the response of an OAR. When $\frac{1}{\alpha}$is near unity the volume effect is

large and when $\frac{1}{\alpha}$ is near 0 the volume effect is small. A large volume effect signifies that the NTCP correlates with the mean dose, while a small volume effect implies that the NTCP correlates with the maximum dose in the OAR (Mayles et al. 2007). NTCP can also be determined through equation 2.12, also known as the relative seriality NTCP model

$$NTCP = \left[1 - \prod_{j=i}^{k} \left(1 - NTCP\left(D_j\right)^s\right)^{V_j}\right]^{\frac{1}{s}} \quad 2.12$$

This model is built on binomial statistics and therefore has a mechanical radiobiological pedigree (Kallman*et al.*, 1992), it handles serial and parallel architecture using FSUs. Equation 2.13 describes the response of the whole organ to an arbitrary dose distribution (Dj) as a function of the response of the whole organ to a homogeneous dose distribution. The number of FSU corresponds with the k bins in the DVH, and s is the relative seriality factor. When s is large the FSUs can be considered to be in series, when s is small the FSUs can be assumed to be arranged in parallel. NTCP(Dj) can be expressed as;

$$NTCP\left(D_j\right) = 2^{\exp^{e\gamma\left(1-\frac{D_j}{D_{50}}\right)}} \quad 2.13$$

Which is based on Poisson statistics to describe cell survival. The γ parameter is the maximum relative slope of the dose response curve and D_{50} is the whole organ uniform dose that would produce a 50% complication probability.

2.4.5 Physical Dose Conversion

2.5 Advantages, Disadvantages and Clinical Acceptance of Radiobiological Model

Presently, the evaluation of a treatment plan is based on the volumetric distribution of the absorbed dose within the patient. However, it is seldom possible to measure dose distribution directly in patients treated with radiation. Data on dose distributions are almost entirely derived from measurements in water phantoms (which are tissue and muscle equivalent)

usually large enough in volume to provide full scatter conditions for a given beam. These basic data are used in a dose calculation system devised to predict dose distribution in an actual patient. So, during the treatment planning process the patient is simulated by a 3-D representation. The dose distribution within the patient is calculated using the electron density distribution provided by the CT slices (Hounsfield Numbers) and correcting for inhomogeneities existing within the patient such as bones and air cavities (Koussi*et al*., 2007). In the so called 'forward optimization' (trial and error) approach, which is mostly used nowadays, the planner changes the configuration of the beams and consequently the dose distribution within the patient trying to satisfy some predetermined criteria (usually tolerance doses for normal tissue and prescribed doses for targets). This is a trial and error process and depends very much of the clinical experience of the planner. Now, that the speed of the computers has increased dramatically many treatment planning systems have implemented the 'inverse planning' approach which uses these predetermined criteria as an input and finds the beam configuration that satisfy them most. However, to simulate the patient by a tissue equivalent computer representation is not clinically very accurate since the response of the various organs to radiation depends on many other factors that are currently not taken into account during the treatment planning process. Such factors are the volume dependence of the organs to radiation, the internal structural organization of the functional subunits for the normal tissues or the density of the clonogenic cells for the targets, the hypoxic cell fraction within the tumor and the fractionation regime, which affects a) repair of sublethal damage; b) redistribution of cells within cell cycle; c) repopulation and d) reoxygenation of the cells. In order to take this information into account in the planning of the treatment one needs to use radiobiological models, which describe the response of the tumors and normal tissues to radiation according to their radiobiological characteristics (Panagiotis *et al*., 2001). This would lead to a major advantage using radiobiological models during treatment planning

process and that is the optimized planning of the radiotherapy treatment which would lead to maximal efficiency in tumor control, keeping complications in normal tissue as low as possible. However, the question of "how reliable will treatment plan-specific endpoint models be?" is seldom addressed. Niemierko has briefly discussed the factors that contribute to uncertainty in such model-based outcome prediction in the context of the quantitative reliability of pulmonary outcome predictions. A brief division of outcome-model predictions in 4 categories is listed below according to Deasy*et al.*, 2001.

1. Model errors are defined as those errors which arise from an inability of the model equations to describe the data available over the applicable range. Model errors are detected primarily by examining residuals between data and model fits and looking for non-random patterns. However, due to the nonlinear and multidimensional nature of the models, it is not always clear which data subsets should be examined to ensure that the model really describes the data. Unfortunately, even if a model fits the available data, it might be applied in a situation unlike that for which data were collected and therefore may fail. There is obviously some amount of model error involved in using empirical models, but it may be negligible compared to the following sources.
2. Parameter uncertainties as defined as uncertainties in the estimated model parameters due to the fact that the amount of patient data is finite. In the hypothetical limit of an infinite amount of non-redundant patient data, and assuming that the models have only a single computational best-fit (i.e., only the local minimum or maximum), model parameters are determined with perfect precision. Of course, there are typically not enough data to determine the model parameters to an accuracy that reduces parameter uncertainties to negligible levels.

3. Biological noise refers to the fact that all of the models are simplifications of highly complex, biologic, dynamic phenomena, in unique individuals. Much of the underlying phenomena appear as random “noise”. It is quite possible that, however, that some component of what appears in one model to be random biological noise may become better understood (predictable), either because more data become available or the data is analyzed in a new way. This recognition may lead to reduction in biological noise through an improved model.
4. Measurement error, for continuous variables, is the difference between the quantified endpoint and the actual value. This source of error can always be a target of improved methodology. Disagreements between model predictions and measurements are due to a mix of model errors, parameter uncertainties, biological noise and measurements errors. According to Joseph et al the incorporation of reliability/uncertainty analysis into software implementation of dosevolume based outcome models is possible and make the use of treatment planning outcome models more justifiable corresponding less misuse. (Joseph *et al*., 2001). It is clear from the literature that radiobiological modeling plays little or no part in considering the various treatment options in clinical trials. In order to use modeling as a precursor to clinical trials there is a need for greater research into the assessment of bio predictive assays which may in future be represented by the genetic characterization of tumor cells, rather than use of classical clonogenic and direct cell kinetic assays respectively, extending models simulating complex biological processes as good as possible. The future is likely to induce great development in radiobiological modeling make clinicians able to individualize and choose among the best recommended (by the models) treatments.

2.6 Physics of Radiation Therapy

In radiotherapy, malignant tumors are treated with ionizing radiation in order to destroy or inactivate tumor cells. This is achieved by the ionization of tumor deoxyribonucleic acid (DNA) by either photons, or charged particles such as electrons, protons or heavier ions. Ionization of the DNA strands, in turn, may lead to double strand breaks in the cell DNA, which are difficult to repair and can lead to cell death. While photons act mostly indirectly via ionization of water in the patient's body forming free radicals, charged particles may damage DNA directly. While other photon based techniques in radiation therapy (such as gamma rays from radioactive isotopes like ^{60}Co), and also charged particle radiation therapy are all important methods of treatment, all patients presented in this thesis were treated using photon beams from medical LINACs. A picture of the front of a medical LINAC is shown in Figure 2.1.

2.6.1 Photon Beam

The photon beam that leaves the LINAC is commonly described in terms of fluence and energy fluence. Fluence is defined as the number of photons N passing through a cross sectional unit area A

$$\Phi = \frac{dN}{dA} \tag{2.14}$$

Since the X-ray beam is polyenergetic, the total fluence is an integral

$$\Phi = \int_0^{E_{max}} \frac{\delta\Phi(E)}{\delta E} dE \tag{2.15}$$

Energy fluence is the energy passing through dA

$$\Psi = \frac{dE}{dA}$$

Once the photon beam strikes a medium it will be attenuated. The interaction cross section σ describes the probability that a photon striking within a unit cross sectional area will interact and the attenuation coefficient μ describes the attenuation of the photonbeam. Sinceμ is

dependentonthedensityofthematerial,themassattenuation coefficient $\frac{\mu}{\rho}$isoftenused,whichdependsontheatomicpropertiesofthemediumand the photon energy, and is independent of density (Almut, 2017).

2.6.2 Linear Energy Transfer

In ion irradiation,notonlytheamountofenergydepositedinavolume(thedose)is of importance but also how the energy depositions are distributed. The spatial distribution of energy depositions influences the effectiveness in producing radiationinduced changes. One way of characterizing this local energy spectrum is by the linear energy transfer (LET). LET is closely related to the collision stopping power andisameasureoftheaverageenergylocallyimpartedtothematerialbyacharged particle per unit length of the particle track (ICRU, 1970).

$$L_{\Delta} = \left(\frac{dE}{dl} \right)_{\Delta} \qquad 2.17$$

where dE is the mean energy loss due to collisions with energy transfers less than a cut-off value Δ, and dl is the distance traversed by the particle. Whereas stopping power focuses on the energy loss of the particle, LET focuses on the energy absorbed by the material. The cut-off value Δ is an energy limit to restrict to energy. losses occurring 'locally' by excluding secondary electrons with energies exceeding Δ. In the unrestricted LET, L∞, all possible energy transfers are included. LET is useful for defining the quality of ionizing radiation. A distinction between low- and high-LET radiation is often made. Low-LET radiation, or sparsely ionizing radiation, such as electrons, experience many interactions with material and the ionizations produced are distributed over a relatively long path resulting in a low ionization density. ^{60}Co γ-rays or X-rays are usually also referred to as low LET radiation, although the definition of LET is limited to charged particles, since the electrons generated

from photon interactions have generally low LET. In contrast, high-LET radiation, such as carbon ions, deposit a large amount of energy in a small distance and produce in that way more clustered, and thereby more severe, DNA damage. Protons may produce high LET in the Bragg peak but belong generally to radiation of low LET. In most experimental situations, there is a distribution of LET values. An average LET at every position can be calculated and the two most common measures are the dose averaged LET and the track (or fluence) averaged LET. A dose averaged LET can be calculated by weighting the LET contribution of each proton by the dose it deposits, and a track averaged LET is obtained by weighting the LET by the number of particles, i.e. it is the arithmetic mean LET. LET is one of the descriptors of the radiation quality and has been found to correlate with the relative biological effectiveness. Alternative measures of radiation quality might be the number of ionizations per path length, or the micro dosimetric quantity dose-mean linear energy. A measure that more uniquely describes the radiation quality would be beneficial.

2.7 **Review of Related Literature**

The goal of radiotherapy is to deliver a sufficient radiation dose to the tumor to provide a high probability of cure while the surrounding healthy tissue is minimally damaged and left functionally and structurally competent. Unfortunately, the accuracy of dose delivery to critical target organs is greatly hindered by uncertainty in treatment parameters which includes but not limited to organ motion and patient positioning. Therefore, knowledge of the treatment errors, their characteristics and causes, the radiobiological techniques to control or reduce them is vital for comprehensive health care. To achieve this goal, a thorough

understanding of the radiotherapy treatment process, set-up errors and radiobiological models in terms of normal tissue complications and tumor control is deemed necessary.

There are quite a number of studies about set-up errors of cancer featuring different radiotherapy modalities which have been conducted.Lin *et al.*, (2012) conducted a single-center retrospective case series analysis to determine the impact of body mass index (BMI) on daily setup variations and frequency of imaging necessary for patients with endometrial cancer treated with adjuvant IMRT with daily image guidance. BMI mean daily shifts, and random and systematic errors in each translational and rotational direction were calculated for each patient. Margin recipes were generated based on BMI. Linear regression and spearman rank correlation analysis were performed. To simulate a less-than-daily image guided radiation therapy (IGRT) protocol, the average shift of the first five fractions was applied to subsequent set-ups without IGRT for assessing the impact on set-up error and margin requirements. A total of 30 patients were included in the analysis. All patients underwent surgery for endometrial cancer, including a total hysterectomy, bilateral salpingo-oophorectomy, and pelvic/para-aortic lymph node dissection for endometrial cancer. Stages ranged from IB to IIIC. Of the patients, six had uterine sarcoma, twenty-one (21) had endometrioid adenocarcinoma, and three had papillary serous carcinoma. One patient received pelvic radiation for a recurrence of endometrial cancer. The median patient age was 59 years (range, 45 to 82 years). The median BMI was 32.9 (range, 23 to 62). Of the 30 patients, 16.7% (n = 5) were normal weight (BMI < 25); 23.3% (n = 7) were overweight (BMI ≥ 25 to < 30); 26.7% (n = 8) were mildly obese (BMI ≥ 30 to < 35); and 33.3% (n = 10) were moderately to severely obese (BMI ≥ 35). On linear regression, mean absolute vertical, longitudinal, and lateral shifts positively correlated with BMI ($p = 0.0127$, $p = 0.0037$, and $p < 0.0001$, respectively). Systematic errors in the longitudinal and vertical direction were found to be positively correlated with BMI category ($p < 0.0001$ for both). IGRT for the first

five fractions, followed by correction of the mean error for all subsequent fractions, led to a substantial reduction in setup error and resultant margin requirement overall compared with no IGRT. The authors concluded that daily shifts, systematic errors, and margin requirements were highest in patients who were obese and as such, tailored use of image-guided IMRT in women with a high BMI receiving pelvic radiotherapy, is thus appropriate.

Chen *et al.*, (2007) conducted a retrospective case series analysis to determine the optimal definition of target margins for patients with esophageal carcinoma and treated with conformal radiation therapy. Pretreatment megavoltage computed tomography(MVCT) scans were used to evaluate setup variations in anterior–posterior (AP), lateral, and superior–inferior (SI) directions and rotational variations, including pitch, roll, and yaw, for patients with pathologically confirmed esophageal carcinoma and treated with helical tomotherapy. A total of 10 patients were included in the analysis; eight had adenocarcinoma, and two had squamous cell carcinoma. After patients were positioned using their skin tattoos/marks, MVCT scans were performed before every treatment and automatically registered to planning kilovoltage CT scans according to bony landmarks. Image registration data were used to adjust patient setups before treatment. A total of 250 MVCT scans were analyzed. Correlations between setup variations and body habitus, including height, weight, relative weight change, body surface area, and patient age, were evaluated. The standard deviations for systematic set-up corrections in AP, lateral, and SI directions and pitch, roll, and yaw rotations were 1.5, 3.7, and 4.8 mm and 0.5°, 1.2°, and 0.8°, respectively. The appropriate averages of random set-up variations in AP, lateral, and SI directions and pitch, roll, and yaw rotations were 2.9, 5.2, and 4.4 mm, and 1.0°, 1.2°, and 1.1°, respectively. Set-up variations were stable throughout the entire course of radiotherapy in all three translational and three rotational displacements, with little change in magnitude. No significant correlations were found between set-up variations and body habitus variables. The authors concluded that daily

MVCT scans before each treatment can effectively detect set-up errors and thus reduce planning target volume margins. This will reduce radiation dose to critical organs and may lower treatment-related toxicities. Even though this study did an extensive research on set-up errors, it did not include the impact of radiobiological models on target organs as well as organs at risks. Also, the sample size considered in this study was about 10 patients which is quite small.

Kotte *et al.*, (2007) conducted a case series analysis to evaluate the intrafraction motion of the prostate during external-beam radiation therapy of patients with prostate cancer. A total of 427 patients with Stage T3Nx/0Mx/0 prostate carcinoma who received IMRT treatment combined with position verification with fiducial gold markers were included in the analysis. For a total of 11,426 treatment fractions (average, 27 per patient), portal images were taken of the first segment of all five beams. The irradiation time of the technique varied between 5–7 min. From these data, the location of gold markers could be established within every treatment beam under the assumption of minimal marker movement. In 66% of treatment fractions, a motion outside a range of 2 mm was observed, with 28% outside a range of 3 mm. The intrafraction marker movements showed that motion directions were often reversed. However, the effect was small. Even with perfect online position-correction at the start of irradiation, intrafraction motion caused position uncertainty, but systematic errors were limited to < 0.6 mm, and random errors to < 0.9 mm. This would result in a lower limit of 2 mm for margins, in the absence of any other uncertainties. The authors concluded that intrafraction motion of the prostate occurs frequently during external-beam irradiation on a time scale of 5–7 min. Margins of 2 mm account for these intrafraction motions. However, larger margins are required in practice to accommodate other uncertainties in the treatment.Prentou*et al.*, (2020)investigated the dosimetric effects of rotational set-up errors in volumetric modulated arc therapy Stereotactic Radiation Surgery (VMAT-SRS) for multiple

brain metastases, and discovered that 0.5◦ - 2◦ set-up errors can have a significant effect on the dose distribution. Clinically unacceptable dose distributions were obtained in some cases even after 0.5◦ rotations which may be caused by position errors. Similar results were obtained by Selvan *et al.,* (2019).

Chiesa *et al.,* (2015) studied rotational set-up errors and their dosimetric effects in VMAT treatment of prostate patient with simultaneously integrated boost (SIB). They found errors over 2◦ in 7% of patient scans. The rotations had no significant effect on prostate coverage, but they did have a significant impact on seminal vesicles coverage. Out of OARs, femoral heads were sensitive to rotations in yaw and rectum was sensitive to rotations in pitch. The dosimetric sensitivity was explained by distance from isocentre and elongated shape.

Another setup uncertainty study done by Oh *et al.*,(2014)where they assessed the setup uncertainties for various tumor sites with CBCT for more than 2200 VMAT treatments. Among those patients whose setup was evaluated, 19 thorax pathologies were treated with a total of 313 fractions. The distribution of setup corrections in all directions and frequencies of 3D vector lengths were analyzed. The setup errors calculated in this study were those defined by Remeijer*et al.,* 2000 as the overall mean error (M), the systematic error (Σ) and the random error (σ). Although a a fairly large population was considered in this study, dosimetric and biological impact of radiobiological models on treatment fraction was not considered.

Dosimetric effects of set-up errors in tangential radiotherapy techniques have been studied by Harron*et al*., in 2008 and Van *et al*.,(2010) among others. Harron*et al*.,(2008) found out that a transversal set-up error of 5 mm or a rotational set-up error of 2◦ does not cause more than 5 % change in the fraction of volume receiving at least 95 % and less than 107 % of the prescribed dose. Van*et al.,* (2010) compared tangential field techniques with different levels of intensity modulation to each other, and found out that the more intensity modulation was

used, the more sensitive the dose distribution was to changes in breast shape. On the other hand, planning techniques with less or no intensity modulation were more sensitive to patient translational set-up errors. With the possibility to correct rotational set-up errors with modern treatment tables and volumetric arc therapy treatment becoming more common, studying rotational set-up errors has become actual. Jain *et al.*, 2008 studied ten patients receiving radiotherapy for breast cancer, each with about nine to fourteen (9-14) fractions. They found inter-fraction rotational errors over 2° around X-axis in 29.2% of fractions, around Y-axis in 15.1% of fractions and around Z-axis in 1.9% of fractions. CBCT images were acquired immediately after daily treatment and automatic image co-registration was used to determine patient positioning variations. Daily PTV contours were used to calculate PTV variations and daily delivered IMRT and theoretically planned tangential RT dose. Their results showed that group systematic (and random) setup errors detected by CBCT were 5.7 (3.9) mm laterally, 2.8 (3.5) mm vertically and 2.3 (3.2) mm longitudinally. Rotations >2 in any axis occurred on 53/106 (50%) occasions. They concluded that CBCT revealed inadequacies of current patient positioning and verification procedures during breast RT and confirmed improved dose homogeneity using IMRT for the patients studied. Although, a more advanced treatment technique was used in this study compared to my study, dosimetric and radiobiological impact using this advanced technique was not considered.Betgen*et al.,* (2015) studied the set-up errors in deep inspiration breath hold (DIBH) treatment of nineteen left-sided breast cancer patients and found out that rotational set-up errors before set-up correction had systematic and random errors between 0.75° and 1.56°. Dosimetric effects of rotational errors alone were not examined in this study. Zhao *et al.,* (2020) simulated translational set-up errors in radiotherapy treatment of left breast and studied the dosimetric impact using forward-planned intensity modulated radiation therapy (FIMRT) and VMAT. The target coverage of VMAT was found to be more sensitive to translational set-up errors of 5 mm or

more, than FIMRT implying that VMAT technique is more likely to deliver radiation more precisely and accuarately.

Krengli*et al.,* in (2013) conducted a prospective study comparing prone and supine WBI for patients with pendulous breasts. Twenty-nine (29) patients with pendulous breasts and infra-mammary folds when supine was selected for prone WBI treatment while fourteen (14) patients were excluded because of insufficient gantry diameter of the CT scanner or low compliance to prone setup position. Besides dosimetric parameters, late effects were assessed during follow-up visits, which ran every four (4) months after six (6) months after radiotherapy for the first two (2) years, and six (6) months afterwards. Statistical analysis of the results to prove significant differences between the two setups was performed with the Student's t-test considering a p-value< 0.05 as statistically significant. The treatment reproducibility for the prone setup was evaluated using portal imaging checks, which showed inter-fraction differences of 2.0 mm, 1.8 mm and 2.5 mm in the lateral, longitudinal and vertical axes. The authors found that CTV and PTV coverage was significantly better in the supine position than in the prone position taking into consideration the irradiation to OARs and target shape. Lung V5, V10, and V20 were significantly lower in the prone position with p-values The heart V5, V10, V20 and LAD mean and maximum doses were lower in 17 patients who were treated for left breast cancer. No significant difference was observed between the patients treated in prone and supine position for either acute or late toxicity. Similarly, Formenti*et. al.,* in 2012 studied the dosimetric differences between supine and prone positioning for whole breast irradiation (WBI) in 400 patients (200 patients had right breast cancer and 200 patients had left breast cancer). Three hundred and fourteen patients had invasive breast cancer, including 47individuals who had involved sentinel or axillary lymph nodes. The patients were simulated in both positions: supine and prone. A 3-D conformal treatment was planned for both datasets, placing the fields on a plane connecting

the midline to the anterior extent of the latissimus dorsi muscle, achieving comparable coverage of the breast in both positions. For all patients, there was a reduction of the in-field lung volumes in the prone position compared with the supine setup: an 82.2% reduction was observed for right breast cancer and a 91.1% reduction for left breast cancer. In patients with left breast cancer, the prone position had an 85.7% reduction of the in-field heart volumes, except for 15% of patients for whom were found of having less in-field heart volume in the supine position. In this study, prone positioning for WBI had reduced the amount of irradiated lung in all patients, and the amount of heart volume irradiated was reduced in 85% of patients with left breast cancer. Mulliez, *et. al.,* (2015) takes into account not only the different positioning with WBI 3- D conformal technique, but also makes a dosimetric comparison with tangential and multi-beam IMRT. Doses to the contralateral breast were similar regardless of positioning or technique. In the supine position, multi beam IMRT was the treatment of choice in this study, and the prone IMRT was superior to any supine treatment for patients with right breast cancer. Prone IMRT obtained better conformity indices, target dose and sparing of the organs-at-risk.

Recently, radiobiological evaluation tools have become available in many treatment planning systems. Normal tissue complication probability (NTCP) tool could be used to biologically evaluate the plan along with dose-volume histogram (DVH)-based evaluation for OAR. Biological parameters, when applied to these biological models, help predict the biological effects on OAR, and are believed to be more directly correlated with treatment outcome than the DVH based parameters (Ampital, 2020). In a study aimed at the determination of the set-up errors for prostate cancer patients used electronic portal imaging device (EPID) as tool to verify the patient treatment positioning (Morsy et al., 2019). Patient set-up was controlled by comparing the Digitally reconstructed radiographs (DRR) with portal images acquired immediately before patient treatment where they evaluated the selected portal images taken

for each patient. The calculation of PTV margins were done according to ICRU Report 62. In addition, their study used an electronic portal imaging device (EPID) to measure the set-up deviations μ for Prostate cancer patients and proposed ways of reducing these errors but failed to measure the impact of these errors using radiobiological models. Similarly, a study on the analysis of set-up errors during CT-scan, simulation, and treatment process in breast cancer patients determined set up errors by calculating the differences in isocenter location, source to surface distance (SSD), central axis lung distance (CLD), and locations of surgical clips implanted during surgery (Rena, 2005). However, their work only looked at the geometric uncertainties without actually considering the risk of overdose or underdose to the organs at risk or the target as the case may be. Similarly, a study on the clinical evaluation of inter-fractional variations for whole breast radiotherapy using 3-dimensional surface imaging evaluated the impact of 3-dimensional (3D) surface imaging on daily patient setup for breast radiotherapy (Shah *et al.*, 2013). In this study, fifty patients undergoing treatment for whole breast radiotherapy were setup daily using an AlignRT system (Vision RT, London, UK) for 3D surface-based alignment. This investigation evaluated the performance of the surface based imaging system for daily breast alignment, the absolute displacements between setup with skin marks and setup with the surface-based imaging system and the dosimetric effect of daily alignments with skin marks versus surface-based alignments contrary to the present study which makes use of a different machine model and calculates the dosimetric effect of set up errors in terms of a generalized equivalent dose.

Surega*et al.,* (2014), quantified the uncertainty of physical dose metrics to predict clinical outcomes of radiotherapy. The radiobiological estimates such as tumor control probability (TCP) and Normal Tissue Complication Probability (NTCP) were made for a cohort of 40 cancer patients (10 brain;19 head andneck;11 cervix) using the Dose Volume parameters. Statistical analysis was performed to determine the correlation of physical plan quality

indicators with radiobiological estimates. The correlation between conformity index (CI) and TCP was found to be good and the dosimetric parameters for optic nerves, optic chiasm, brain stem, normal brain and parotids correlated well with the NTCP estimates. However, this study did not consider the biological impact of these physical indicators on organs at risk. Furthermore, Boughalia and his colleagues in 2015 conducted a research on nasopharyngeal cancer where he quantified patients set up errors using the NTCP and TCP models. In this study, 20 patients treated for nasopharyngeal cancer were enrolled in a radiotherapy and oncology department where systematic and random errors were quantified. The dosimetric and biological impact of these set-up errors on the target volume and the organ at risk (OARs) coverage were assessed using calculation of dose volume histogram, gEUD, TCP and NTCP. The standard deviations (SDs) of the systematic set-up and random set-up errors were calculated for the lateral and subclavicular fields and results were obtained. This work took into account the impact of these set up errors on the overall treatment but failed to quantify the extent of these errors and possible ways of reducing these errors.

Lee *et al.,* in 2021 conducted a research on the clinical implications of geometric and dosimetric uncertainties of inter and intra-fractional movement during volumetric modulated arc therapy for breast cancer patients where they evaluated the necessity of pre-treatment and intra-fractional cone-beam computed tomography (CBCT) by analyzing inter- and intra-fractional CBCT images of breast cancer patients receiving RT. From 57 patients, 1206 pre-treatment CBCT and 1067 intra-fractional CBCT images were collected. Geometric movements of patients were measured quantitively in both inter- and intra-fractional CBCT, and changes in dosimetric parameters were evaluated in selected patients with extreme intra-fractional movement. Modified plans reflecting large changes in intra-fractional position in 10 selected cases revealed insufficient target coverage in seven cases and more than 20-fold

increase in the volume of heart receiving at least 25 Gy in two cases. Intra-fractional verification, as well as pre-treatment verification, were considered in patients using DIBH.

Mukundan*et al.*,(2020) evaluated the dosimetric and isocentric variations due to patient set errors in CT-based treatment planning for breast cancer by electronic portal imaging where a total of 360 EPIs in 60 patients receiving breast/chest wall irradiation were evaluated. Cumulative dose–volume histograms (DVHs) were analyzed for mean doses to lung (V20) and heart (V30), setup source to surface distance (SSD) and central lung distance (CLD), and shifts in anterior-posterior (AP), superior-inferior (SI), and medial lateral (ML) directions and results showed that random errors ranged from 2 to 3 mm for the breast/chest wall (medial and lateral) tangential treatments and 2–2.5 mm for the anterior supraclavicular nodal field. Systematic errors ranged from 3 to 5 mm in the AP direction for the tangential fields and from 2.5 to 5 mm in the SI and ML direction for the anterior supraclavicular nodal field. Similarly, Liang *et al* conducted a research in 2020 where they investigated the consequences of residual set-up error on target dose distribution using various image registration strategies for breast cancer treated with intensity-modulated proton therapy (IMPT). Among 11 post-lumpectomy patients who received IMPT, 44 dose distributions were computed. They divided the setup error into the posture error and breast error. Patients with a large posture error and those with good posture setup but a large breast error were identified to evaluate the effect of posture error and breast error. The results showed that 4/11 patients had ≥1% decrease in breast CTV D_{95}, one (1) of whom developed breast edema while the other 3 all had a $> 2^{o}$ posture error. The CTV D_{95} variation was within 1% for the patients with good posture setup but $>2^{o}$ breast error.

In 2022, Luchao*et al.*, published an article on the effect of sterotactic body radiation therapy combined with thermoplastic fixation on set-up errors in breast cancer patients undergoing radiotherapy. Ninety breast cancer patients undergoing radiotherapy who were treated in their

hospital (May 2019-May 2020) were selected as the research objects and equally divided into the experimental group and control group according to the order of hospitalization, with 45 patients in each group. The control group received conventional radiotherapy combined with breast bracket, and the experimental group received SBRT combined with thermoplastic fixation and they concluded that implementing SBRT combined with thermoplastic fixation in breast cancer patients undergoing radiotherapy can effectively improve set-up efficiency and treatment accuracy and reduce set-up errors.

Similary, Ioana*et al.*, (2022) studied the factors impacting on set-up analysis and error management during breast cancer radiotherapywhere they compiled and discussed the set-up errors that occurred due to treatment and positioning factors. In view of this, a systematic search of the scientific literature in the Medline/PubMed databases was performed over the 1990–2021-time period, with 93 articles found to be relevant for the study and they concluded that clinics should evaluate, according to their socio-economic prospects, the most adequate options for breast cancer patient setup in order to deliver an effective treatment without compromising the patients' quality of life. Seonghee*et al.,* in 2022 evaluated the efficiency and accuracy of the daily patient setup for breast cancer patients by applying surface-guided radiation therapy using the halcyon system instead of conventional laser alignment based on the skin marking method. They retrospectively investigated 228 treatment fractions using two different daily patient setup methods. The accuracy of the residual rotational error of the surface-guided radiation therapy system was evaluated by using an in-house breast phantom. The residual translational error was analyzed using the couch position difference in the vertical, longitudinal, and lateral directions between the reference computed tomography and daily kilo-voltage cone beam computed tomography acquired from the record and verification system. Based on the results they obtained, they concluded that surface-guided radiation therapy improves the accuracy and efficiency of patient setups in

breast cancer patients using the halcyon system, which has limitations in correcting the rotational offset.Comparing treatment uncertainty for ultra-vs. standard hypofractionated investigated postoperative ultra-hypofractionated radiation therapy (UHFRT) in 5 fractions (fx) for breast cancer patients In this retrospective study, treatment uncertainties occurring in patients treated with 5fx (5fx-group) were evaluated using electronic portal imaging device (EPID)-based in-vivo dosimetry (EIVD) and compared with the results from patients treated with conventionally HFRT (15fx-group) to validate the new technique and to evaluate if the shorter treatment schedule could have a positive effect on the treatment uncertainties. In conclusion, their research showed that EPID-based in-vivo dosimetry (EIVD) demonstrated that UHFRT for breast cancer results in less FFs compared to standard hypofractionated radiation therapy (SHFRT. Similarly, Mankinen*et al.,* (2022) conducted a research on the dosimetric effect of respiratory motion on planned dose in whole-breast volumetric modulated arc therapy using moderate and ultra-hypofractionation of respiratory motion on the planned dose in free-breathing right-sided whole-breast irradiation (WBI) was studied by simulating hypofractionated VMAT treatment courses. Only ten patients with phase-triggered 4D-CT images were included in the study. VMAT plans targeting the right breast were created retrospectively with moderately hypofractionated (40.05 Gy in 15 fractions of 2.67 Gy) and ultra-hypofractionated (26 Gy 5 fractions of 5.2 Gy) schemes. 3D-CRT plans were generated as a reference and they concluded from results obtained that respiratory motion of less than 5 mm in magnitude did not result in clinically significant changes in the planned free-breathing WBI dose. The 5 mm margins were sufficient to account for the respiratory motion in terms of CTV dose homogeneity and coverage for VMAT techniques. Steep dose gradients near the PTV edges might decrease the CTV coverage. No clinical significance was found due to the choice of fractionation.*Kang et al.,* (2022) evaluated the dosimetric and radiological parameters in four radiotherapy regimens for synchronous

bilateral breast cancer and found out that IMRT exhibited similar target coverage and a certain degree of dosimetric improvement in OAR sparing compared to the other techniques and although IMRT significantly increased monitor unit compared to VMAT, which is the best option in terms of delivery efficiency, there was only a 22% increase in delivery time.In the case of target volume correction, breathing motion or breast volume changes in the positive margin (outside the patient) is a factor that can easily be taken care of in 3D conformal planning by opening the field and creating a "skin flash" area. The position of the MLCs on an inverse planned treatment conforms to the target, making it difficult to integrate this area. As with any other radiation treatment delivery, immobilization devices help to reduce inter- and intra-fraction motion of the target during irradiation. The current use of IGRT plays an important role in helping minimize the effect of inter-fraction motion by analyzing patient positioning daily and performing online correction of set offs. Approaches such as deep inspiration breath-hold techniques during VMAT irradiation are suggested in literature (Tsai, *et al.,* 2012) (Michalski, *et al.,* 2012) in order to avoid significant variations in dosage to the PTV as well as to reduce the dose to delivered to the heart volume and lungs. Gating techniques have also been suggested (Nicolini, *et al.,* 2010), but their implementation is not time effective in most institutions. Nicolini*et al.,*(2010) has been able to explore both possibilities: delivering respiratory gated VMAT and accounting for respiratory motion during the treatment planning. The respiratory gating approach used for the Real-time Position Management (RPM) respiratory gating system was from Varian in a group of six patients and it was tested on Octavius phantom. The gated delivery was compared with the non-gated planed dose and the dosimetric impact was a mean delta MU <0.2% for all gating conditions. The gated VMAT did not affect the quality of dose delivery but it did interrupt a single arc 20 to 50 times during delivery, which can be time consuming and difficult to use if the patient does not have regular breathing patterns. On their other approach, Nicolini*et al.,*

(2010) expanded the contour of the breast area to the outside of the CT image and made its density equivalent to soft tissue to extend the dose fluence outside of the body contour to account for changes in size and position of the target and other tissues due to respiratory movement or edema. VMAT plans were optimized for six patients for whom three datasets were used: an original planning CT and a planning CT with an artificial expansion of 10 mm and 5 mm outside of the body in the breast region which was assigned a hounsfield unit (HU) number equivalent to that of soft tissue. It was concluded that the target coverage could be compromised if no action is taken towards correcting for edema or respiratory motion in modulated radiation treatments. If no steps are taken in case of important changes in morphology, for example 10 mm, the target dose could be affected with 4% average reduction, while a 5 mm discrepancy could lead to a 5% reduction in v95% rising to 25% in the case of 10 mm. This study only included whole breast irradiation treatment plans and did not include radiation treatments in which the internal mammary or supra-clavicular nodes were involved. In order to further analyze the importance of having an optimization PTV structure that accounts for volume changes, Michalski, *et al.*, (2012) analyzed eighteen articles about the inter- and intra-fraction motion during radiation therapy to the whole breast in the supine position, ranging from the years 1991 to 2008. The motion was measured foreach image set acquired for each patient based on five parameters: central lung distance, central irradiated width, central beam edge-to-skin distance, cranio-caudal distance and/or central breast distance. From the seven groups that reported the intrafraction motion of the target in breast cancer patients never exceeded 5 mm. The intrafraction motion is naturally smaller than interfraction motion, since interfraction motion includes changes in the tissue such as edema or tumor shrinkage. Michalski *al.*, (2012) recommends a clinical PTV margin of 5 mm for all whole breast radiotherapy.

Kaveh *et al.*,(2021) investigated and compared the radiobiological factors of the tumor and organs at risk in two different radiation therapy techniques of breast cancer where Dose-volume histograms (DVHs), Tumor control probability (TCP), and normal tissue complication probability (NTCP) curves were used to compare the dosimetric and radiobiological parameters of the tissues in the breast cancer radiation therapy technique and the results obtained revealed that the maximum doses in planning target volume (PTV) with mean values of 109% and 110% in the SI and dual-isocentric technique (DIT) were not significantly different in both techniques and that they were indeed at the optimum level based on the RTOG 1005 protocol. The dose homogeneity index in mono-isocentric technique (MIT) was more than that in DIT, while the conformity index and the mean TCP did not show a significant difference in the two techniques. Furthermore, minimum, mean, and maximum dose in the lung and the probability of pneumonitis decreased in MIT. On the other hand, the maximum dose, the dose of 33%, 66%, and 100% of the heart, and the probability of pericarditis in MIT were lower than DIT.

On dosimetric comparison studies, in 2010, Popescu *et al.,* conducted a study comparing 3-D conventional, IMRT and VMAT techniques on 5 previously treated patients. Her team demonstrated the possibility to produce high quality plans using VMAT for large treatment volumes of an average of 945 cc by using two coplanar arcs of 190° with a 2 cm overlap jaws. Her group concluded that this technique successfully covered the large PTV regardless of the short MLC travel distance of varian machines (15 cm). The VMAT plans had a total of 386 MLC segments, giving enough control points to achieve an optimal dose distribution as well as to spare OARs, regardless of the long optimization time (10 hours). They concluded that the PTV homogeneity was similar across all techniques being compared. The average heart volumes receiving >30 Gy for VMAT, IMRT, and 3-D conformal were 2.6% ± 0.7%, 3.5% ± 0.8%, and 16.4% ± 4.3%, respectively, and the average ipsilateral lung volumes

receiving >20 Gy were 16.9% ± 1.1%, 17.3% ± 0.9%, and 37.3% ± 7.2%, respectively. The healthy tissue volume percentages receiving 5 Gy were significantly larger with VMAT (33.1% ± 2.1%) and IMRT (45.3% ±3.1%) than with 3-D conformal (19.4% ± 3.7%). VMAT decreased the number of monitor units by 30% and the treatment time by 55% compared with IMRT. In more advanced approaches, Popescu and her team have also compared traditional 3D conformal techniques with static couch VMAT and simultaneous couch rotation VMAT in 20 patients. The VMAT plans consisted of a single 200 to 240-degree arc, while the VMAT with couch rotation consisted of two tangential couch arcs with the same isocenter with simultaneous non-coplanar gantry rotation directions. Even though the VMAT with dynamic couch rotation yielded superior results to static couch VMAT in OARs sparing, the mean dose to the ipsilateral breast increased by up to 15% compared to 3D conformal technique. The dynamic couch VMAT resulted in superior target coverage when compared to 3D-CRT and VMAT being the V95%: 98.2% vs. 97.1% respectively. This type of treatment planning requires a modification of the VMAT algorithm to link the couch and gantry rotation.

Various treatment mobilization techniques have shown that having a radiation treatment plan with a good dose distribution does not guarantee a successful treatment course delivery if the immobilization setup is not reproducible. Having an effective immobilization system can make the positioning variations minimal and improve the total outcome of the radiotherapy treatment. There are specific immobilization devices for specific cancer sites as well as techniques. For WBI, the most common immobilization devices are butterfly boards and vaclok bags in the supine position and prone breast boards. The study of the effectiveness of an immobilization device has been studied using two-dimensional (2D) and three-dimensional (3D) information. Two-dimensional information can be obtained through MV portal images as well as kV radiographs with the disadvantages that one cannot assess

rotational variations and that image quality might pose a difficulty measuring other parameters. The integration of three-dimensional (3D) imaging not only facilitates the setup positioning during treatment, but also can provide additional information in a similar way to a simulation CT dataset. Therefore, 3D images provide more information than 2D images and it can be said that they are superior tools to assess the reproducibility of immobilization devices. Inverse planned radiotherapy delivers highly conformal dose distribution to spare critical organs and normal tissues while achieving optimal target coverage. Image-guidance during treatment delivery as well as a reduction in setup uncertainty become more important to guarantee correct treatment delivery. In a study by Cheng, *et al.,* 2014 daily treatment set-up MVCT data from 212 patients was evaluated in terms of reproducibility and set-up corrections using an accuracy helical tomotherapy unit. Within the sample population, 41 patients were evaluated for chest radiation treatment accounting for a total of 862 treatment fractions. Cheng assessed the reproducibility by looking at the lateral, longitudinal and vertical locations of a point in each MVCT as a measure of translational deviation and roll locations for each patient. The systematic error was calculated as the average error over all the treatment fractions and random error was calculated as the average magnitude of errors that were expected to be distributed as a Gaussian function about a mean. In this study, the prone breast group used the CIVCO Medical Solutions prone board while the supine breast group used a vaclok and a headrest. Cheng and his team discovered that for the breast cases, the systematic error in the long position, and the random errors for the lateral, long and vertical positions were greater for the prone breast group than the supine breast group by 2.2, 3.8, 2.0 and 1.7 mm respectively. The mean 3D vectors of the prone breast group and the supine breast group were 13.9 and 7.2 mm respectively. For the prone breast, shifts more than 6 mm were more frequent (91.2%) than for the supine breast group (66.2%). No breast volumes were obtained for either group, but the authors did note that the treatment region is

more mobile in patients with large breasts. For the rest of the study, the overall set-up accuracy was acceptable with mean set-up variations being less than 10 mm.

In 2019, Wang and his colleagues carried out a research to compare differences in setup error assessment and correction between planar kilovolt images and cone beam computed tomography images for external beam partial breast irradiation during free breathing. Nineteen patients who received external beam partial breast irradiation after breast-conserving surgery were recruited. Interfraction setup error was acquired using planar kilovolt images and cone beam computed tomography. After online setup correction, the residual error was calculated, and the setup error was compared. The residual error and setup margin were quantified for planar kilovolt and cone beam computed tomography images.Discrepancy between the setup errors observed with planar kilovolt and cone beam computed tomography was obvious in the anteroposterior direction. Compared to cone beam computed tomography, the elapsed treatment time was smaller when the initial alignment used kilovolt planar imaging. Whether using planar kilovolt or cone beam computed tomography, residual errors can be reduced to 1.5 mm for external beam partial breast irradiation procedures.

The study on Ipsilateral lung normal tissue complication probability parameters for different dose calculation algorithm (DCA) in radiotherapy of breast cancer carried out by Kavousi*et al.*, (2020) determined the NTCP parameter values for different DCAs in left-sided breast radiotherapy, using the Lyman-Kutcher-Burman (LKB) model. The methodology recommended by International Atomic Energy Agency TEC-DOC 1583 was used to establish the accuracy of dose calculations of different DCAs treatment planning of 15 patients with left-sided breast cancer was performed by the mentioned DCAs and NTCP of the left-lung normal tissue were calculated for each patient individually, using the LKB model. For the pencil beam (PB) algorithm, the NTCP parameters were taken from previously published

values and new model parameters obtained for each DCA, using the iterative least squares methods. This research confirmed that the NTCP values for a given treatment type are different for the different DCAs. Thus, it is essential to introduce appropriate NTCP parameter values according to DCA adopted in TPS, to obtain a more precise estimation of lung NTCP. Hence, new parameter values, classified according to the DCAs, must be determined before introducing NTCP estimation in clinical practice.

Yao *et al*., (2019) conducted a case series analysis to investigate the setup uncertainties and to establish an optimal imaging schedule for the prone-positioned whole breast radiotherapy. Twenty prone-positioned breast patients treated with tangential fields from 2015 to 2017 were retrospectively enrolled in this study. The prescription dose for the whole breast treatment was 266 Gy × 16 for all of the patients and the treatments were delivered with the source to surface distance (SSD) setup technique. At every fraction of treatment, the patient was set up based on the body localization tattoos. Mega-voltage (MV) portal imaging was then taken to confirm the setup; if a discrepancy (> 3 mm) was found between the portal images and corresponding plan images, the patient positioning was adjusted accordingly with couch movement. Based on the information acquired from the daily tattoo and portal imaging setup, three sets of data, named as weekly imaging guidance (WIG), no daily imaging guidance (NIG), and initial 3 days then weekly imaging guidance (3 + WIG) were sampled, constructed, and analyzed in reference to the benchmark of the daily imaging guidance (DIG). A comparison of the setup uncertainties, target coverage (D_{95}, D_{max}), V5 of the ipsilateral lung, the mean dose of heart, the mean and max dose of the left-anterior-descending coronary artery (LAD) among the four-imaging guidance (IG) schedules were made. Relative to the daily imaging guidance (IG) benchmark, the NIG schedule led to the largest residual setup uncertainties; the uncertainties were similar for the WIG and 3 + WIG schedules. Little variations were observed for D_{95} of the target among NIG, DIG and WIG.

The target Dmax also exhibited little changes among all the IG schedules. While V5 of the ipsilateral lung changed very little among all 4 schedules, the percent change of the mean heart dose was more pronounced; but its absolute values were still within the tolerance. However, for the left-sided breast patients, the LAD dose could be significantly impacted by the imaging schedules and could potentially exceed its tolerance criteria in some patients if NIG, WIG and 3 + WIG schedules were used. The authors concluded that for left-side whole breast treatment in the prone position using the SSD treatment technique, the daily imaging guidance can ensure dosimetric coverage of the target as well as preventing critical organs, especially LAD, from receiving unacceptable levels of dose. For right-sided whole breast treatment in the prone position, the weekly imaging setup guidance appears to be the optimal choice.

Ding *et al.*, *(*2022)evaluated the robustness of multi-field IMRT and VMAT plans to target motion for left-sided BC radiotherapy. In this study, 7-field hybrid IMRT (7F-H-IMRT) and 2-arc VMAT (2A-VMAT) plans were generated for ten left-sided BC patients. Shifts of 3 mm, 5 mm, and 10 mm in six directions were introduced and the perturbed dose distributions were recalculated. The dose differences (ΔD) of the original plan and perturbed plan corresponded to the plan robustness for the structure. Results showed higher $\Delta D_{98\%}$, $\Delta D_{95\%}$, and ΔD_{mean} of CTV were observed in 2A-VMAT plans, which induced higher tumor control probability reductions. A higher ΔDmean of CTV Boost was found in 7F-H-IMRT plans despite lower $\Delta D_{98\%}$ and $\Delta D_{95\%}$. Shifts in the S-I direction exerted the largest effect on CTV and CTV Boost. Regarding OARs, shifts in R, P, and I directions contributed to increasing the received dose. The 2A-VMAT plans performed better dose sparing, but had a higher robustness in a high-dose volume of the left lung and heart. The 2A-VMAT plans decreased the max dose of LAD but exhibited lower robustness. They concluded that the 2A-VMAT

plans showed higher sensitivity to position deviation. Shifts in the S-I direction exerted the largest effect for CTV and CTV Boost.

Electronic Portal Imaging (EPI) is commonly used to identify and correct for interfraction variability in tangential breast irradiation. Based on the institutional policy, EPI registration is performed by either radiation oncologist or therapist. Little data is available on the inter-observer agreement in EPI registration among different health practitioners. However, Jereczec-fossa and his team in 2022 analyzed inter-observer agreement among radiation oncologists and therapists in the evaluation of EPI for breast cancer radiotherapy verification. EPI data of 40 patients treated with tangential fields were independently reviewed by a radiation oncologist (on-line, just before treatment) and off-line by junior and senior therapists. Displacement of each EPI image with respect to the digital reconstructed radiographs (DRRs) was quantified using manual EPI registration based on bony marks with the corresponding DRRs. Agreement between observers was evaluated using weighted Cohen's Kappa statistics. In 95% out of 720 EPI-DRR comparisons, the EPI-DRR misalignment was < 5 mm. The difference between observers was < 2 mm in 666 (92.5%) out of all 720 delta values. High inter-observer agreement was found, with weighted Cohen's Kappa values attesting evaluation overlaps ranging from moderate (among therapists) to almost perfect (among radiation oncologist and therapists). The high agreement among the observers demonstrated the precision of breast localization using EPI. These findings suggest that routine EPI-based patient set-up verification in breast cancer radiotherapy can be safely entrusted to trained therapists.

In breast cancer radiotherapy, significant discrepancies in dose delivery can contribute to underdosage of the tumor or overdosage of normal tissue, which is potentially related to a reduction of local tumor control and an increase of side effects. To study the impact of these factors in breast cancer radiotherapy, a meta-analysis of the clinical data reported by

Mavroidis *et al.*, (2002) showing the patient setup and breathing uncertainties characterizing three different irradiation techniques, were employed. The uncertainties in dose delivery are simulated based on fifteen breast cancer patients (5 mastectomized, 5 resected with negative node involvement (R-) and 5 resected with positive node involvement (R+)), who were treated by three different irradiation techniques, respectively. The positioning and breathing effects were taken into consideration in the determination of the real dose distributions delivered to the CTV and lung in each patient. The combined frequency distributions of the positioning and breathing distributions were obtained by convolution. For each patient the effectiveness of the dose distribution applied is calculated by the Poisson and relative seriality models and a set of parameters that describe the dose-response relations of the target and lung. Results showed that the combined effects of positioning uncertainties and breathing can introduce a significant deviation between the planned and delivered dose distributions in lung in breast cancer radiotherapy. The positioning and breathing uncertainties do not affect much the dose distribution to the CTV. The simulated delivered dose distributions show larger lung complication probabilities than the treatment plans. This means that in clinical practice the true expected complications are underestimated. Radiation pneumonitis of Grade 1–2 is more frequent and any radiotherapy optimization should use this as a more clinically relevant endpoint (Tzikas*et al*., 2012). In 2022, Zhu and her colleagues investigated the effect of stereotactic radiotherapy (SBRT) combined with thermoplastic fixation on set-up error in breast cancer (BC) patients undergoing radiotherapy.Ninety BC patients undergoing radiotherapy who were treated in their hospital (May 2019-May 2020) were selected as the research objects and equally divided into the experimental group and control group according to the order of hospitalization, with 45 patients in each group. The control group received conventional radiotherapy combined with breast bracket, and the experimental group received SBRT combined with thermoplastic fixation. The incidences of adverse reactions, 1-

year survival rates, and set-up errors were compared between the two groups. Results showed that Implementing SBRT combined with thermoplastic fixation in BC patients undergoing radiotherapy can effectively improve set-up efficiency and treatment accuracy and reduce set-up errors. Compared with the breast bracket, the combination of SBRT and thermoplastic fixation has higher application value, and further studies are conducive to providing patients with a better solution plan.

The challenge of bilateral breast cancer for the radiation oncologist is to limit the dose to multiple important organs-at-risk and reducing the chance of overlapping tangential fields to limit hotspots. Dhar *et al.*,(2022) studied a simple technique to verify the setup accuracy of breast tangential fields using the electronic portal imaging device (EPID) for bilateral breast cancer. A 74-year-old female, received postoperative radiotherapy following bilateral breast conservative surgery. Standard CT-based simulation and target delineation was done, followed by treatment planning using classical field arrangements with two separate isocenters, one for each breast (keeping identical anteroposterior and superior-inferior coordinates). The planned doses were 45 Gy/25# for whole breasts, plus tumor bed boost of 15 Gy/6# and 50 Gy/25# to left supraclavicular fossa. The study validated a simple EPID-based technique for routine use in the field matching for radiotherapy of bilateral breast cancer.

All these research carried out by the different authors had their various limitations which includes ignoring the effects of the impact of these set up errors on treatment, establishing the extent of these set up errors and evaluating the magnitude and its effects in terms of radiobiological parameters. The conclusion that Radiobiological modelling is helpful in ranking the rival treatment plans, can be used to optimize the treatment plan established for cancer patients and that as we advance in knowledge, the gEUD, TCP and NTCP will be more suitable tools to assess the treatment plans before treating the patients. No research

about dosimetric sensitivity to systematic and random set-up errors in breast EBRT in Nigeria has been done to the best of my knowledge. Based on the aforementioned research, the sensitivity of breast cancer treatments should not be as high as in the case of other types of cancer mentioned because the PTV and relevant OARs in radiotherapy of the breast are significantly larger than those in radiotherapy of other types of cancers.

CHAPTER THREE

MATERIALS AND METHODS

3.1 Equipment

The list of equipment used in this study is given below;

1 Linac (3D-CRT) (Elekta Synergy platform MLC12)

2 Treatment Planning System (TPS) (Monaco 5.11 3DCRT/IMRT/VMAT)

3 Computed Tomography Simulator (Philips Big Bore CT scanner)

4 Immobilization Device (Breast board with arm rest, head rest, knee rest)

5 Electronic Portal Imaging Device (EPID) (iView GT Elekta)

6 Records of patients from the respective hospital

7 Software used for analysis (SPSS v 26 and Windows 10)

3.2 Method

Treatment procedures such as patient selection, contouring of the target and organ at risks, immobilization, treatment simulation and planning, radiobiological assessmentwere carried out. Data were collected at each step and analysed using suitable softwares.

3.2.1 Patient Selection

Two hundred breast cancer patients that received external beam radiotherapy treatment (thirty-four had their breast intact and one hundred and sixty-six, mastectomized) at the National Hospital Abuja from December 2017 to March 2020 were consecutively identified. All patients were treated by different radiation oncologists and fell within the age range of 20 to 80 years. Once the patients were selected from the computerized treatment planning system to be transferred to the photon treatment planning system, sensitive patient information wereanonymized. Each patient was assigned a research number in the format X, where X is an index from 1 to 200. Treatment plans were carried out using treatment modalities of the LINAC with energy levels 6MV., 10MV and 15 MV for photons and 4, 6, 9, 12,15 and 18 MeV for electrons. The clinical plans were carried out on a 3DCRT/IMRT/VMATTreatment Planning System using CT scans from previously treated patients.

3.2.2 Contouring

Patients were treated in the supine position and the free breathing CT scans were obtained from the chest wall. Planning target volumes (PTV) were generated by the radiation oncologists for all original EBRT plans and subsequently transferred to the photon TPS.After importing of CT images into the treatment planning system, the Gross Tumor Volume (GTV) and Clinical Target Volume (CTV) were electronically contoured by the Oncologist and Medical Physicist. In addition to the treated region, the lung and heart were selected and contoured by the oncologist as Organs at Risk (OARs). To obtain the planning target volumes in the chest wall region, the size of margin considered was 0.5cm in all directions on CTVs, to allow for spatial uncertainties arising from setup errors and physical motions during treatment, was applied. All treatment plans were designed with 6MV LINACs by using the

Monaco 5.11 treatment planning software. The breast and the surrounding organs at risk (heart, contralateral breast and lungs) were outlinedaccording to International Commission on Radiation Units and Measurements (ICRU) Reports 50 and 62 (ICRU 1993, 2000). The volumes of these organs are shown in figure 2.4.

3.2.3 Immobilization and Simulation

All patients considered in this study were immobilized in the supine position with customized arm rest, breast board, knee rest and head rest. Radiation fields were simulated and optical fields projection were marked on the thermoplastic mold for subsequent positioning and treatment. The images were transferred to Monaco (Version 5.11 3DCRT/IMRT/VMAT) to serve as reference images for comparison with the portal images

3.2.4 Treatment Planning

In treating breast cancer, prescribed doses per fraction (PD/Fr) assigned to PTV for different patients were an average of 50/25Gy respectively for 200 patients. The selection of an appropriate energy for dose calculation depends on factors such as: tumor size, the stage of tumor, tumor depth, homogeneity or heterogeneity of tissues, density of tumor and normal tissues that are on the radiation beam's path administered for treatment planning. For all the plans, we used two tangential fields, the medial and lateral tangential with different weights at angles. For the purpose of appropriate dose coverage on the target and protecting the sensitive organs, shaping to the field by use of blocks on different fields was done and all fields according to the PTV size were shielded. All of the other parameters including beam arrangement, Number of beams, weight of beams, the dose prescription- the way of the shielding, etc., were considered.

3.2.5 Portal Imaging and Evaluation

For this study, we acquire portal images using iView GT Elekta. This is an image intensifier that captures the image of the structure on its view through a detector. It is mounted on the Linear accelerator (LINAC) with a detector size of 40x40cm. The EPID images were acquired at a reduced dose rate of 400 Monitor Unit (MU) per min and a maximum of 2MU were delivered per field for portal acquisition. A double exposure portal image of the anterior and lateral fields was obtained. For each patient portal images per field were acquired on the first day of treatment and any other day the radiologists deemed necessary. As iView GT Elekta does not have image automatic overlaying and fusion ability, the portal vision software allowed detection and quantification of the set-up error by comparison and superposition with the portal image and the reference images. The superposition was performed by achieving the best possible matching of the outlines. The anatomic landmarks of interest were the lateral, anterior-posterior and Superior-Inferior of the chest wall which were easily identifiable on both images. The considered daily set-up errors were the displacement measured between the landmarks of the DRR and the ones of the daily PIs. After demonstration of the technique by the radiation oncologists, one radiographer carried out all the measurements to avoid inter-observer variation. A radiation oncologist randomly checked 5% of all displacements and re-verified measurements in case of outliers during the process of image analysis for the purpose of documentation and analysis; anterior, superior and lateral shifts were coded as positive shifts and posterior, inferior and Left sided shifts were coded as negative shifts. Some of the potential sources of errors such as Laser alignments, display accuracy, iso-centric accuracy and jaw reproducibility were not taken into consideration. It is assumed that the routine periodic quality assurance employed for the LA would ensure minimal impact of the aforesaid

3.2.6 Organs at Risk (OARs)

The following parameters from the dose volume histograms were obtained between plans for each patient.

Organs at Risk (OARs):

1. Dose volume histogram for each organ (Ipsilateral breast, Ipsilateral lung, Heart, contralateral lung, contralateral breast).
2. Minimum, maximum and mean dose to each OAR and standard deviations with respect to portal shifts
3. Volume of lungs (ipsilateral & contralateral) receiving 2, 5, 10, 20, 50 Gy or more.
4. Volume of heart receiving 2, 5, 10, 20, 50 Gyor more.
5. Volume of breast (ipsilateral and contralateral) receiving at least 5 Gyor more

The organs at risk that we are most interested in are the lungs (ipsilateral and contralateral), heart, breast (ipsilateral and contralateral).

3.2.7 Plan Analysis

Dose Volume Histogram (DVH) metrics were extracted to compare the dose coverage of the target volumes and the dose sparing of OARs.For the comparison of treatment plans, a radiobiological based plan evaluation was also carried out. There are different models available in literature for the prediction of tumor cure and normal tissue complication probabilities. (Niermeko*et al*., 1997)**.** In this study, we used Equivalent Uniform Dose (EUD) based radiobiological modelling, which is very effective in predicting the effect of more heterogeneous dose distributions (Gay *et al*.,2007). The EUD is the uniform dose that gives the same radiobiological effect, if delivered over the same number of fractions as does the non-uniform dose distribution of interest. According to Niemierko's model, the EUD is given in equation 3.6 (Niermeko*et al*., 1999).

3.3 Radiobiological Assessment

Radiation treatment plans should not be evaluated on physical quantities alone such as the DVH values mentioned in this research but also on the radiobiological responses. It has been shown that the inclusion of non-dosimetric factors such as normal tissue complication probability and tumor control probability for organs at risk with dose volume metrics increase the predictive power of complication incidence. (Li *et al*., 2012).

3.3.1 Tumor Control Probability Calculations (TCP)

TCP is the probability that the tumor is completely eradicated. A radiation therapy plan represents a volumetric distribution of radiation dose. Tumor control probability for a tumour volume is calculated using the Webb and Brenner model (Brenner, 1993; Webb and Nahum, 1993; Li *et al*., 2012), which accounts for repopulation**.** The expression for Tumor Control Probability is given as

$$TCP = \frac{1}{1+\left(\frac{TCD_{50}}{gEUD}\right)^{4\gamma_{50}}} \tag{3.1}$$

Where gEUD = generalized Equivalent Uniform Dose.

TCD_{50} is the given dose for which we have 50% of tumor control probability.

γ_{50} is the slope of the response dose curve.

Table 3.1. Parameters used in the radiobiological models for calculation of TCP and NTCP.

Structures		**n**	**m**	**α**	γ_{50}	TCD_{50}	TD_{50}	α/β	**References**
Tumour	Breast			-7.2	2	45.75		10	Willneret al., 2002
									Guerrero et al., 2003
									Hall et al., 2000
Organs -	Heart	0.87	0.10	3	3		50	1.8-2	Emami et

at-risk (OAR)									al., 1991
	Lung	0.87	0.18	1	2		24.5	1.8-2	

3.3.2 Normal Tissue Complication Probability (NTCP)

The probability that a given dose of radiation will cause an organ or structure to experience complications considering the specific biological cells of the organ or structure. The NTCP was also calculated using the following equation

$$NTCP = \frac{1}{1+\left(\frac{TD_{50}}{EUD}\right)^{4\gamma_{50}}} \qquad 3.2$$

TD_{50} is the uniform dose given to the entire organ that results in 50% complication risk

γ_{50} is the slope of the response dose curve.

gEUD is the generalized equivalent uniform dose as given in equation 3.3

Table 3.1 lists the radiobiological parameters used for left breast irradiation in both regimens, using the EUD based model.

3.3.3 Equivalent Uniform Dose (EUD)

The concept of EUD for tumors was introduced by Niemierko, and is defined as the biologically equivalent dose which, if given uniformly, leads to the same cell kill in the tumor volume as the actual non-uniform dose distribution (Niemierko., 1997). He generalized this concept to apply to normal tissues as well. (Niemierko., 1999).The phenomenological formula used for the generalized EUD (i.e. Normal and Tumor cells) is given by

$$gEUD = \left(\sum_{i}^{N} V_i D_i^{\alpha}\right)^{\frac{1}{\alpha}} \qquad (3.3)$$

In this expression, D*i* is the dose in the ith voxel.

"α" is a tissue-specific parameter that describes the volume effect.

V_i is fractional organ volume receiving a Dose of D*i*.

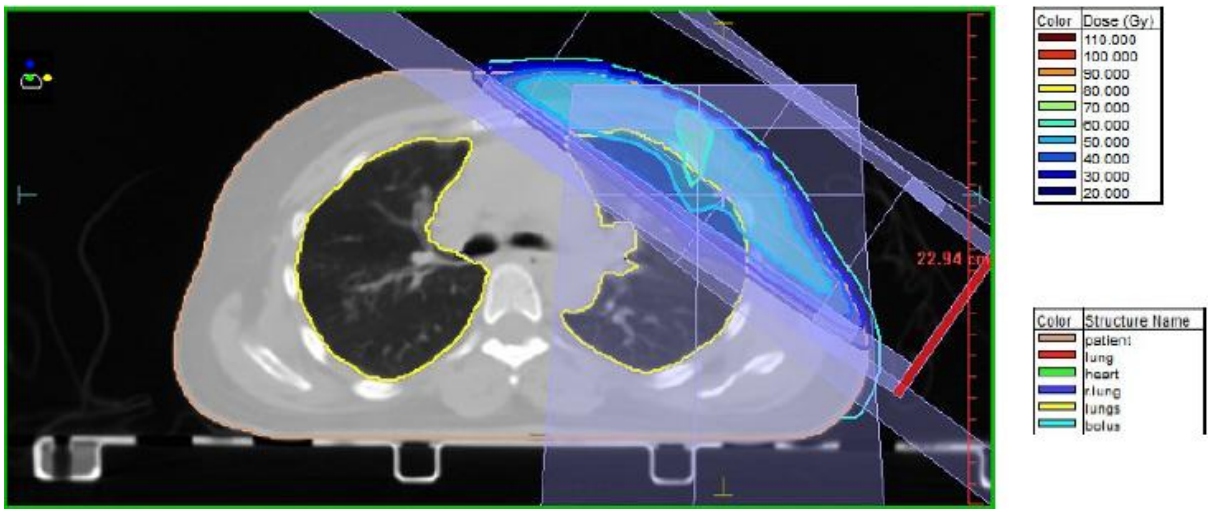

Figure 3.1. A sample of a contoured patient volume used in this study, PTV, lungs and heart.(National Hospital Abuja, Nigeria).

3.3.4 Patient Set-up Errors

Set-up errors are a combination of systematic and random errors. Systematic error was calculated as the average deviation of a particular reference structure between simulation and treatment and is given by:

$$\sum = \frac{\sum_{i}^{N} \Delta_i}{N} \tag{3.4}$$

where N is the total number of portal images acquired for a particular field, and Δ_i is the calculated deviation from the ith treatment fraction.

Random errors(δ) were calculated for each treatment fraction as the standard deviation (SD) of the systematic error for a given anatomical feature from the average deviation. The random error may be calculated individually for each patient and each direction, and it is calculated as:

$$\delta = \sqrt{\sum_{i}^{N} \frac{\left(\Delta_i - \Sigma\right)^2}{\left(N-1\right)}} \tag{3.5}$$

3.3.5 Margin Calculation

An optimum margin is the aperture that ensures the dose received by the target with the least possible amount of irradiation to the normal tissue. In this study, the margin was calculated according to the formula proposed in the62nd report of the International Commission on Radiation Units and measurement(ICRU 62) and formulas proposed by other authors given as;

$$ICRU\ 62 = \sqrt{\sum^2 + \delta^2} \quad (3.6)$$

$$Stroom\ = \sqrt{2\Sigma_{group}\ + 0.7\sigma_{group}} \quad (3.7)$$

$$Van\ Herk = \sqrt{2.5\Sigma_{group}\ + 0.7\sigma_{group}} \quad (3.8)$$

$$McKenzie = 1.3\Sigma_{group}\ + 0.7\sigma_{group} \quad (3.9)$$

3.4 Statistical Analysis

Data obtained for patient set-up errors were analyzed using the Statistical Package for Social Sciences (SPSS version 26). Dose information was collected to evaluate PTV coverage and doses to OARs. Mean dose (Dmean), maximum dose (Dmax), dose to 50%, 75%, 90% and 98% were reported for PTV coverage comparisons. Dmean, Dmax, and volumes receiving specific doses were calculated for the OARs. Comparisons of dose-volume data for the technique used in this study was made by t-test. P value <0.05 was considered statistically significant. Data was analyzed by calculating means, range, median, and standard deviations. The data were presented as the mean ± SD. Windows was used for the analysis.

CHAPTER FOUR

RESULTS AND DISCUSSION

4.1 Results

4.2 Systematic and Random Errors Quantification

Systematic (Σ) and random (σ) errors were calculated using Equations 3.7 and 3.8. The systematic component of the displacement represents displacement that was present during the entire course of treatment. For an individual patient, the systematic displacement was assessed by mean values of all the displacements and for the whole population, the systematic error was represented by the standard deviation (SD) from the values of mean displacement for all individual patients. The random errors represent day-to-day variation in the set-up of the patient. For each patient, dispersion around the systematic displacement was calculated to assess the random displacement. For the whole population, the distribution of random displacements was expressed by the root mean square of SD of all patients. The population

systematic error (Σ) in Lateral (L), Anterior Posterior (AP) and Superior Inferior (SI) direction were 6.61, 4.61 and 11.43 mm respectively. The population random error (σ) in the corresponding directions were 4.77, 3.85 and 8.17 mm respectively. The overall mean in the corresponding directions were 6.30, 4.43 and 10.99 mm respectively. Table 4.1 present the results summary of the systematic, random and margin components.

Table 4.1: Parameters to describe set-up errors and margin calculations in the Lateral, Anterior- Posterior and Superior-Inferior directions. All values are in mm.

		Lateral	**Anterior-Posterior**	**Superior-Inferior**
1	**Population Set up error**			
	Overall Mean	6.30	4.43	10.99
	Random component (δ)	4.48	3.86	8.16
	Systematic component ($\boldsymbol{\Sigma}$)	6.61	4.61	11.43
2	**Margin Calculation**			
	1 C R U 62	7.98	6.01	14.06
	Stroom*et al.*,1999	4.04	3.31	6.26
	Van Herk *et al.*,2000	4.43	3.59	5.33
	Mc Kenzie *et al.*,2000	3.29	2.71	4.04

4.3 Margin Calculation

The CTV-PTV margins were calculated using Equations 3.9-3.12. Using Equation 3.9, the values of the CTV-PTV margin in the L; AP; and SI direction were 7.98, 6.01 and 14.06 mm respectively. The corresponding values were 3.29, 2.71 and 4.04 mm using Equation 3.10 and 4.04, 3.31 and 6.26 mm with Equation 3.11. The variation in the margin values is as a result of the definition by the different authors such as Stroom et al in 1999 who defined a margin as one that covers 99% of the CTV with a dose of 95% and Van Herk et al (2000) as one that yields a minimal dose to the CTV of 95% for 90% of the patient's population.Random errors blur the dose distribution whereas systematic errors cause a shift of the cumulative dose distribution relative to the target. In fact, it has been consistently shown that systematic errors are of higher dosimetric consequences than random errors. Stroom's margin recipe $(2\Sigma + 0.7\sigma)^{1/2}$ ensures that on an average, 99% of the CTV receives more than or equal to 95% of the prescribed dose. The formula by Van Herk $(2.5\Sigma + 0.7\sigma)^{1/2}$ seems to be the most

appropriate as it ensures that 90% of patients in the population receive a minimum cumulative CTV dose of at least 95% of the prescribed dose. Owing to the anatomy of the breast region, the internal target motion was considered negligible. The PTV margin was calculated using Equation 3.9 and was found to be equal to 3.29mm, 2.71mm and 4.04 mm in the corresponding directions.

4.4 Displacements in the Lateral, Anterior-Posterior and Superior-Inferior Directions

The displacements in 140 portal images taken before treatment of the subjects considered in this study were measured. Equations (3.7–3.8) were used to calculate the systematic set-up deviation for a patient P, the random set-up deviation for a patient P, the overall mean systematic errors, the random set-up errors for all the patients and the systematic set-up errors for all the patients respectively as presented in Table 4.1.

The distribution of the breast set-up deviations at lateral (L), superior-inferior (S-I) and Anterior-Posterior (AP) directions are depicted in Figure 4.1 As shown in the figure, the redundancy of displacements in the directions is within −5 to >20 mm.

Figure 4.1 shows the distribution of the interfractional patient set-up errors for the breast; the displacements ($\boldsymbol{\mu}$) of the co-ordinate of the breast between the digitally reconstructed radiograph (DRR) and imaging portals plotted for thelateral (L), anterior-posterior (A-P) and Superior-Inferior (S-I) directions.

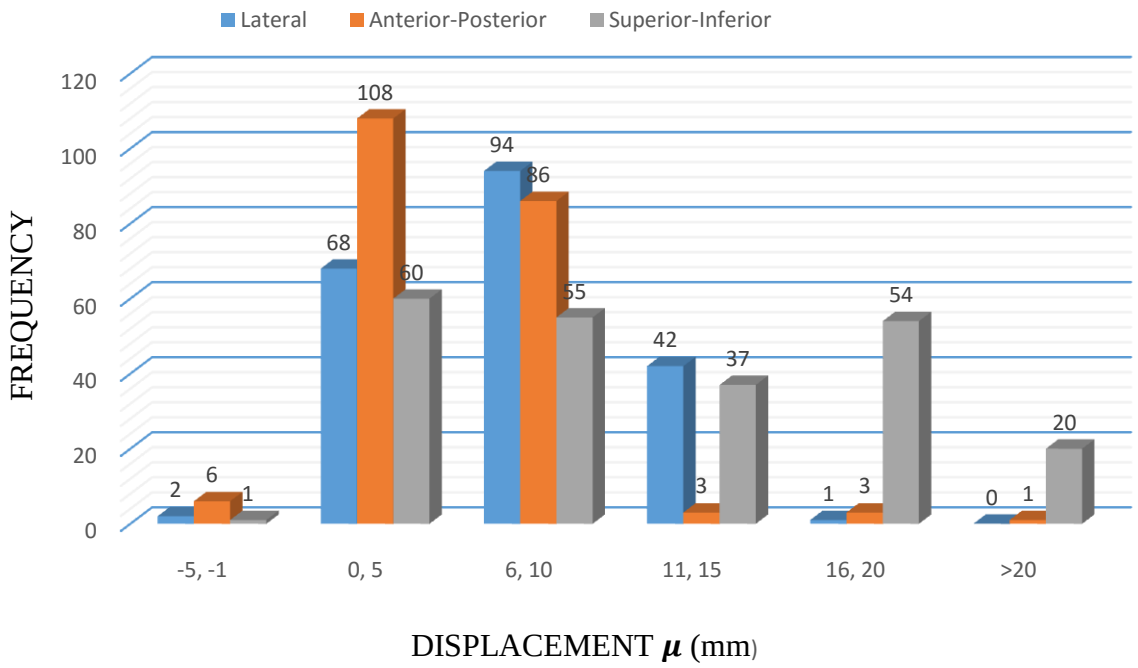

Fig 4.1: Displacement Frequency in the Different Direction

Unlike other software used in portal devices, iView GT Elekta is not equipped with anatomy matching and fusion module. Therefore, image analysis was done by comparing the reference simulator image with portal images using fixed bony landmarks, a very good surrogate for breast cancers. To avoid the possibility of variation in manual measurements, two different points were used for evaluation of displacements in the lateral, anterior-posterior and superior-inferior direction. In validating the results obtained, online digital measurements were compared with manual measurements. Emphasis was laid on the technique of manual measurements by precisely choosing the same points on reference and portal images. To ensure the quality of image analysis, random cross checking, by a radiation oncologist were carried out.

Figure 4.1show that large deviations occurred in all three directions and this is largely due to the lack of portal images for most of the subjects considered in this study. This lack of portal images was largely due to the inexperience of the radiotherapists on how to extract portal

images from the electronic portal imaging device. Fig 4.1 shows that 66% (137 out of 207) of the population treated for breast radiotherapy had a deviation beyond the recommended standard value in the lateral directionwhich is intolerable. Set up errors of this order can potentially lead to significant reductions in clinical target volume coverage as well as increase the tolerance dose to organs at risk. A deviation in the direction of the lateral tangential for breast radiotherapy has serious effects on the lungs. The results of this study implies that 66% of the patients will have serious lung complications. In the Anterior-Posterior direction, it is observed that 44.92% of the patient population had a deviation exceeding the 5mm range and the dosimetric consequences of this is that more dose goes to the media sternum and can have serious health implications. The Superior-Inferior direction shows that 80.2% of the population had a deviation exceeding the 5mm range. This is highly intolerable as it implies that a deviation to the inferior border leads to unacceptable accumulation of radiation dose to the liver while that to the superior border leads to dosimetric consequences that can affect the head of humerus.

A major drawback of this study as mentioned earlier was the lack of automatic anatomy matching and image fusion facilities in iView GT elekta portal imaging device which could have resulted in reduction in the accuracy of measurements. However, to compensate for this, an attempt was made to manually verify measurements using appropriately scaled out print outs on graph paper. Secondly, for systematic and random errors to be reduced greatly, an average minimum of four portal images per patient on a weekly basis is required. More than half of the patients considered in this study had no portal images taken during treatment while others had a maximum of just two portals taken for the entire course of treatment. Thirdly, this study did not attempt to measure rotational errors or intra fraction displacements because Electronic Portal Imaging Devices (EPID) can only quantify systematic and random errors but are unable to detect or quantify rotational errors.

The set-up accuracy which is not comparable with standard is also a reflection of the experience and training of the radiation therapy staff. Even though there is a high commitment on the part of the radiation therapy staff to treat patients, there is paucity of skills and experience on the use of portal imaging device for proper patient positioning which resulted in the lack of use of this equipment and hence results in a wide systematic and random error which leads to a high dosimetric consequence on patients.

In the analysis of magnitudes and directions of all displacements (n=207) for the lateral fields, 0.96% ≤ -5mm to -1mm, 32.85% $\leq 0mm - 5mm$, 45.41% $\leq 6mm - 10mm$, 20.29% $\leq 11 - 15mm$, 0.48% $\leq 16mm - 20mm$ and 0% >20mm. In the AP direction, the corresponding values were 2.89% ≤ -5mm to -1mm, 52.17% $\leq 0mm - 5mm$, 41.54% $\leq 6mm - 10mm$, 1.45% $\leq 11mm - 15mm$, 1.45% $\leq 16mm - 20mm$ and 0.48% >20mm. For the S-I direction field, 0.48% ≤ -5mm to -1mm, 28.98% $\leq 0mm - 5mm$, 26.57% $\leq 6mm - 10mm$, 17.87% $\leq 11mm - 15mm$, 26.08% $\leq 16mm - 20mm$ and 9.66% >20mm (Table 4.2).

Table 4.2. Magnitude and directions of all displacements of the electronic portal images compared with the digitally reconstructed radiographs

≤ -5,1mm		**≤0,5mm**	**≤ 6,10mm**	**≤11,15mm,**	**≤16,20mm**	**>20mm**
L	0.966%	32.85%	45.41%	20.289%	0.48%	0%
A-P	2.89%	52.173%	41.54%	1.45%	1.45%	0.48%
S-I	0.48%	28.98%	26.57%	17.87%	26.08%	9.66%

These results show that for all directions, more than half of the subjects considered in this study had a deviation that exceeded the 5mm recommended margin. This has serious dosimetric consequences as unwanted radiation dose might be delivered to the lungs, heart,

liver, mediasternun and the head of femur thereby under-dosing the target organ. This can lead to treatment induced death rather than disease induced fatalities. At National Hospital, the action level considered is 5mm and this is in line with the ICRU 62 guideline for margins considered for breast cases. However, the findings from this thesis demonstrates that 66.2,44.9 and 80.2% set up deviation in the lateral, Anterior-Posterior and Superior-Inferior directions respectively exceeded the 5mm range. Only about 33, 55 and 29 % were within the 5mm range for the L, A-P and S-I directions. This is intolerable when compared with the ICRU 62 guideline for margins considered for breast cases. The reason for this difference could be as a result of not acquiring daily electronic portal reference images.

Table 4.3 represents a comparison between the results obtained of present study with similar works. As seen in table 4.3, there is no good agreement between this study's data and other similar studies. This is as a result of the fact that out of 207 subjects considered in this study, less than 1% (0.48%) had only 3 portals, 19.8% had only 2 portals, 26.1% had 1 portal and 53.6% had no portals at all. All these portals were recorded for the entire course of treatment. In the case of the studies compared with this study, more than 90% of the subjects had at least 12 portals taken throughout the entire course of their treatment schedules. Another reason could be lack of regular use of lasers for proper patient alignment with the beam of radiation from the linear accelerator. Comparing the Digital Reconstructed Radiographs (DRRs) with the portal images taken is vital to reducing errors and achieving more reliable results. In all of the studies compared in Table 4.3, the set-up accuracy in radio-therapeutic treatment was assessed and this depends on the treatment site, portal images taken, the device of immobilization and the institution involved. In this studies, set up errors were quite large and exceeded the 5mm. The major contributory factor to this was the lack of the use of portal images which was largely due to lack of knowledge on the use of this device by the staff of the institution. Only 1 patient had 3 portals, 41 patients had just two portals, 54 patients had

only 1 portal and 111 had no portals during the entire course of treatment. According to the ICRU 62 recommendation, every patient should at least have 4 portal imaging every week. Ideally, each patient considered in this study should have a minimum of 15 portals throughout the course of treatment but this was clearly not the case.

Table 4.3: Population systematic (Σ) and random (σ) errors of selected contemporary studies and correlation with probability of target volume coverage

Studies (Year)	**Σ(mm)**	**σ(mm)**	**Displacements or Errors**	**Place of Study**	**Type of Machine used**	**Frequency of electronic portal images taken**
Mourik (2011)	L,0.13 C-C, 0.14 A-P, 0.15	L 0.3 C-C 0.29 A-P 0.38	<2% not within standard margin	The Netherlands Cancer Institute	Intensity Modulated Radiation Therapy (IMRT)	Daily
Alderliesten (2012)	L ,1.6 C-C, 1.6 A-P, 1.6	L 1.3 C-C 1.3 A-P 1.3	100% within standard margin	The Netherlands Cancer Institute	Cone-Beam Computed Tomography (CBCT).	Daily
Jain (2008)	L,5.7 V, 2.8 L, 2.3	L3.9 V3.5 L3.2	Not reported	Radiation Oncology Centre, University of Manchester	Intensity Modulated Radiation Therapy (IMRT)	Daily
Shah (2012)	A-P, 4.1 S-I, 2.7 L, 2.6	A-P 3.2 S-I 2.2 L 2.2	100% within standard margin	M.D Anderson cancer centre Orlando, Florida	3 Dimensional surface imaging	Daily
Thomsen (2014)	FF,1.1 LF, 1.4	FF, 1.5 LF, 1.7	97.3% within standard margin	Aarhus University Hospital, Denmark	Image-Guided Radiotherapy (IGRT)	Daily
Noghreiyan (2019)	CL(AP),0.49 L(AP), 0.24 DV (L), 0.27 CL(L), 0.38	CL(AP),0.27 L(AP), 0.15 DV (L), 0.16 CL(L), 0.23	95% within standard margin	Imam Reza Radiation Oncology Center (Mashhad,Iran	3-Dimensional Conformal Radiotherapy (3DCRT	Daily
Present study	L, 6.61 A-P, 4.61 S-I, 11.43	L, 4.48 A-P, 3.85 S-I, 8.17	80% displacements not within standard margin	National Hospital Radiotherapy Centre, Abuja Nigeria.	3D-Conformal Radiotherapy Technique	Electronic portals rarely taken

L=Lateral, V= Vertical, L= Longitudinally, A-P=Anterior-Posterior, S-I= Superior-Posterior, CC=Cranio-Caudal, FF=First field, LF=Last field, CL=Caudocranial longitudinal, DV=Dorsoventral Vertical.

Table 4.4: Dose limits for the OARs during breast radiation therapy planning

Organ	**Dose Constraints**
Ipsilateral Lung	$D_{mean} < 10Gy$
Contralateral Lung	$D_{mean} < 10Gy$
Heart	$D_{mean} < 4Gy$ $D_{max} < 40Gy$

Contralateral Breast	$D_{mean} < 2.5Gy$ $D_{max} < 3Gy$

Danish Breast Cancer Cooperative, accessed June 2012, www.dbcg.dk.

4.5 Dosimetric Analysis

The dosimetric results for the target and organ at risk for 3D-CRT plan with the mean valuesand standard deviation are presented in appendix Iand Fig 4.2 (a-c). The plan meets the target constraint that 95% of the PTV breast must receive at least 95% of the prescription dose.The p values for multiple comparisons using one sample T test are also presented.From Table 4.4and Fig 4.2(a-c), it was observed that, both the mean dose of the contralateral lung, ipsilateral lung and the heart were significantly lower when compared with the contralateral breast (0.210Gy, 0.336Gy, and 0.371Gy Vs 0.49Gy) respectively. The mean dose to the CB is significantly higher when compared to the other OARs (heart, CL and IL).

Similarly, the mean dose to the target organ (IB) is significantly lower than that of the OARs (CB, IL, CL and heart). The mean minimum dose and maximum dose in the contralateral lung is significantly lower than for all the organs (9.587Gy, 1.028Gy) respectively. The value for maximum dose (Dmax) for the ipsilateral breast is higher than all the other organs except for the contralateral breast. However, the ipsilateral breast produced a higher value for the minimum dose (Dmin) when compared to the other organs. A significant difference is observed in the values for D_{50}, D_{75}, D_{90}, D_{98} for the Ipsilateral breast and the organs at risks with the heart having the lowest mean value as seen in appendix I.

Fig 4.2(a-c)shows that all patients received doses within the standard dose constraint recommended by Radiation Therapy Oncology Group (RTOG) as seen in Table 4.4 to the CB, IL, CL and heart excluding five and twelve patients exceeded the recommended RTOG

constraints to the heart and contralateral breast respectively indicating that the organs would be affected negatively.

Figure 4.2 (a-c);presentsparameters calculated for the target organ and OARs in 3D-CRT.The mean values of the minimum, maximum and mean dose of a**)** Ipsilateral Breast (IB) and Contralateral Breast (CB)**.** b**)** Ipsilateral Lung(IL) and Contralateral Lung (CL)c)The Heart.

x; mean, max, min

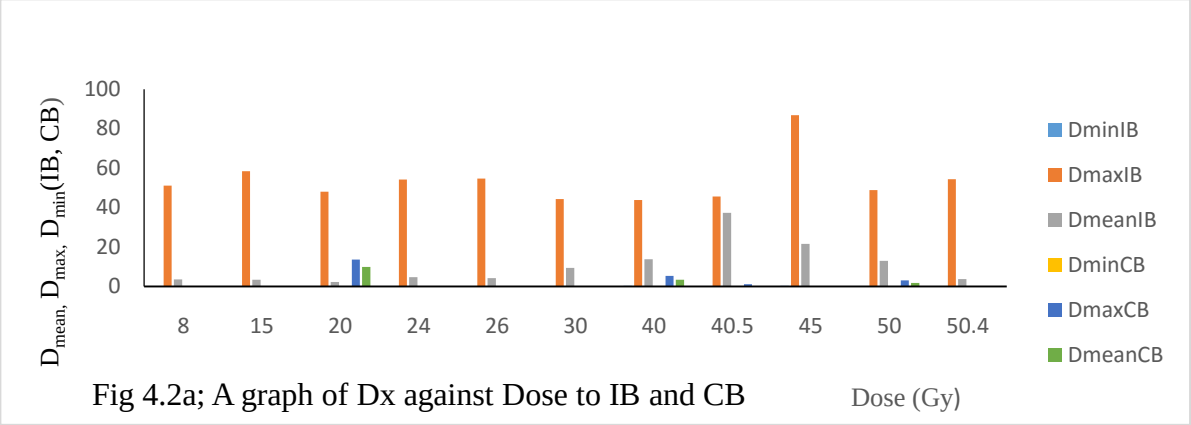

Fig 4.2a; A graph of Dx against Dose to IB and CB

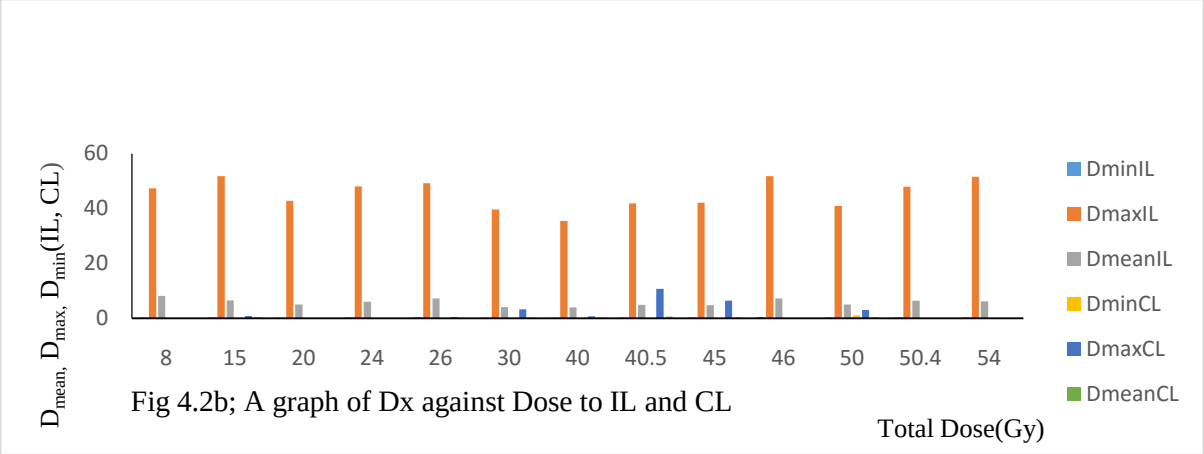

Fig 4.2b; A graph of Dx against Dose to IL and CL

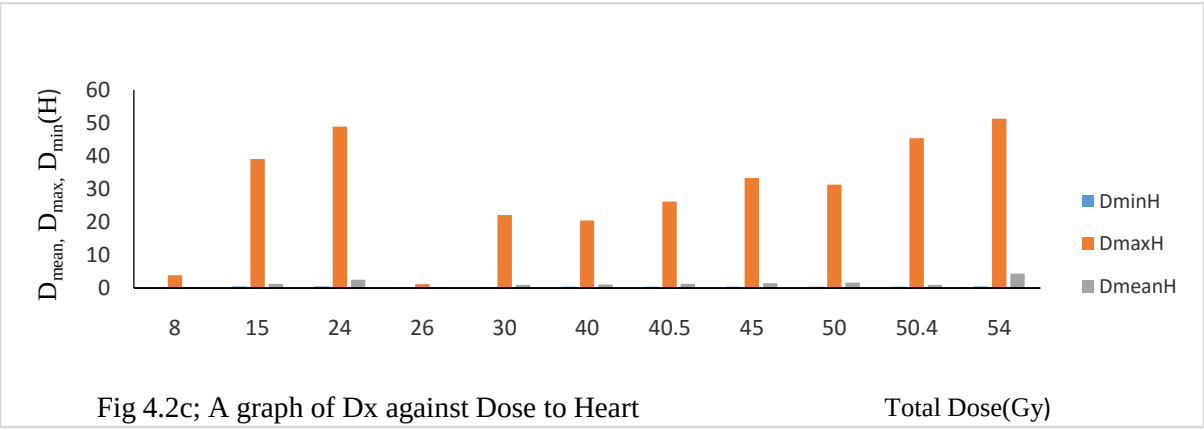

Fig 4.2c; A graph of Dx against Dose to Heart

Figure 4.2 (a-c)gives the dose of 50%, 75%, 90% and 98% volume of the heart, Ipsilateral Breast(IB), Contralateral Breast(CB), Ipsilateral Lung (IL) and Contralateral Lung (CL). It is

observed that the mean dose to 50%, 75%, 90% and 98% of the planning target volume was generally lower in the heart and contralateral lung with no significant differences between these two and significantly higher in the ipsilateral lung and ipsilateral breast. The values for the heart are acceptable values according to RTOG and ICRP and unacceptable for values in the IL.

Figure 4.3(a-c**)** presents parameters calculated for the target and OARs. a) the dose of 50%, 75%, 90% and 98% volume of the heart. b) the dose of 50%, 75%, 90% and 98% volume of the ipsilateral breast and contralateral breast c) the dose of 50%, 75%, 90% and 98% volume of the ipsilateral lung and contralateral lung. (x=50, 75, 90 and 98).

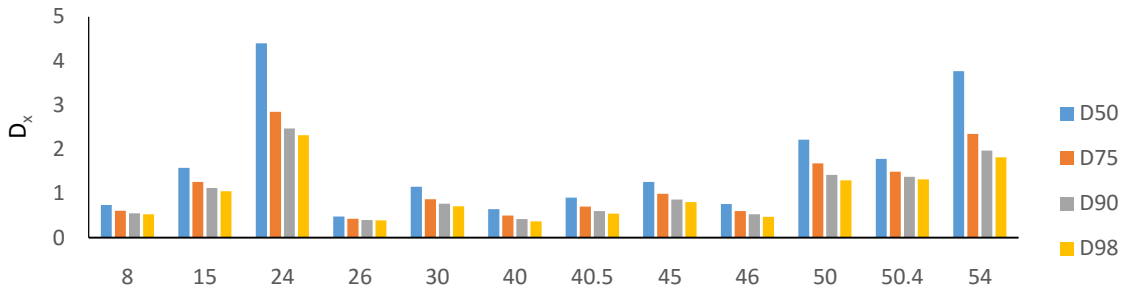

Fig 4.3a; The dose of 50%, 75%, 90% and 98% volume of the heart.

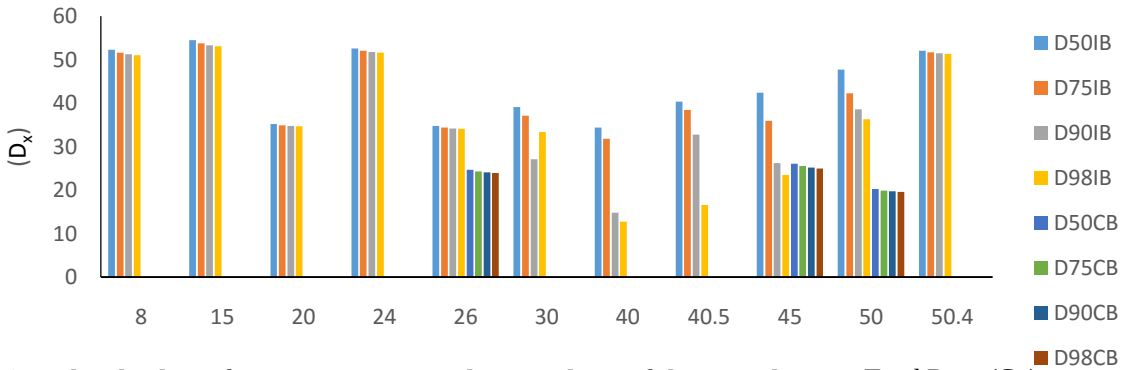

Fig 4.3b; The dose of 50%, 75%, 90% and 98% volume of the IB and CB

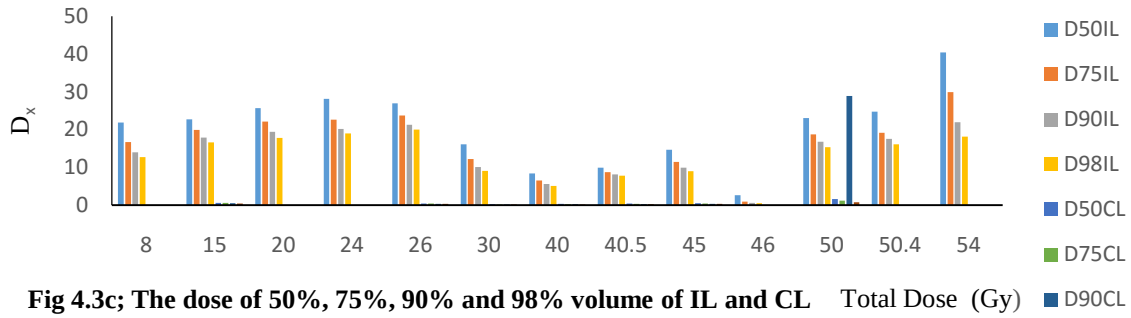

Fig 4.3c; The dose of 50%, 75%, 90% and 98% volume of IL and CL

Table 4.6 gives an evaluation report of the treatment plans using different radiobiological models. An evaluation of the treatment plans using the radiobiological indices (NTCP and TCP) reveals that the treatment plans have lowtumor control, with small normal tissue complication probability. The calculated NTCP for the heart and combined lungs was 0.99% and 1% respectively for values at D_{50}, D_{75}, D_{90} and D_{98} respectively. This model (LKB) gives a high value for the heart and lungs. These values are however within the Quantitative Analysis of Normal Tissue Effects in Clinic (QUANTEC) value of 1% for the heart and 5% to the lungs. In addition, the TCP values for the Contralateral breast and Ipsilateral Breast were quite very low as seen in Table 4.6.This low TCP corresponding with low NTCP implies that the treatment plans for the breast cases handled in this study were poor.

Table 4.6. NTCP and TCP analysis for the different organs

Parameter	Organs		p-Value
NTCP(%)	Heart	Combined Lungs	
D50	0.99	1	< 0.05
D75	0. 99	1	< 0.05
D90	0.99	1	< 0.05
D98	0.99	1	< 0.05
Parameter	Organs		p-value
TCP(%)	Contralateral Breast	Ipsilateral Breast	
D_{50}	3.02E-21	1.53E-21	< 0.05
D_{75}	2.68E-24	1.23E-23	< 0.05
D_{90}	5.80E-26	8.31E-26	< 0.05
D_{98}	5.98E-27	6.75E-32	< 0.05

NTCP; Normal Tissue Complication Probability, TCP; Tumor Control Probability; D_{50}, D_{75}, D_{90}, D_{98}; dose that goes to 50%,75%,90% and 95% of the planning target volume.

Fig 4.4;(a-c)Show the relationship between gEUDand volume of the CL irradiated and between gEUD and volume of the heart irradiated.

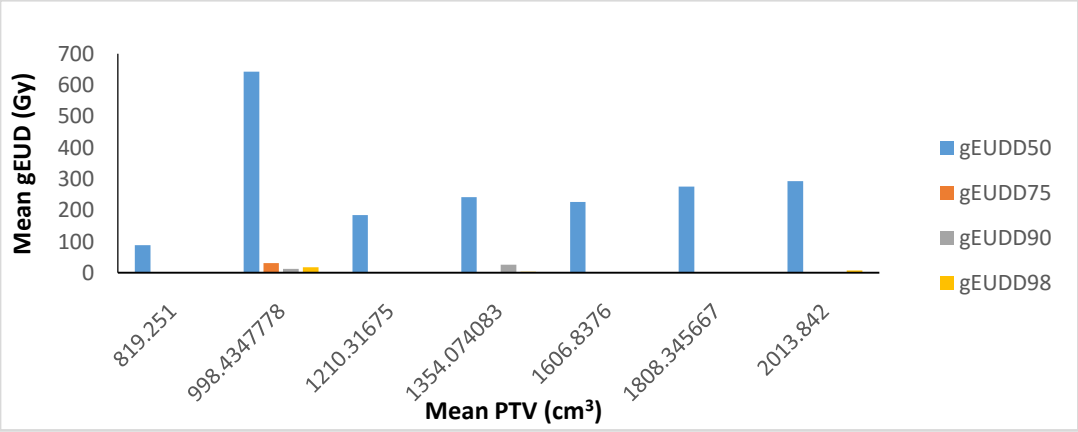

Fig 4.4(a): Relationship between gEUD and volume of the CL irradiated

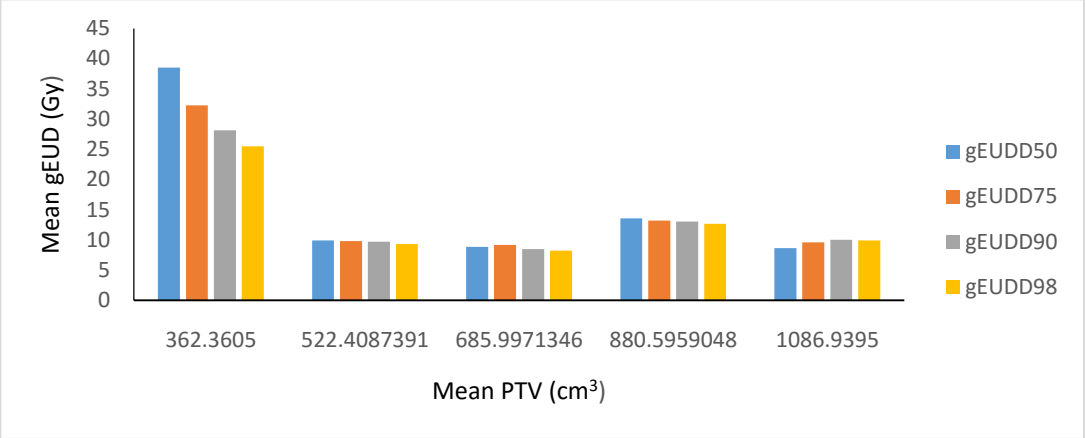

Fig 4.4(b): Relationship between gEUD and volume of the heart irradiated.

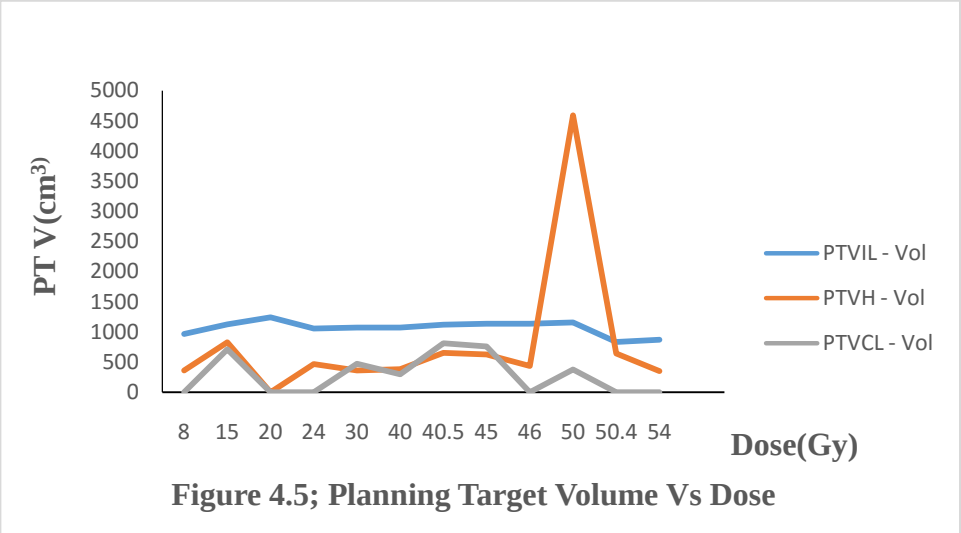

Figure 4.5; Planning Target Volume Vs Dose

In showing the relationship between gEUD and volume of the heart irradiated, Figures 4.4(a-b)shows that there is a positive relationship between volume of organs irradiated and gEUD. In Figure4.4(a-b), it is observed that the volume range (1901-2100), (901-1100), (1301-1500) and (901-1100) had a higher value of gEUD at D50, D75, D90 and D98 respectively. While at low doses the volume range (700-900), (900-1100), (1100-1700) and (1701-1900) had a lower value of gEUD at D_{50}, D_{75}, D_{90} and D_{98} respectively; indicating that when irradiating the breast, it is safer to irradiate the CL at smaller volumes than at larger volumes.

Interestingly, the results in 4.4(a-b)shows that at higher value of gEUD at D_{50}, D_{75}, D_{95} and D_{98}, it is safer to irradiate the heart at higher volumes than at lower volumes during breast treatment.

Figure 4.5shows the distribution of the maximum dose to the planning target volume(PTV) of the Organs at Risk (paired lungs and heart). The majority of the patients PTV were exposed to a mean dose of 50Gy to the heart; 20-50Gy to the ipsilateral Lung and 40.5-45Gy to the contralateral lung. This shows that the heart received a higher maximum dose than the combined lungs. The maximum dose to the contralateral lung was generally the lowest. In 3D-CRT, the heart is exposed to doses <40Gy. However, we realized that there is no achievable safe dose.

4.5.1 Dosimetric Evaluation

The overall objective of this retrospective study is to check the acceptability of treatment plan by incorporating radiobiological evaluation tools. The physician considers the delivered dose to the target volume, along with the side effects of radiation to the surrounding healthy tissues. The final decision on treatment planning is usually dependent on the tumor position, the extent of the disease, the physician's preference of the estimates of treatment and its complications. The goal of radiotherapy therefore, plays an important role in maximizing tumor control and minimizing normal tissue toxicity. Radiotherapy treatment plans are generally assessed by evaluating the 3D dose distributions calculated by a treatment planning system by analyzing the dose distribution superimposed on images of the patient anatomy and by examining DVHs, which are 2D representation of 3D dose information, for each organ or tumor volume of interest (Varadharajan*et al*., 2014).

The difficulties encountered in 3D-CRT are heterogeneous dose distribution, hot or cold spots due to irregular breast contour, normal tissue protection and difficulty in establishing dose consistency and dose homogeneity. The 3D-CRT technique is superior to other

techniques in low doses regarding normal tissue, integral dose, and duration of treatment (Hensen*et al*., 2013). Although, dose-adjusted RT with dose escalation, increased homogeneity in PTV, increased dose conformity, protection of critical organs such as the heart, lung, significant reductions in early and late effects and successful cosmetic results demonstrate that this technique is advantageous; patient positioning, increase in organ contingency amongst other factors, are seen as disadvantages of this technique (Zhao *et al*., 2015).

In this study, 200 patients hadirradiation to whole breast following breast conservation surgery with 3DCRT technique at National Hospital, Abuja during the study period. All patients were treated with tangential breast fields and an anterior field for supraclavicular fossa in node positive patients. The organ at risk doses that were assessed in this study includes dose to ipsilateral lung, heart, contralateral lung and contralateral breast. DVH indices were compared to assess the dose coverage for target volumes and the dose sparing for OARs. The value of NTCP and TCP was calculated with previously published models to assess effect on the organ at risk.

Our analysis from Fig 4.2(a-c) and Table 4.4 shows that there is a good balance of the dose sparing of OARs with the standard dose constraint. Taylor *et al*., (2015) published a review article on heart dose in breast cancer, summarizing 149 articles and 398 regimens, showing that the mean heart dose was 5.4Gy (range between 1.6-8) in the 3D breast cancer radiotherapy. The values obtained in this study was 0.37Gyfor 3D-CRT which was below the lower limit of Taylor's article. The value obtained in the study by Adam et al., (2015) for the mean and maximum heart dose in the 3D technique were 13 Gy and 51Gyrespectively, which were higher than the values in this study for 3D-CRT(Table 4.4). From Table 4.4, it is seen that the recommended mean and maximum dose constraints for the heart is <4Gy and <40Gy respectively indicating that the results of this study falls within the dose constraints thereby

posing acceptable heart complications. Ohashi *et al*., (2009) claimed that cardiac complications would be minimized if the heart receives less than 26Gy. This reduced mean and maximum dose value may be because of the appropriate shield of the heart during treatment planning of the breast.On the other hand, Fig 4.2 (a-c)shows that the dose absorbed by 50%, 75%, 90% and 98% of the planning target volume and OARs are within the standard dose constraints except for the ipsilateral lung whose values are generally higher than the recommended values indicating that the ipsilateral lung is prone to unacceptable complications.

The probability of normal tissue complications for the heart in this study is calculated to be 0.998 (Table 4.6) which has a statistically significant difference between the different doses ($p<0.05$).This is consistent with the study by Astudillo*et al*., (2015)who reported 0-1 for heart NTCP and in agreement with the information in Fig4.2(a-c) showing that the heart is not within acceptable complications.According to the protocol published by the RTOG, the mean dose for the combined lungs for breast radiotherapy should be less than 10Gy. The values obtained from this study is consistent with the RTOG protocol indicating that a very low complication would arise from the lung with a low probability of lung complications such as pneumonitis and fibrosis.

Table 4.6 also shows the results of the TCP values for the IB and CB. Comparing these values, it is observed that the TCP values for CB and IB are generally low for values of D_{50}, D_{75}, D_{90}, D_{98}. By dosimetric analysis, this treatment plan did not achieve better tumour control and delivered lower doses than required to the target organ. This may lead to further proliferation of the tumor to nearby organs.From the information from Figure 4.4a**,** it is observed clearly that irradiating the CL at small volume during breast treatment is safer as this ensures that smaller doses are administered to the CL. However, Fig 4.4bshows that at higher value of gEUD at D_{50}, D_{75}, D_{95} and D_{98}**,** it is safer to irradiate the heart at higher

volumes than at lower volumes during breast treatment. Figure 4.5shows the distribution of the maximum dose to the planning target volume(PTV) of the Organs at Risk (paired lungs and heart). The majority of the patients PTV were exposed to a mean dose of 50Gy to the heart; 20-50Gy to the ipsilateral Lung and 40.5-45Gy to the contralateral lung. This shows that the heart received a higher maximum dose than the combined lungs.

In this study therefore, 3D-CRT is compared based on dosimetric and radiobiological evaluations. We sought to compare the minimum, maximum and mean doses absorbed by the organ at risks during breast radiotherapy with the QUANTEC and RTOG protocol in order to generate better radiotherapeutic plans to guide clinical decision-making. Various DVH parameters were commonly used to evaluate treatment plan in clinical practice (Zhang *et al*., 2018,Wang *et al*., 2013, Martin*et al*.,2011). However, the radiobiological analysis in view of the DVH curve as a whole might play a more critical role in determining the overall quality of treatment plan. To date, there is little or no data of published articles which is based on dosimetric and radiobiological evaluation on radiotherapy plans in Nigeria. Therefore, the radiobiological parameters such as TCP and NTCP were also calculated in this study. As reported in this study,all patients received mean and maximum doses within the standard dose constraint recommended by RTOG to the CB, IL, CL and heart. However, a few patients exceeded the recommended RTOG constraints to the heart and contralateral breast respectively indicating that the organs would be affected negatively. For doses administered to 50%, 75%, 90% and 98% volume of the heart, IB, CB, IL and CL respectively, we observed that the values for the heart are acceptable according to RTOG and QUANTEC and unacceptable for values in the IL**.** Additionally, the relationship between gEUD and volume of the OARs irradiated, indicates that when irradiating the breast, it is safer to irradiate the CL at smaller volumes than at larger volumes and to irradiate the heart at larger volumes than at smaller volumes. Similarly, in the distribution of the maximum dose to the Planning Target

Volume of the combined lungs and heart, we realized that there is no achievable safe dose.In order to strengthen the reliability of our data, three independent predicting models were utilized in our study. Interestingly, we observed the similar trends of TCP and NTCP, and then further confirmed our results reliable. Taken together, we strongly suggest radiobiological evaluation should be widely adopted in clinical settings to cover the deficiency of dosimetric analysis.

CHAPTER FIVE

SUMMARY, CONCLUSIONS AND RECOMMENDATIONS

5.1 Summary

The findings from this study provided information on the systematic and random errors in radiotherapy in terms of the generalized equivalent uniform dose, Normal Tissue Complication Probability and Tumour Control probability. The analysis was carried out using windows and the SPSS technique. Systematic and random errors were quantified using equations from the ICRU as well as from authors adopted from literature. The key findings from this study include the following;

1. The systematic error (Σ) in Lateral (L), Anterior Posterior (AP) and Superior Inferior (SI) direction were found to be 6.61, 4.61 and 11.43 mm respectively while the random error (σ) in the corresponding directions were 4.77, 3.85 and 8.17 mm respectively. These values deviate from the international recommended standard.
2. The PTV margin was found to be equal to 3.29mm, 2.71mm and 4.04 mm in the corresponding directions.Thedisplacement between the DRR and imaging portals plotted for thelateral (L), anterior-posterior (A-P) and Superior-Inferior (S-I) direction obtained showsa wide variation from the recommended values and this mainly due to the inexperience of the radiotherapists to extract portal images from the Electronic Portal Imaging Device implying that complications may arise at the organ at risks

situated at the Lateral (L), Anterior Posterior (AP) and Superior Inferior (SI) directions.

3. Comparing this study with similar studies showed that no good agreement exists between this study's data and other compared work which is due to the fact that more than 50% had no imaging portals taken.
4. Even though all patients received doses within the standard dose constraint recommended by Radiation Therapy Oncology Group (RTOG) to the CB, IL, CL and the heart, a few patients exceeded the recommended RTOG constraints to the heart and contralateral breast which has negative consequences to the organs.
5. Comparing the values of the IB and CB, this study shows that the TCP values for CB and IB were generally low which by dosimetric analysis implies that the treatment plan did not achieve a better tumour control. This could potentially harm the other organ at risks considered in this study.

In summary, the results from this study shows that radiobiological evaluation if adopted in clinical settings will cover the deficiency of dosimetric analysis as it enables treatment to be more precise and accurate with minimal errors in patient position set-up.

5.2 Conclusions

In this study, displacements of portal images from simulator images were measured for calculating both systematic and random errors. Systematic error can arise from various factors, the most important being transfer errors from simulator to treatment unit as well as the lack of the use of the electronic portal imaging device. Random errors are related to any accidental error during setup. This study clarified the importance of using high quality fixation devices for all breast patients and demonstrates the feasibility of implementing an EPID-based protocol to improve field set-up verification in an active radiotherapy practice.

The maintenance of technical condition related errors within known and acceptable limits must be ensured by regular applyication of quality assurance(QA) procedures for all equipment involved in the radiotherapy procedure chain.

From the various graphs, it is seen that the study does not compare well with the published set-up error data and exceeds the 5mm margin recommended by the ICRU. For fig 3.2a, it can be seen that 66% of the population had a deviation beyond the 5mm margin in the lateral direction, which implies that there could be serious impact on the lungs of these population. Figure 3.2b shows that over 40% exceeded the recommended 5mm margin in the anterior-posterior direction leading to a high dosimetric consequence to the media sternum and in Fig 3.2c, it is observed that about 80% of the population will have their head of femur greatly affected because of exceeding the 5mm margin.

This result clearly shows that due to the lack of use of the electronic portal-imaging device for proper patient set-upand positioning, patients may be largely affected by treatment-induced errors rather than disease induced fatalities. It is suggested therefore that before adopting any published margin recipe, factors that can potentially influence upon margins should also be taken into consideration to ensure adequacy of target volume coverage.Similarly, the study evaluated and quantified a computerized treatment planning system using radiobiological models. The Lyman Kutcher and Burnam (LKB) model and Equivalent Uniform Dose (EUD) models were used in calculating the Normal Tissue Complication Probability (NTCP) of the Paired Lungs, Heart and Contralateral Breasts of breast cancer patients. The web Brenner Model was used in determining the Tumor Control Probability(TCP) for the ipsilateral and contralateral breast. These indices are function of the toxicity to the Organs at Risk (OARs) and tumor control of the target organ due to exposure of high photon radiation energy. The results show that for both models (EUD and LKB), the paired lungs is more at risk, followed by the heart, next is the contralateral breast. In addition,

there was a significant positive relationship between lung organ volume and Equivalent Uniform Dose (EUD). Also, the fractionation schemes gave values within and above the QUANTEC and RTOG standard and therefore can be introduced into clinical trials for the treatment of breast cancer patients where appropriate. This protocol will save time for both the patients and clinicians and reduce failure of the Linear Accelerator (LINAC) machine, which is a major challenge in most radiotherapy centers in Nigeria.

5.3 Recommendations

i. EPID is a reliable device for the correction of geometrical inter-fraction errors in radiotherapy departments where the common treatment is 3DCRT. Therefore, to overcome systematic and random errors, it is recommended that the portal images must be taken at least twice every week.

ii. From this study, it was observed that there were significant differences in the three major (Lateral, Anterior-Posterior and Superior-Inferior) displacements. Therefore, to manage random and systematic errors effectively it is suggested that set-up errors need to be evaluated weekly to update departmental local PTV margin.

iii. There is the need for the Management of National Hospital Abuja to train its radiotherapist on how to properly use the Electronic Portal Imaging Device.

iv. There is also the need to evaluate CTV-PTV margin for other types of cancers. Example, head and neck, pelvic cancer, cervical cancer etc. It is recommended that a new departmental local PTV margin be established in prescribing CTV-PTV margin prior to treatment commencement.

v. It is important to use NTCP/TCP parameter sets based on calculations and treatments similar to those for which the NTCP/TCP has to be calculated; additionally, it is necessary to improve models and obtain more robust clinical related radiobiological parameters.

vi. Long follow up periods with breast patients are becoming a widespread phenomenon in Nigeria and may allow better understanding of the effect of the different DVH curves of the normal and target tissues. A close follow up on patient's toxicity profiles and correlations with a specific treatment planning method should be studied.

REFERENCES

Adam D, M.D., Popa R., &Ciocaltei, V. (2015). *Volumetric- modulated arc therapy vs. 3D- conformal radiotherapy for breast cancer. Rom Rep Phys*. 1;67:978-86.

Akinde, O.R., Phillips A., &Oguntunde, O., &Afolayan, O. A. (2015). *Cancer MortalityPattern in Lagos University Teaching Hospital, Lagos, Nigeria. Journal of cancer epidemiology*. 842032. 10.1155/2015/842032.

Akpo, E.E., Akpo, M.O., &Akhator, A. (2010). *Breast cancer knowledge and screening practices among Nigerian medical students internet J. Health* 11(2):6-9.

American Cancer Society (2009). *Breast cancer: Early detection.* Retrieved April 18th 2012 fromhttp://www.cancer.org/docroot/CRI/content/CRI_2_6x_Breast_Cancer_Early_De tec tion.asp.

American Cancer Society (2020). *Breast Cancer Facts & Figures*. *Atlanta: American Cancer Society, Inc*. 2019.

Amitpal, S.S., (2020)"Evaluation of Optimal Technique for Left Breast Irradiation" (2020). Graduate Theses and Dissertations. https://scholarcommons.usf.edu/etd/8682

Anbumani, S., Arunai, N., Prabhakar, G., Anchineyan, P., Bilimagga, R. S., Palled, S. R., &Chairmadhurai, A. (2014). *Quantification of uncertainties in conventional plan evaluation methods in Intensity Modulated Radiation Therapy*. Official journal of the Balkan Union of Oncology, 19(1), 297–303.

Arabloo, J., Hamouzadeh, P., Mousavinezhad, S. M., Mobinizadeh, M., Olyaeemanesh, A., &Pooyandjoo, M. (2016). *Health technology assessment of image-guided radiotherapy (IGRT): A systematic review of current evidence. Medical Journal of the Islamic Republic of Iran*. 30, 318. Retrieved from http://www.ncbi.nlm.nih.gov/pubmed/27390688.

Aras, S., İkizceli, T., &Aktan, M. (2019). Dosimetric Comparison of Three-Dimensional Conformal Radiotherapy (3D-CRT) and Intensity Modulated Radiotherapy Techniques (IMRT) with Radiotherapy Dose Simulations for Left-Sided Mastectomy Patients. *European journal of breast health*, *15*(2), 85–89. https://doi.org/10.5152/ejbh.2019.4619

Astudillo, V., Paredes, G., Resendiz, G., Posadas, V., Mitsoura, E., & Rodriguez, L. et al. (2015*). TCP and NTCP radiobiological models: conventional and hypo fractionated treatments in radiotherapy*. 2015;47(7):13.

Atean, I., Pointreau, Y., Barillot, I., & Kirova, Y. M. (2012). Volumes de délinéation dans le traitement des cancers du sein : volumes cibles et organes à risque (Organs at risk and target volumes: definition for conformal radiation therapy in breast cancer). *Cancer radiotherapie : journal de la Societefrancaise de radiotherapieoncologique*, *16*(5-6), 485–492. https://doi.org/10.1016/j.canrad.2012.06.002.

Australian Institute of Health and Welfare (2009b). *Breast Screen Australia monitoring report. Cancer series* no. 48.Cat. no. CAN 44. Canberra.

Australian Institute of Health and Welfare (2009c). *National Cancer Statistics Clearing House protocol 2009*. Canberra.

Barendsen, G. (1982). *Dose fractionation, dose rate and iso-effect relationships for normal tissue responses. International Journal of Radiation Oncology*Biology* Physics*, 8(11):1981–1997.

Betgen, A. et al. "Assessment of set-up variability during deep inspiration breath hold radiotherapy for breast cancer patients by 3D-surface imaging". In: Radiotherapy and oncology 106.2 (Feb. 2013), pp. 225–230. doi: 10.1016/ j.radonc.2012.12.016.

Bhide, S. A., & Nutting, C. M. (2010). *Recent advances in radiotherapy. BMC Medicine*, 8(1), 25. https://doi.org/10.1186/1741-7015-8-25.

Boughalia, A., Marcie, S., Fellah, M., Chami, S., &Mekki, F. (2015). *Assessment and quantification of patient set-up errors in nasopharyngeal cancer patients and their biological and dosimetric impact in terms of generalized equivalent uniform dose (gEUD), tumour control probability (TCP) and normal tissue complication probability (NTCP).* The British journal of radiology, 88(1050), 20140839. https://doi.org/10.1259/bjr.20140839.

Boyle, P., & Levin, B., Eds. (2008) *World Cancer Report 2008. International Agency for Research on Cancer (IARC)*, Geneva, 1-6-2010.

Brenner, D.J., & Hall, E.J. (1999). *Fractionation and protraction for radiotherapy of prostate carcinoma. International Journal of Radiation Oncology* Biology* Physics*, 43(5):1095–1101.

Brenner, D. J. (1993*). Dose, volume, and tumour-control predictions in radiotherapy* Int. J. Radiat. Oncol. Biol. Phys. 26 171–9.

Burnet, N. G. (2004). *Defining the tumour and target volumes for radiotherapy. Cancer Imaging*, 4(2), 153–161. https://doi.org/10.1102/1470-7330.2004.0054.

Chadwick, K., & Leenhouts, H. (1973). *A molecular theory of cell survival*. Physics in Medicine and Biology, 18(1):78.

Chan, TY., Tan, P.W., Tan., C.W., & Tang, J. I. (2015). *Assessing radiation exposure of the left anterior descending artery, heart and lung in patients with left breast cancer: A dosimetric comparison between multicatheter accelerated partial breast irradiation and whole breast external beam radiotherapy.* Radiotherapy and Oncology. 2015;117(3):459-66.

Chao, K. S., Deasy, J. O., Markman, J., Haynie, J., Perez, C. A., Purdy, J. A., & Low, D. A. (2001). *A prospective study of salivary function sparing in patients with head-and-neck cancers receiving intensity-modulated or three-dimensional radiation therapy: initial results. International Journal of Radiation Oncology, Biology, Physics, 49(4), 907–16*. Retrieved from http://www.ncbi.nlm.nih.gov/pubmed/11240231.

Chapman, J.D., Nahum, A.E. (2015). Radiotherapy treatment planning: Linear-quadratic radiobiology (1st ed). CRC Press. Pages 190 eBook ISBN9780429193637 London. https://doi.org/10.1201/b18349.

Chen, Y.J., Han, C., Liu, A., et al.(2007). Setup variations in radiotherapy of esophageal cancer: evaluation by daily megavoltage computed tomographic localization. Int J Radiat Oncol Biol Phys. 2007 Aug 1;68(5):1537-45.

Cheng, K., & Wu., V. (2014). Comparison of the effectiveness of different immobilization systems in different body regions using daily megavoltage CT in helical tomotherapy. The British Journal of Radiology BJR, 87, 20130494-20130494.

Chapman, J.D., Nahum, A. E. (2015). *Radiotherapy treatment planning*: Linear-quadratic radiobiology (1st ed.) CRC Press. Pages190 eBook ISBN9780429193637 London. https://doi.org/10.1201/b18349.

Chiesa, S., et al. (2015) "Adaptive optimization by 6 DOF robotic couch in prostate volumetric IMRT treatment: rototranslational shift and dosimetric consequences". In: Journal of Applied Clinical Medical Physics 16.5 (2015). doi: 10.1120/jacmp.v16i5.5525.

Chapman, J.D., Nahum, A. E. (2015). *Radiotherapy treatment planning*: Linear-quadratic radiobiology (1st ed.) CRC Press. Pages190 eBook ISBN9780429193637 London. https://doi.org/10.1201/b18349.

Christina, F. (2018). Global, Regional, and National Cancer Incidence, Mortality, Years of Life Lost, Years Lived with Disability, and Disability-Adjusted Life-years for 32 Cancer Groups, 1990 to 2015: *A Systematic Analysis for the Global Burden of Disease Study. JAMA oncology*, *3*(4), 524–548. https://doi.org/10.1001/jamaoncol.2016.5688.

Chvetsov, A., Dempsey, J., &Palta, J. (2007). *Optimization of equivalent uniform dose using the L-curve criterion*. Phys. Med. Biol., 52:5973–5984.

Dale, R., & Jones, B. (2007). *Radiobiological Modelling in Radiation Oncology (1st ed.). London: British Institute of Radiology*. Retrieved from http://www.amazon.co.uk/RadiobiologicalModelling-Radiation-Oncology-Roger/dp/090574960X.

Dasu, A., & Toma-Dasu, I. (2012). *Prostate alpha/beta revisited – an analysis of clinical results from 14 168 patients.* Acta Oncologica, 51(8):963–974.

Dearnaley, D. P., Hall, E., Lawrence, D., Huddart, R. A., Eeles, R., Nutting, C. M., & Horwich, A. (2005). *Phase III pilot study of dose escalation using conformal radiotherapy in prostate cancer:* PSA control and side effects. British Journal of Cancer, 92(3), 488–498.

Dhar D, Mallik S, Goswami J. Validation of a simple technique for accurate treatment delivery for bilateral breast irradiation using the electronic portal imaging device. J Can Res Ther [serial online] 2022 [cited 2023 Jan 24];18:1159-61. Available from: https://www.cancerjournal.net/text.asp?2022/18/4/1159/356552

Ding, Z.; Zeng, Q.; Kang, K.; Xu, M.; Xiang, X.; Liu, C. (2022) Evaluation of Plan Robustness Using Hybrid Intensity-Modulated Radiotherapy (IMRT) and Volumetric Arc Modulation Radiotherapy (VMAT) for Left-Sided Breast Cancer. *Bioengineering*, *9*, 131. https://doi.org/10.3390/bioengineering9040131.

Elsässer, T., Krämer, M., & Scholz, M. (2008). *Accuracy of the Local Effect Model for the prediction of biologic effects of carbon ion beams in vitro and in vivo.* InternationalJournalofRadiationOncology*Biology*Physics,71(3):866– 872.

Emami B, Lyman J, Brown A, Cola L, Goitein M, Munzenrider JE, et al. (1991) Tolerance of normal ssue to therapeu- c irradiaon. Int J Radiat Oncol Biol Phys, 21: 109-122.

Feng, F. Y., Kim, H. M., Lyden, T. H., Haxer, M. J., Feng, M., Worden, F. P., Eisbruch, A. (2007). *Intensity-modulated radiotherapy of head and neck cancer aiming to reduce dysphagia: early dose-effect relationships for the swallowing structures*. International Journal of Radiation Oncology, Biology, Physics, 68(5), 1289–98. https://doi.org/10.1016/j.ijrobp.2007.02.049.

Ferlay, J., Shin, H. R., Bray, F., Forman, D., Mathers, C., & Parkin, D. M. (2010). *Estimates of worldwide burden of cancer in 2008*: GLOBOCAN 2008. International journal of cancer, 127(12), 2893–2917. https://doi.org/10.1002/ijc.25516.

Ferlay, J., Steliarova-Foucher, E., Lortet-Tieulent, J., Rosso, S., Coebergh, J.W., Combe,r H., Forman, D., & Bray, F. *Cancer incidence and mortality patterns in Europe*: estimates for 40 countries in 2012. Eur J Cancer. 2013 Apr;49(6):1374-403. doi: 10.1016/j.ejca.2012.12.027. Epub 2013 Feb 26. PMID: 23485231.

Ferlay, J., Soerjomataram, I., Dikshit, R., Eser, S., Mathers, C., Rebelo, M., Parkin, D.M., Forman, D., & Bray, F. (2015). *Cancer incidence and mortality worldwide: sources, methods and major patterns in GLOBOCAN 2012*. Int J Cancer. 2015 Mar 1;136(5):E359-86. doi: 10.1002/ijc.29210. Epub 2014 Oct 9. PMID: 25220842.

Ferlay, J., Soerjomataram, I., &Ervik., Morten & Dikshit., Rajesh &Eser., Sultan &Rebelo, M., Parkin, D.M & Forman., David & Bray, Freddie. (2014). GLOBOCAN 2012 v1.0, *cancer incidence and mortality worldwide:* IARC cancer base no. 11 [Internet]. International Agency for Research on Cancer, Lyon.

Fiagan, Y. A. C., Bossuyt, E., Machiels, M., Nevens, D., Billiet, C., Poortmans, P., Gevaert, T., & Verellen, D. (2022). Comparing treatment uncertainty for ultra- vs. standard-hypofractionated breast radiation therapy based on in-vivo dosimetry. *Physics and imaging in radiation oncology*, *22*, 85–90. https://doi.org/10.1016/j.phro.2022.05.003

Formenti, S., Dewyngaert, J., Jozsef, G., & Goldberg, J. (2012). Prone vs Supine Positioning for Breast Cancer Radiotherapy. JAMA, 308(9), 861-861.

Fowler, J. F., Toma-Dasu, I., and Dasu, A. (2013). *Is the α/β ratio for prostate tumours really low and does it vary with the level of risk at diagnosis?* Anticancer research, 33(3):1009–1011.

Gay, H.A., Niemierko, A. (2007). *A free program for calculating EUD-based NTCP and TCP in external beam radiotherapy*. PhysicaMedica. 2007;23(3):115-125.

Gerstner, N., Wachter, S., Knocke, T. H., Fellner, C., Wambersie, A., &Pötter, R. (1999). *The benefit of Beam's eye view based 3D treatment planning for cervical cancer. Radiotherapy and Oncology*: Journal of the European Society for Therapeutic Radiology and Oncology, 51(1), 71– 8. Retrieved from http://www.ncbi.nlm.nih.gov/pubmed/10386719.

Gilbeau, L., Octave-Prignot, M., Loncol, T & Renard L., Scalliet, P & Gregoire, V. (2001). *Comparison of setup accuracy of three different thermoplastic masks for the treatment of brain and head and neck tumors*. Radiotherapy and oncology: journal of the European Society for Therapeutic Radiology and Oncology. 58. 155-62. 10.1016/S0167-8140(00)00280-2.

Goodhead, D. T. (1994). *Initial events in the cellular effects of ionizing radiations: clustered damage in DNA.* International journal of radiation biology, 65(1):7– 17.

Guerrero M and Li XA (2003) Analysis of a large numver of clinical studies for breast cancer radiotherapy: esmaon of radiobiological parameters for treatment planning. Phys Med Biol, 48: 3307-26.

Hall EJ (2000) Radiobiology for the radiologist. 5th ed. LippincoQ Williams & Wilkins. USA.

Harro, E. et al. "Dosimetric Effects of Setup Uncertainties on Breast Treatment Delivery". In: Medical dosimetry 33.4 (Feb. 2008), pp. 293–298. doi: 10.1016/ j.meddos.2008.01.003.

Herman, M. G. (2005). *Clinical use of electronic portal imaging*. Seminars in radiation oncology, *15*(3), 157–167. https://doi.org/10.1016/j.semradonc.2005.01.002.

Henson, K.E., McGale, P., Taylor, C., & Darby, S.C. (2013). *Radiation-related mortality from heart disease and lung cancer more than 20 years after radiotherapy for breast cancer*. Br J Cancer 2013; 108: 179-182. (PMID: 23257897).

Hirsch, J. S., &Holzknecht, G. (1926). *The Principles and Practice of Roentgen Therapy*. British Journal of Radiology: BIR Section, 31(308), 114–115. https://doi.org/10.1259/bir.1926.0028.

Humphreys, M., Urbano, M.T.G., &Mubata, C. et al. *Assessment of a customisedimmobilisation system for head and neck IMRT using electronic portal imaging*. Radiother Oncol 2005; 77 (1): 39–44.

International Commission on Radiation Units and Measurements. (1994). *ICRU Report, 50*. Bethesda, MD: ICRU Publications; 1994. Prescribing, recording and reporting photon beam therapy.

International Commission on Radiation Units and Measurements. (2000). *ICRU Report, 62*. Bethesda, MD: ICRU Publications; 2000. Prescribing, recording and reporting photon beam therapy. International commission on radiation units and measurement, prescribing, recording and reporting photon beam therapy.

International Commission on Radiation Units and Measurements. (1993a). *Prescribing, Recording, and Reporting Photon Beam Therapy Report 50*. Journal of the ICRU.

International Commission on Radiation Units and Measurements. (1993b). Prescribing, recording and reporting photon beam therapy. *ICRU report 50*. ICRU report. https://doi.org/10.2307/3578862.

International Commission on Radiation Units and Measurements. (1999). *ICRU Report 62.* Prescribing, Recording, and Reporting Photon Beam Therapy (Supplement to ICRU Report 50). Journal of ICRU, Ix +52. https://doi.org/10.1259/bjr.74.879.740294.

International Commission on Radiation Units and Measurements. (2010). *Report 83*. The International Commission on Radiation Units and Measurements. Journal of the ICRU, 10(1), 27–38. https://doi.org/10.1093/jicru/ndq001.

Ioana-Claudia, Costin., Loredana, G. Marcu. (2022). Factors impacting on patient setup analysis and error management during breast cancer radiotherapy, Critical Reviews in Oncology/Haematology, Volume 178,2022,103798, ISSN 1040-8428, https://doi.org/10.1016/j.critrevonc.2022.103798. (https://www.sciencedirect.com/science/article/pii/S1040842822002220)

Jackson, S. P. (2002). *Sensing and repairing DNA double-strand breaks*. Carcinogenesis, 23(5):687–696.

Jain, P. et al. (2008) “Inter-fraction motion and dosimetric consequences during breast intensity-modulated radiotherapy (IMRT)”. In: Radiotherapy and oncology 90.1 (Nov. 2008), pp. 93–98. doi: 10.1016/j.radonc.2008.10.010.

Jassal, K., Bisht, S., &Kataria, T. (2013). *Comparison of Geometrical Uncertainties in Breast Radiation Therapy with Different Immobilization Methods*. Journal of Nuclear Medicine & Radiation Therapy. 04. 10.4172/2155-9619.1000140.

Jemal, A., Bray, F., Forman, D., O'Brien, M., Ferlay, J., Melissa, B.S., Maxwell, D., & Parkin, M.D. (2012). *Cancer burden in Africa and opportunities for prevention*. https://acsjournals.onlinelibrary.wiley.com/toc/10970142/2012/118/18. https://doi.org/10.1002/cncr.27410.

Jereczek-Fossa, B.A., Santoro, L., Colangione, S.P., Morselli, L., Fodor, C.I., Vischioni, B., Rozza, D., Leppa, A.L., Cambria, R., Leonardi, M.C., Morra, A., Baroni, G., Zurrida, S., &Orecchia, R. (2013). Electronic portal imaging registration in breast cancer radiotherapy verification: analysis of inter-observer agreement among different categories of health practitioners. *Neoplasma*, *60 3*, 302-8.

Joiner, M. C., Marples, B., Lambin, P., Short, S. C., &Turesson, I. (2001). *Low dose hypersensitivity: current status and possible mechanisms.* International Journal of Radiation Oncology* Biology* Physics, 49(2):379–389.

Joiner, M., & Johns, H. (1988). *Renal damage in the mouse: the response to very small doses per fraction*. Radiation research, 114(2):385–398.

Joseph, O., Deasy, K. S., Clifford Chao, M.D., & Jerry, M., (2001). *Uncertainties in model-based outcome predictions for treatment planning*, int. j. radiation oncology biol. phys., vol. 51, no. 5, pp. 1389–1399, 2001.

Kallman, P., Agren, A., &Brahme, A. (1992). *Tumour and normal tissue responses to fractionated non-uniform dose delivery*. Int. J. Radiat. Biol. 1992, 62:249–262.

Kang, S. W., Kang, S., Lee, B., Song, C., Eom, K. Y., Jang, B. S., Kim, I. A., Kim, J. S., Cho, W., Shin, D. S., Kim, J. Y., & Chung, J. B. (2022). Evaluation of the dosimetric and radiobiological parameters in four radiotherapy regimens for synchronous bilateral breast cancer. *Journal of applied clinical medical physics*, *23*(8), e13706. https://doi.org/10.1002/acm2.13706.

Karlsson, K.H., &Stenerlöw, B. (2004). *Focus formation of DNA repair proteins in normal and repair-deficient cells irradiated with high-LET ions. Radiation research*, 161(5):517–527.

Kaveh S.T., Sediqeh, H., Marzieh S., Ahmad, S., Mohammad, M. M., Hussain G. (2021). Tumor Control Probability (TCP) and Normal Tissue Complication Probability (NTCP) in Mono and Dual-isocentric Techniques of Breast Cancer Radiation Therapy. ShiraniTak Abi et al. Arch Breast Cancer 2021; Vol. 8, No. 3:192-202. DOI: 10.32768/abc.202183192-202.

Kavousi, N., Nedaie, H.A.G., Somayeh E., Mahbod S., Sajad, H.M. Ipsilateral lung normal tissue complication probability parameters for different dose calculation algorithms in radiotherapy of breast cancer. (2020). Journal of Cancer Research and Therapeutics 16(6):p 1323-1330, Oct–Dec 2020. | DOI: 10.4103/jcrt.JCRT_1149_19

Kellerer, A. M., & Rossi, H. H. (1978). *A generalized formulation of dual radiation action.* Radiation Research, 75(3):471–488.

Kharia, D. (2018). *Radiobiological Optimization of Lung and Prostate Radiotherapy Treatments - A Macroscopic Approach*.https://ethos.bl.uk/OrderDetails.do?uin=uk.bl.ethos.771137.

Kirkpatrick, J. P., Brenner, D. J., & Orton, C. G. (2009). *The linear-quadratic model is inappropriate to model high dose per fraction effects in radiosurgery*. Medical physics, 36:3381.

Kotte, A.N., Hofman, P., Lagendijk, J.J., et al., (2007) Intrafraction motion of the prostate during external-beam radiation therapy: analysis of 427 patients with implanted fiducial markers. Int J Radiat Oncol Biol Phys. 2007 Oct 1;69(2):419-25.

Koussi, E., (2007). *Evaluation of dose-response models and determination of several radiobiological parameters*. http://hdl.handle.net/10889/596.

Krengli, M., Masini, L., Caltavuturo, T., Pisani, C., Apicella, G., Negri, E., . . . Gambaro, G. (2013). Prone versus supine position for adjuvant breast radiotherapy: A prospective study in patients with pendulous breasts. Radiation Oncology, 8, 232.

Kutcher, G., Burman, C., Brewster, L., Goitein, M., & Mohan, R. (1991). *Histogram reduction method for calculating complication probabilities for three dimensional treatment planning evaluations*. Int. J. Radiat. Oncol. Biol. Phys., 21:137–146.

Kupelian, P. A., Reddy, C. A., Carlson, T. P., Altsman, K. A., & Willoughby, T. R. (2002). *Preliminary observations on biochemical relapse-free survival rates after short-course intensity-modulated radiotherapy (70 Gy at 2.5 Gy/fraction) for localized prostate cancer*. International Journal of Radiation Oncology, Biology, Physics, 53(4), 904–12. Retrieved from http://www.ncbi.nlm.nih.gov/pubmed/12095556.

Lambert, B. (2001). Chapter 3 Radiation*: early warnings; late effects in Late lessons from early warnings: the precautionary principle* 1896-2000. EEA. Retrieved from http://www.eea.europa.eu/publications/environmental_issue_report_2001_22.

Lea, D., &Catcheside, D. (1942). *The mechanism of the induction by radiation of chromosome aberrations in tradesoantia*. Joumal of Genetics, 44:216–245.

Lee, J.J.B.; Lee, I.J.; Choi, Y.; Jeon, M.J.; Jung, I.H.; Lee, H. (2021). *Clinical Implications of Geometric and Dosimetric Uncertainties of Inter- and Intra-Fractional Movement during Volumetric Modulated Arc Therapy for Breast Cancer Patients*. *Cancers* **2021**, *13*, 1651. https://doi.org/10.3390/cancers13071651

Li, A. X., Alber, M., Deasy, J., Jackson, A., & Kyung-Wook, K. J. (2012). *The use and QA of biologically related models for treatment planning*: Report of AAPM Task Group 166 Med Phys 39.

Liang, X., Mailhot Vega, R.B., Li, Z. *et al.* (2020). Dosimetric consequences of image guidance techniques on robust optimized intensity-modulated proton therapy for treatment of breast Cancer. *Radiat Oncol* **15**, 47 (2020). https://doi.org/10.1186/s13014-020-01495-6

Lievens, Y., Nulens, A., Gaber, M. A., Defraene, G., De Wever, W., Stroobants, S., & Van den Heuvel, F. (2011). *Intensity-modulated radiotherapy for locally advanced non-small-cell lung cancer: a dose-escalation planning study*. International Journal of Radiation Oncology, Biology, Physics, 80(1), 306–13. https://doi.org/10.1016/j.ijrobp.2010.06.025.

Lin, L.L., Hertan, L., Rengan. R., et al. (2012) Effect of body mass index on magnitude of setup errors in patients treated with adjuvant radiotherapy for endometrial cancer with daily image guidance. Int J Radiat Oncol Biol Phys. 2012 Jun 1;83(2):670-5.

Luchao Zhu, Jun Liu, Yimin Li, Qiaolu Yang, Qiong Wu, Qing Lin, Sijia Chen, "Effect of Stereotactic Body Radiation Therapy Combined with Thermoplastic Fixation on Set-Up Errors in Breast Cancer Patients Undergoing Radiotherapy", Computational and Mathematical Methods in Medicine, vol. 2022, Article ID 8370842, 7 pages, 2022. https://doi.org/10.1155/2022/8370842.

Lyman, J. (1985). *Complication probability as assessed from dose-volume histograms*. Radiat. Res., 104:13–19.

Lyman, J.T. (1985). *Complication probability as assessed from dose-volume histograms*. Radiat Res Suppl. 1985;8:S13-S19.

Mankinen, M., Virén, T., Seppälä, J. *et al.* (2022). Dosimetric effect of respiratory motion on planned dose in whole-breast volumetric modulated arc therapy using moderate and ultra-hypofractionation. *Radiat Oncol* **17**, 46 (2022). https://doi.org/10.1186/s13014-022-02014-5

Marks, L. B., Yorke, E. D., Jackson, A., Ten Haken, R. K., Constine, L. S., Eisbruch, A., Bentzen, S. M., Nam, J., Deasy, J. O. (2010*). Use of normal tissue complication probability models in the clinic*. International journal of radiation oncology, biology, physics, 76(3 Suppl), S10-9.

Mavroidis P., Axelsson S., Hyödynmaa S., Rajala J., Pitkänen M. A., Lind B. K., Brahme A. (2002) Effects of positioning uncertainty and breathing on dose delivery and radiation pneumonitis prediction in breast cancer. *Acta Oncol* 41, 471–485 (2002).

Mayles, P., Nahum, A., & Rosenwald, J. (2007). *Handbook of radiotherapy physics theory and practise*. Taylor and Francis.

McKenzie, A.L. (2000). *How should breathing motion be combined with others errors when drawing margins around clinical target volume*? Br J Radiol 2000; 73: 973–7. 24.

McKenzie, A., Van Herk, M., &Mijnheer, B. (2002). *Margins for geometric uncertainty around organs at risk in radiotherapy*. Radiother Oncol 2002; 62: 299–307. doi: 10.1016/s0167-8140(02)00015-4.

Michalski, A., Atyeo, J., Cox, J., & Rinks, M. (2012). Inter- and intra-fraction motion during radiation therapy to the whole breast in the supine position: A systematic review. Journal of Medical Imaging and Radiation Oncology, 56(5), 499-509.

Morsy, M., Ahmed, A. (2019). *Measure the Errors of Treatment Set-Ups of Prostate Cancer Patient Using Electronic Portal Imaging Device (EPID)*. IOSR Journal of Applied Physics. 10. 55-59. 10.9790/4861-1002015559.

Mukundan, H., Mukherjee, D., Tyagi, K., Taneja, S., Ranjan, S., &Sahu, S. (2020). Dosimetric and isocentric variations due to patient setup errors in CT-based treatment planning for breast cancer by electronic portal imaging. *Medical journal, Armed Forces India, 76*(1), 51–57. https://doi.org/10.1016/j.mjafi.2018.07.008

Mulliez, Thomas, Bruno Speleers, Indira Madani, Werner De Gersem, Liv Veldeman, and Wilfried De Neve. "Whole Breast Radiotherapy in Prone and Supine Position: Is There a Place for Multi-beam IMRT?" Radiation Oncology 8.15 (2013): 151.

National Institute of Health. (2010). *Common Terminology Criteria for Adverse Events v4.0 (CTCAE). (Vol. 2009).* Retrieved from http://evs.nci.nih.gov/ftp1/CTCAE/CTCAE_4.03_2010-0614_QuickReference_5x7.pdf.

Nggada H., &Yawe, K., Abdulazeez, J., & Khalil, M. (2008). *Breast Cancer Burden in Maiduguri, North Eastern Nigeria.* The breast journal. 14. 284-6. 10.1111/j.1524-4741.2008.00576.x.

Nicolini, G., Vanetti, E., Clivio, A., Fogliata, A., &Cozzi, L. (2010). Pre-clinical evaluation of respiratory-gated delivery of volumetric modulated arc therapy with RapidArc. Physics in Medicine and Biology Phys. Med. Biol., 55(12), 347-57

Niemierko A. (1997). *Reporting and analysing dose distributions: A concept of equivalent uniform dose.* Medical Physics 24 (1),103-110 (1997).

Niemierko, A. (1999). *A generalized concept of Equivalent Uniform Dose (EUD)*, Medical Physics 26 (6), 1100 (1999).

Niemierko, A. A. (1999). *Generalized concept of equivalent uniform dose (EUD*). Med Phys. 1999;26(6):1100.

Niemierko, A. (1997). *Reporting and analyzing dose distributions: a concept of equivalent uniform dose.* Medical physics. 1997;24(1):103-10.

Nutting, C. M., Morden, J. P., Harrington, K. J., Urbano, T. G., Bhide, S. A., & Clark, C. (2011). Parsport trial management group. *Parotid-sparing intensity modulated versus conventional radiotherapy in head and neck cancer* (PARSPORT): a phase 3 multicentrerandomised controlled trial. The Lancet. Oncology, 12(2), 127–36. https://doi.org/10.1016/S14702045(10)70290-4.

Oh, Y., Baek, J., Kim, O., & Kim, J. (2014). Assessment of setup uncertainties for various tumor sites when using daily CBCT for more than 2200 VMAT treatments. Journal of Applied Clinical Medical Physics, 15(2), 85-99.

Ohashi, T., Takea, A., ShigematsU, N., Fukada, J., Sanuki, N., Amemiya, A., et al. (2009). *Dose distribution analysis of axillary lymph nodes for three dimensional conformal radiotherapy with a field-in-field technique for breast cancer*. International Journal of Radiation Oncology Biology Physics. 2009;73(1):80-7.

Remeijer, P., Geerlof, E., Ploeger, L., Gilhuijs, K., Herk, M., &Lebesque, J. (2000). 3-D portal image analysis in clinical practice: An evaluation of 2-D and 3-D analysis techniques as applied to 30 prostate cancer patients. International Journal of Radiation Oncology, Biology, Physics, 46(5), 1281-1290.

Panagiotis, M. (2001). *Determination and use of radiobiological Response Parameters in Radiation therapy Optimization*, Division of Medical Radiation Physics, Department of Oncology-Pathology, Karolinska Institutet, Stockholm 2001.

Pawel K., (2004). *Clinical aspects of normal tissue complication probability*. Rep Pract Oncol Radiother 2004; 9:261-7, review paper.

Popescu, C., Wai, E., Ansbacher, W., Salter, L., Olivotto, I., Beckham, W., & Otto, K. (2010). Volumetric Modulated Arc Therapy (VMAT) Improves Dosimetry and Reduces Treatment Time Compared to 9-field Conventional Intensity Modulated Radiotherapy (cIMRT) for Locoregional Radiotherapy of Left-sided Breast Cancer. International Journal of Radiation Oncology Biology Physics, 76(1), 287- 195.

Prentou, G et al., "Dosimetric impact of rotational errors on the quality of VMAT-SRS for multiple brain metastases: Comparison between single- and two-isocenter treatment planning techniques". In: Journal of Applied Clinical Medical Physics 21.3 (2020), pp. 32–44. doi: 10.1002/acm2.12815.

Radiotherapy Oncology Group. (2015). *RTOG/EORTC Late Radiation Morbidity Scoring Schema.* Retrieved October 23, 2015, from https://www.rtog.org/ResearchAssociates/AdverseEventReporting/RTOGEORTCLate Radiation MorbidityScoringSchema.aspx.

Rena, L. (2005). *Analysis of Set-up Errors during CT-scan, Simulation, and Treatment Process in Breast Cancer PatientsRadiat Oncol J.* 2005;23 (3): 169-175.

Royal College of Radiologists (RCR). (2008). *The timely delivery of radical radiotherapy: standards and guidelines for the management of unscheduled treatment interruptions, Third edition.* Retrieved from http://www.sascro.co.za/downloads/BFCO_RT_Interruptions.pdf.

Selvan, K.T., et al. (2019) "Dosimetric Effect of Rotational Setup Errors in SingleIsocenter Volumetric-Modulated Arc Therapy of Multiple Brain Metastases". In: Journal of Medical Physics 44.2 (2019). doi: 10.4103/jmp.JMP_103_18.

Seonghee, K. S., Jin, S., ital., J. H., Chang, S., Bum-Sup, Jang., Kyung, H. S., Chang, H. C., Jung-in, K., (2022). Evaluation of surface-guided radiation therapy for breast cancer using the Halcyon system. https://doi.org/10.21203/rs.3.rs-2356561/v1.

Schlegel, W. (2006). *New Technologies in Radiation Oncology*, ISBN : 978-3-540-00321-2.

Scholz, M., Kellerer, A., Kraft-Weyrather, W., & Kraft, G. (1997). Computation of cell survival in heavy ion beams for therapy. Radiation and environmental biophysics, 36(1):59–66.

Shah, A. P., Dvorak, T., Curry, M. S., Buchholz, D. J., & Meeks, S. L. (2013). *Clinical evaluation of interfractional variations for whole breast radiotherapy using 3-dimensional surface imaging*. Practical radiation oncology, *3*(1), 16–25. https://doi.org/10.1016/j.prro.2012.03.002.

Stewart, B. W., Bray, F., Forman, D., Ohgaki, H., Straif, K., Ullrich, A., & Wild, C. P. (2016). *Cancer prevention as part of precision medicine: 'plenty to be done'*. *Carcinogenesis*, *37*(1), 2–9. https://doi.org/10.1093/carcin/bgv166.

Stewart, R., & Li, X. (2007). BGRT: *Biologically guided radiation therapy the future is fast approaching!* Med. Phys., 34:3739–3751.

Stroom, J.C., &Heijmen, B.J. (2002). *Geometrical uncertainties, radiotherapy planning margins, and the ICRU-62 report*. Radiother Oncol 2002; 64: 75–83. doi: 10.1016/s0167-8140(02)00140-8.

Taylor, C.W., Wang, Z., Macaulay, E., Jagsi, R., Duane, F., & Darby, S.C. (2015). *Exposure of the heart in breast cancer radiation therapy: a systematic review of heart doses published during 2003 to 2013*. International Journal of Radiation Oncology* Biology* Physics. 2015;93(4):845-53.

Teoh, M., Clark, C. H., Wood, K., Whitaker, S., & Nisbet, A. (2011). Volumetric modulated arc therapy: a review of current literature and clinical use in practice. The British Journal of Radiology, 84(1007), 967–96. https://doi.org/10.1259/bjr/22373346

Thames, H.D., Zhang, M., Tucker, S.L. et al. (2004*). Cluster models of dose–volume effects*. Int J Radiat Oncol Biol Phys. 2004;59(5):1491- 1504.

Troeller, Almut., (2017). *Normal tissue complication probability modelling: influence of treatment technique, fractionation, and dose calculation algorithm*. Dissertation, LMU München: Faculty of Medicine.

Troeller, A., Sohn, M., Grills, I., Guckenberger, M., Belderbos, J., Sonke, J., Hope, A., Werner- ¨ Wasik, M., Xiao, Y., & Yan, D. (2015). TH-AB-304-06: *Investigation of Fractionation Issues in NTCP Modeling of Pneumonitis: An Analysis of Common NTCP Models for HypoFractionated and Standard-Fractionated Data*, Medical Physics 42(6):3701. doi:10.1118/1.4926121.

Tsai, P., Lin, S., Lee, S., Yeh C., Huang, Y. (2012). The feasibility study of using multiple partial volumetric-modulated arcs therapy in early stage left-sided breast cancer patients. Journal of Applied Clinical Medical Physics, 13(5), 62-73.

Tzikas A, Komisopoulos G, Ferreira BC, et al. Radiobiological Evaluation of Breast Cancer Radiotherapy Accounting for the Effects of Patient Positioning and Breathing in Dose Delivery. (2012) A Meta Analysis. Technology in Cancer Research & Treatment. 2013;12(1):31-44. doi:10.7785/tcrt.2012.500274

Van, M.A., et al. “Effects of setup errors and shape changes on breast radiotherapy”. In: International Journal of Radiation Oncology, Biology, Physics 79.5 (Apr. 2011), pp. 1557–1564. doi: 10.1016/j.ijrobp.2010.07.032.

Van H.M. Errors and margins in radiotherapy**.** *SeminRadiat Oncol* 2004, **14:** 52-64. 10.1053/j.semradonc.2003.10.003

Varadharajan, E., & Swaminathan S, et al. (2014). Biological evaluation of 3D conformal radiotherapy and intensity modulated radiotherapy plans in different clinical situations. JIPMER Journal of cancer. 2014;3(1):35-43.

Wang W, Yu T, Xu M, Shao Q, Zhang Y, Li J. (2019). Setup Error Assessment and Correction in Planar kV Image- Versus Cone Beam CT Image-Guided Radiation

Therapy: A Clinical Study of Early Breast Cancer Treated With External Beam Partial Breast Irradiation. Technology in Cancer Research & Treatment. 2019;18. doi:10.1177/1533033819853847

Wedenber, M. (2013) *From Cell Survival to Dose Response – Modeling Biological Effects in Radiation Therapy*. ISBN 978-91-7549-250-6.

Webb, S. (1994). *Optimum parameters in a model for tumour control probability including interpatient heterogeneity* Phys. Med. Biol. 39 1895–914.

Webb, S., & Nahum, A. E. (1993). *A model for calculating tumour control probability in radiotherapy including the effects of inhomogeneous distributions of dose and clonogenic cell density* Phys. Med. Biol. 38 653–66.

Willner J, Baier K, Caragiani E, Tschammler A, Flentje M (2002) Dose, volume, and tumor control predicons in primary radiotherapy of non-small-cell lung cancer. Int J Radiat Oncol Biol Phys, 52: 382-89

Wolfgang A. Tomé, Ph.D.1 Minesh P. Mehta, M.D.1 Sanford L. Meeks, Ph.D.2 John M. Buatti, M.D.2

World Health Organization (WHO). (2020). *Global Health Estimates 2020: Deaths by Cause, Age, Sex, by Country and by Region, 2000-2019*. WHO; 2020. Accessed December 11, 2020. who.int/data/gho/data/themes/mortality-and-global-health-estimates/ghe-leading-causes-of-death.

Yao S, Zhang Y, Nie K, et al. Setup uncertainties and the optimal imaging schedule in the prone position whole breast radiotherapy.(2019) Radiat Oncol. 2019 May 9;14(1):76.

Zelefsky, M. J., Fuks, Z., Hunt, M., Lee, H. J., Lombardi, D., Ling, C. C., & Leibel, S. A. (2001). *High dose radiation delivered by intensity modulated conformal radiotherapy improves the outcome of localized prostate cancer*. The Journal of Urology, 166(3), 876–81. Retrieved from http://www.ncbi.nlm.nih.gov/pubmed/11490237.

Zhao, Y. et al. “Impact of Positioning Errors on the Dosimetry of Breath-HoldBased Volumetric Arc Modulated and Tangential Field-in-Field Left-Sided Breast Treatments”. In: Frontiers in Oncology 10 (Oct. 2020), pp. 237–238. doi: 10.3389/fonc.2020.554131.

Zhao, H., He, M., Cheng, G., Han, D., Wu, N., Shi, D., Zhao, Z., &Jin, J. (2015). *A comparative dosimetric study of left-sided breast cancer after breast-conserving surgery treated with VMAT and IMRT*. Radiat Oncol 2015; 10: 231. (PMID: 26577189).

Zhu, L., Liu, J., Li, Y., Yang, Q., Wu, Q., Lin, Q., & Chen, S. (2022). Effect of Stereotactic Body Radiation Therapy Combined with Thermoplastic Fixation on Set-Up Errors in Breast Cancer Patients Undergoing Radiotherapy. *Computational and mathematical methods in medicine, 2022*, 8370842. https://doi.org/10.1155/2022/8370842.

APPENDIX

APPENDIX I**;** Summary of DVH analysis for PTV and OARs for the cohort of 200 breast cancer patients included in this study, for 3D-CRT. Data are shown as mean values plus or minus one standard error; in brackets the standard deviation.

DVH Parameter	**OARs and the Breast for PTV values**									
	Ipsilateral Breast	p-value	Ipsilateral Lung	p-value	Contralateral Breast	p-value	Contralateral Lung	p-value	Heart	p-value
Dmax($mean \pm SE$)(SD)	0.079±0.026 (16.307)	0.008	0.336±0.165 (2.226)	0.000	0.490±0.090 (18.041)	0.181	0.210±0.178 (1.448)	0.051	0.371±0.090 (1.001)	0.020
Dmin($mean \pm SE$)(SD)	52.12±3.400 (0.325)	0.828	43.78±0.009 (0.125)	0.000	27.234±4.034 (1.327)	0.00	9.587±0.013 (0.108)	0.161	30.758±0.013 (0.143)	0.000
Dmax($mean \pm SE$)(SD)	13.53±1.310 (42.334)	0.000	5.195±0.867 (11.691)	0.000	16.158±5.386 (24.089)	0.133	1.028±1.925 (15.367)	0.009	1.545±1.692 (18.768)	0.000
PTV($mean \pm SE$)(SD)	18389.470 ±2115.536 (26338.227)		1175.334±23.535 (318.372)	0.000	906.421±121.15 (283.655)		1185.739±34.916(283.655)	0.013	5147.002±4486.849 (49761)	0.041
D_{50}($mean \pm SE$)(SD)	45.82±1.807 (22.496)	0.000	21.058±1.370 (18.484)	0.000	21.073±5.059 (22.64)	0.086	8.600±7.443 (60.468)	0.052	1.949±0.197 (2.182)	0.010
D_{75}($mean \pm SE$)(SD)	41.134±1.100 (3.669)	0.000	17.048±1.16 (15.687)	0.000	20.679±5.000 (22.360)	0.086	0.871±0.401 (3.259)	0.049	1.471±0.131 (1.458)	0.000
D_{90}($mean \pm SE$)(SD)	36.42±1.480 (18.431)	0.000	15.141±1.084 (14.628)	0.000	20.466±4.961 (22.185)	0.086	18.501±17.797 (144.585)	0.314	1.253±0.105 (1.167)	0.000
D_{98}($mean \pm se$)(SD)	34.14±1.680 (20.77)	0.000	13.900±1.025 (13.88)	0.000	20.345±4.939 (22.087)	0.086	0.614±0.230 (1.870)	0.052	4.387±3.221 (35.581)	0.000

SD=standard deviation; Dmax, maximum dose; Dmean, mean dose; Dmin, minimum dose. $D_{x,}$ dose to the x% of the volume; PTV, planning target volume; OARs, Organ at Risk.

APPENDIX II: Beam Parameters for Patients

Beam Number	1	4	6	7
Description	MED	LAT	APSU	RTSU
Field ID				
Treatment Unit	Linac1	Linac1	Linac1	Linac1
Machine ID	SYNERGY MLCI2 - 6M	SYNERGY MLCI2 - 6M	SYNERGY MLCI2 - 6M	SYNERGY MLCI2 - 6M
Machine Energy	6.0 MV	6.0 MV	6.0 MV	6.0 MV
Modality	Photon	Photon	Photon	Photon
Algorithm	CC	CC	---	---
Setup	SAD	SAD	SAD	SAD
SSD (cm)	93.82	89.51	96.87	76.86
Gantry (deg)	307.0	127.0	0.0	270.0
Collimator (deg)	3.2	356.8	0.0	0.0
Couch (deg)	0.0	0.0	0.0	0.0
Asymmetric	Yes	Yes	Yes	Yes
Width1 (cm) / Label	1.59 / X1	5.19 / X1	7.50 / X1	12.00 / X1
Width2 (cm) / Label	5.19 / X2	1.59 / X2	7.50 / X2	7.50 / X2
Length1 (cm) / Label	1.90 / Y2	1.90 / Y2	10.00 / Y2	10.00 / Y2
Length2 (cm) / Label	18.31 / Y1	18.31 / Y1	7.50 / Y1	12.00 / Y1
MLC Model	ELEKTAMLCi2	ELEKTAMLCi2	ELEKTAMLCi2	ELEKTAMLCi2
Couch	Not Assigned	Not Assigned	Not Assigned	Not Assigned
Bolus	Not Assigned	Not Assigned	Not Assigned	Not Assigned
Number of Blocks	0	0	0	0
Isocenter x (cm)	9.61	9.61	9.61	9.61
Isocenter y (cm)	-1.10	-1.10	-1.10	-1.10
Isocenter z (cm)	20.00	20.00	20.00	20.00

Beam Number	1	2	4	5
Description	MED	LAT	APSU	RTSU
Field ID				
Treatment Unit	Linac1	Linac1	Linac1	Linac1
Machine ID	SYNERGY MLCI2 - 10	SYNERGY MLCI2 - 10	SYNERGY MLCI2 - 6M	SYNERGY MLCI2 - 6M
Machine Energy	10.0 MV	10.0 MV	6.0 MV	6.0 MV
Modality	Photon	Photon	Photon	Photon
Algorithm	CC	CC	---	---
Setup	SAD	SAD	SAD	SAD
SSD (cm)	93.39	85.01	93.56	76.65
Gantry (deg)	310.0	130.0	0.0	270.0
Collimator (deg)	10.6	349.4	0.0	0.0
Couch (deg)	0.0	0.0	0.0	0.0
Asymmetric	Yes	Yes	No	Yes
Width1 (cm) / Label	1.90 / X1	8.59 / X1	12.00 / X1	12.00 / X1
Width2 (cm) / Label	8.59 / X2	2.00 / X2	12.00 / X2	7.50 / X2
Length1 (cm) / Label	2.80 / Y2	2.80 / Y2	12.00 / Y2	12.00 / Y2
Length2 (cm) / Label	16.20 / Y1	16.20 / Y1	12.00 / Y1	12.00 / Y1
MLC Model	ELEKTAMLCi2	ELEKTAMLCi2	ELEKTAMLCi2	ELEKTAMLCi2
Couch	Not Assigned	Not Assigned	Not Assigned	Not Assigned
Bolus	Not Assigned	Not Assigned	Not Assigned	Not Assigned
Number of Blocks	0	0	0	0
Isocenter x (cm)	6.62	6.62	6.62	6.62
Isocenter y (cm)	-2.57	-2.57	-2.57	-2.57
Isocenter z (cm)	16.20	16.20	16.20	16.20

Beam Number	1	2	5	6
Description	MED	LAT	APSU	RTSU
Field ID				
Treatment Unit	Linac1	Linac1	Linac1	Linac1
Machine ID	SYNERGY MLCI2 - 6M	SYNERGY MLCI2 - 6M	SYNERGY MLCI2 - 6M	SYNERGY MLCI2 - 6M
Machine Energy	6.0 MV	6.0 MV	6.0 MV	6.0 MV
Modality	Photon	Photon	Photon	Photon
Algorithm	CC	CC	---	---
Setup	SAD	SAD	SAD	SAD
SSD (cm)	95.38	92.57	98.42	80.07
Gantry (deg)	302.0	126.0	0.0	270.0
Collimator (deg)	5.5	354.5	0.0	0.0
Couch (deg)	0.0	0.0	0.0	0.0
Asymmetric	Yes	Yes	Yes	Yes
Width1 (cm) / Label	2.70 / X1	4.00 / X1	7.50 / X1	12.00 / X1
Width2 (cm) / Label	4.00 / X2	2.60 / X2	7.50 / X2	7.50 / X2
Length1 (cm) / Label	4.90 / Y2	4.90 / Y2	12.00 / Y2	12.00 / Y2
Length2 (cm) / Label	12.60 / Y1	12.60 / Y1	7.50 / Y1	12.00 / Y1
MLC Model	ELEKTAMLCi2	ELEKTAMLCi2	ELEKTAMLCi2	ELEKTAMLCi2
Couch	Not Assigned	Not Assigned	Not Assigned	Not Assigned
Bolus	Not Assigned	Not Assigned	Not Assigned	Not Assigned
Number of Blocks	0	0	0	0
Isocenter x (cm)	10.15	10.15	10.15	10.15
Isocenter y (cm)	-3.91	-3.91	-3.91	-3.91
Isocenter z (cm)	14.55	14.55	14.55	14.55

APPENDIX III: Plan Report for Patients

Plan Information

Treatment Orientation: Head First Supine

Max Dose in Plan (Gy): 55.765

Max Dose Location (cm): X = -10.40 Y = -3.90 Z = 16.20

Grid Information

Grid Spacing (cm): 0.30

Calculate Dose Deposition to: Medium

Force entire volume to be treated as water: No

Assigned CTtoED File: DICOM3.CTCIRSPHANTOM2

# of Calculation Points: 4098204

Prescription Information: [A]

Rx Site	Prescribe To:	Rx Dose (Gy)	Fractional Dose (Gy)	Number of Fractions
2ASC	Interest Point 1	50.000	2.000	25

Actual Dose(Gy): 50.000

Rescale: No user normalization applied

Algorithm: Collapsed Cone Photon

Delivery Mode: 3D

Beam Information

Scan Reference Coordinates (cm): X = -0.06 Y = -0.16 Z = 16.35

Beam #	Description	Treatment Unit	Modality	Energy	Gantry (deg)	Coll. (deg)	Couch (deg)	Isocenter X(cm)	Isocenter Y(cm)	Isocenter Z(cm)	# of Segs	MU/Fx
1	LAT	Linac1	Photon	10.0 MV	234.0	6.0	0.0	-12.50	1.50	21.00	0	129.59
2	MED	Linac1	Photon	10.0 MV	55.0	354.0	0.0	-12.50	1.50	21.00	0	90.67
4	APSU	Linac1	Photon	6.0 MV	0.0	0.0	0.0	-12.50	1.50	21.00	1	0.00
5	RTSU	Linac1	Photon	6.0 MV	270.0	0.0	0.0	-12.50	1.50	21.00	1	0.00
										Total:	2	220.26

StudySet Information

Studyset ID: CT2 **# of Slices:** 98 **Pixel Size:** 0.12 **Scan Orientation:** Head First Supine

Plan Information

Treatment Orientation: Head First Supine

Max Dose in Plan (Gy): 55.877

Max Dose Location (cm): X = 9.00 Y = -2.09 Z = 20.40

Grid Information

Grid Spacing (cm): 0.30 **Assigned CTtoED File:** DICOM3.CTCIRSPHANTOM2

Calculate Dose Deposition to: Medium **# of Calculation Points:** 3993500

Force entire volume to be treated as water: No

Prescription Information: [A]

Rx Site	Prescribe To:	Rx Dose (Gy)	Fractional Dose (Gy)	Number of Fractions
LT BREAST	Interest Point 3	50.000	2.000	25

Actual Dose(Gy): 50.000

Rescale: No user normalization applied

Algorithm: Collapsed Cone Photon

Delivery Mode: 3D

Beam Information

Scan Reference Coordinates (cm): No Scan Reference Point has been selected

Beam #	Description	Treatment Unit	Modality	Energy	Gantry (deg)	Coll. (deg)	Couch (deg)	Isocenter X(cm)	Y(cm)	Z(cm)	# of Segs	MU/Fx
1	MED	Linac1	Photon	10.0 MV	303.0	4.2	0.0	8.70	-2.39	13.20	0	127.31
2	LAT	Linac1	Photon	10.0 MV	125.0	355.8	0.0	8.70	-2.39	13.20	0	90.13
5	APSU	Linac1	Photon	6.0 MV	0.0	0.0	0.0	8.70	-2.39	13.20	1	0.00
6	RTSU	Linac1	Photon	6.0 MV	270.0	0.0	0.0	8.70	-2.39	13.20	1	0.00
										Total:	2	217.44

APPENDIX IV: Dose Volume Histogram Statistics for Patients

Structure	Volume (cm^3)	Plan Name	Min Dose Gy	Max Dose Gy	Mean Dose Gy	Cold Ref Gy	Vol < (cm^3)	% Vol < Cold Ref	Hot Ref Gy	Vol > (cm^3)	% Vol > Hot Ref	% Inside Calc Vol	Inside StudySet
Heart	579.345	617916BB	0.363	49.234	1.408							100.00	Yes
Left Lung	805.985	617916BB	0.305	51.084	5.140				25.000	57.220	7.10	100.00	Yes
Right Lung	1004.665	617916BB	0.187	2.057	0.417							100.00	Yes
patient(Unsp.Tiss.)	25790.055	617916BB	0.006	54.723	1.754							99.48	No
target vol. 1	348.860	617916BB	0.000	55.127	44.166							100.00	Yes

Resolution: 0.10 **cm** **Bin Width:** 0.010 **Gy**

All DVH data is based on DVH resolution and bin width for ALL beams with calculated dose.

Structure	Volume (cm³)	Plan Name	Min Dose Gy	Max Dose Gy	Mean Dose Gy	Cold Ref Gy	Vol < (cm³)	% Vol < Cold Ref	Hot Ref Gy	Vol > (cm³)	% Vol > Hot Ref	% Inside Calc Vol	Inside StudySet
Heart	533.480	396456	0.451	47.512	1.649							100.00	Yes
LT Chest wall	117.615	396456	0.000	53.744	44.333							100.00	Yes
Lt Lung	879.015	396456	0.473	48.398	6.174				25.000	79.226	9.01	100.00	Yes
R Lung	960.970	396456	0.350	1.993	0.550							100.00	Yes
RT Breast	690.530	396456	0.000	19.588	0.902							100.00	Yes
patient(Unsp.Tiss.)	21374.840	396456	0.013	54.794	3.655							99.42	No

Resolution: 0.10 **cm** **Bin Width:** 0.010 **Gy**

All DVH data is based on DVH resolution and bin width for ALL beams with calculated dose.